Specialized Philippine Enterprise Reference of Experts and Scientists (SPHERES)

Volume 4 Issue No. 2 **December 2020**

INFORMATION RESOURCES AND ANALYSIS DIVISION
Science and Technology Information Institute
Department of Science and Technology
Gen. Santos Ave., Bicutan, Taguig City, Philippines

ABOUT THE SPECIALIZED PHILIPPINE ENTERPRISE REFERENCE OF EXPERTS AND SCIENTISTS (SPHERES)

The Division of Documentation of the National Institute of Science and Technology published the first volume of the Philippine Men of Science in 1964. It contained one hundred one bio-bibliographies of living men and women in the field of science and technology. It keeps track of our scientists and their contributions for the information and benefit of all. The compilation aims to provide interested users a useful and effective reference.

In 2012, the 24th volume of the Philippine Men of Science was uploaded online to make it more visible and accessible to users. Subsequently, the publication was renamed as the Philippine Men and Women of Science in 2013 to adopt a gender-sensitive title.

Today, the publication is given a new name – Specialized Philippine Enterprise Reference of Experts and Scientists (SPHERES).

The SPHERES brand introduces a new function with a new focus. When it comes to Filipino scientists and experts and their bio-bibliographic information, this compilation serves as a specialized reference for the public. Now with a gender-neutral emphasis and an inclusive sphere of influence, SPHERES is the name to remember.

Each volume of SPHERES consists of two issues annually.

For any inquiries on our publication:
Telefax: (632) 8837-2071 to 82, local 2135
E-mail: spheres@stii.dost.gov.ph WWW: http://spheres.dost.gov.ph/

CONTENTS

EXPERTS AND SCIENTISTS **PAGE**

Aherrera, Jaime Alfonso M. …… 1

Researches

- BAG6 Variant rs805303 is Nominally Associated with ACEi-induced Cough Among Filipinos 2
- The Klotho Variant rs36217263 Is Associated With Poor Response to Cardioselective Beta-Blocker Therapy Among Filipinos 2
- Disease characteristics of takayasu's arteritis among filipino patients seen at rheumatology clinics 3
- Clinical Profile and MACE in Patients who Underwent Revascularization for Left Main Coronary Artery and Left Main Equivalent Coronary Artery Disease in UP-PGH 4
- Cardiac events occurred commonly among apparently healthy Filipinos with the Brugada ECG pattern in the LIFECARE cohort 4
- "The Sticky LAD": Large Intracoronary Thrombus in an Aneurysmal Left Anterior Descending Artery Presenting as ST-Elevation Myocardial Infarction 5
- "Too Young to Have a Broken Heart": Spontaneous Coronary Artery Dissection Causing ST-Elevation Myocardial Infarction in a Young Adult: A Case Report 6
- Systolic Anterior Motion of Mitral Valve Subchordal Apparatus: A Rare Echocardiographic Pattern in Non-Obstructive Hypertrophic Cardiomyopathy 7
- A Rare Case of Pneumopericardium in the Setting of Tuberculous Constrictive Pericarditis 8
- Pulmonary vein mass with extension to the left atrium diagnosed by echocardiography 9
- PS 08-01 The Neutrophil-Lymphocyte Ratio (NLR) Predicts Severity of stable Coronary Artery Disease determined by the syntax score 9
- PS 02-23 Association of the Platelet–Lymphocyte Ratio (PLR) with outcomes in patients admitted for Acute Coronary Syndrome 10

- PS 14-78 Renal Artery Stenosis in Takayasu's Arteritis causing early-onset hypertension: a report of four cases at the UP-Philippine General Hospital 11
- PS 17-81 Prognostic Impact of Coronary Collaterals in Acute Coronary Syndrome (ACS): a meta-analysis (PICCACS STUDY) 12
- Prediction of Symptomatic Embolism in Filipinos With Infective Endocarditis Using the Embolic Risk French Calculator 13
- The Triply Twisted Heart: Cyanosis in an Adult With Situs Inversus, Levocardia, Double Outlet Right Ventricle, and Malposition of the Great Arteries 14
- APSC2015-1204 The Platelet-To-Lymphocyte Ratio (PLR) Is a Predictor of In-Hospital Mortality in Filipinos With Acute Coronary Syndrome: A Prospective Cohort 14
- APSC2015-1177 The Neutrophil-Lymphocyte Ratio Predicts Severity of Coronary Artery Disease Using the Syntax Score 15
- APSC2015-1178 Depression and Anxiety in Adult Filipinos With Congenital Heart Disease Using the Validated Filipino Version of the Hospital Anxiety and Depression Score (HADS) 15
- APSC2015-1176 Risk of Death and Adverse Outcomes in Adult Filipinos Admitted for Infective Endocarditis: A Prospective Cohort 15
- Cardiac tamponade as a rare manifestation of systemic lupus erythematosus: A report on four cases in the philippine general hospital 16
- Coarctation of the Aorta and a Parachute Mitral Valve in an Adult With Differential Cyanosis 17
- GW25-e0613 Clinical profile and predictors of outcomes of patients with mitral stenosis undergoing percutaneous transseptal mitral commissurotomy 17
- GW25-e0537 Association of the neutrophil–lymphocyte ratio (NLR) with outcomes in patients admitted for an acute coronary syndrome 18
- "The heart is blind" endogenous endophthalmitis secondary to endocarditis in a patient with systemic lupus erythematosus 18
- PW054 Acquired Arteriovenous Fistula of the Right Common Iliac Artery and Left Common Iliac Vein and Bilateral Lower Extremity Deep Venous Thrombosis in a Woman Presenting as High Output Failure 18

- A Comparison of 12 Lead Electrocardiogram and 2d-Echocardiography Derived Ejection Fraction among Patients with Depressed Ejection Fraction 18
- "Double Trouble" Wolff Parkinson White Syndrome and Mitral Stenosis Presenting as a Stroke in the Young 19
- When Stemi Is Not Stemi HIV Myocarditis Mimicking St-Elevation Myocardial Infarction on Electrocardiogram: A Case Report 19
- Pulmonic Valve Endocarditis with an underlying ventricular septal defect: a report on three cases at the Philippine General Hospital 19
- An unparsimonious quandary: Mitral stenosis and ventricular septal defect complicating systemic lupus erythematosus and pregnancy 19
- Routine angioplasty after fibrinolytic therapy for ST-segment elevation myocardial infarction: An updated meta-analysis (RAFT-STEMI) 20
- Clinical and Echocardiographic Profile and Outcomes of Peripartum Cardiomyopathy: The Philippine General Hospital Experience 21
- Febuxostat versus allopurinol for hyperuricemia and gout: a meta-analysis (Fame study) 22

Galay, Remil Linggatong …… 23

Researches

- Development of a Loop-Mediated Isothermal Amplification (LAMP) Assay Targeting the Citrate Synthase Gene for Detection of Ehrlichia canis in Dogs 23
- Molecular Detection of Rickettsia Spp. and Coxiella Burnetii in Cattle, Water Buffalo, and Rhipicephalus (Boophilus) Microplus Ticks in Luzon Island of the Philippines 24
- Molecular detection of Anaplasma spp. in blood and milk of dairy cattle in the Philippines 25
- Molecular detection of tick-borne pathogens in canine population and Rhipicephalus sanguineus (sensu lato) ticks from southern Metro Manila and Laguna, Philippines 25
- Induction of intracellular ferritin expression in embryo-derived Ixodes scapularis cell line (ISE6) 26

- Glutathione S-transferases play a role in the detoxification of flumethrin and chlorpyrifos in Haemaphysalis longicornis 27
- Hemolymph defensin from the hard tick Haemaphysalis longicornis attacks Gram-positive bacteria 28
- Vector competence of Haemaphysalis longicornis ticks for a Japanese isolate of the Thogoto virus 29
- Characterization and expression analysis of a newly identified glutathione S-transferase of the hard tick Haemaphysalis longicornis during blood-feeding 29
- Evaluation of vaccine potential of 2-Cys peroxiredoxin from the hard tick Haemaphysalis longicornis 31
- Immunofluorescent detection in the ovary of host antibodies against a secretory ferritin injected into female Haemaphysalis longicornis ticks 31
- Synchronous Langat Virus Infection of Haemaphysalis longicornis Using Anal Pore Microinjection 32
- Ticks' antioxidant complex: A defense stronghold and a potential target for their control 33
- Characterization and antiviral activity of a newly identified defensin-like peptide, HEdefensin, in the hard tick Haemaphysalis longicornis 34
- 2-Cys peroxiredoxin is required in successful blood-feeding, reproduction, and antioxidant response in the hard tick Haemaphysalis longicornis 35
- Host Immunization with Recombinant Proteins to Screen Antigens for Tick Control 36
- RNA Interference — A Powerful Functional Analysis Tool for Studying Tick Biology and its Control 36
- Induction of gene silencing in Haemaphysalis longicornis ticks through immersion in double-stranded RNA 37
- Virucidal activity of Haemaphysalis longicornis longicin P4 peptide against tick-borne encephalitis virus surrogate Langat virus 38
- Impaired cellular immune response to injected bacteria after knockdown of ferritin genes in the hard tick Haemaphysalis longicornis 39
- A novel C-type lectin with triple carbohydrate recognition domains has critical roles for the hard tick Haemaphysalis longicornis against Gram-negative bacteria 39

- Functional analysis of recombinant 2-Cys peroxiredoxin from the hard tick Haemaphysalis longicornis 40
- Ticks and Tick-borne Diseases 40
- Identification of the Babesia-responsive leucine-rich repeat domain-containing protein from the hard tick Haemaphysalis longicornis 40
- Iron metabolism in hard ticks (Acari: Ixodidae): The antidote to their toxic diet 41
- Evaluation and comparison of the potential of two ferritins as anti-tick vaccines against Haemaphysalis longicornis 41
- Two Kinds of Ferritin Protect Ixodid Ticks from Iron Overload and Consequent Oxidative Stress 43
- Expression analysis of autophagy-related genes in the hard tick Haemaphysalis longicornis 43
- Inhibitory effect of cyclophilin A from the hard tick Haemaphysalis longicornis on the growth of Babesia bovis and Babesia bigemina 44
- Multiple ferritins are vital to successful blood feeding and reproduction of the hard tick Haemaphysalis longicornis 45
- Host-derived transferrin is maintained and transferred from midgut to ovary in Haemaphysalis longicornis ticks 45
- Target of rapamycin (TOR) controls vitellogenesis via activation of the S6 kinase in the fat body of the tick, Haemaphysalis longicornis 46
- HlSRB, a Class B Scavenger Receptor, Is Key to the Granulocyte-Mediated Microbial Phagocytosis in Ticks 47
- Scavenger Receptor Mediates Systemic RNA Interference in Ticks 47
- Anti-babesial activity of a potent peptide fragment derived from longicin of Haemaphysalis longicornis 48
- Tick Longicin Implicated in the Arthropod Transmission of Toxoplasma Gondii 49

Paraan, Francis Norman C. …… 51
- Selective capture of CO2 over N2 and CH4: B clusters and their size effects 51
- Strong chemisorption of CO2 on B10-B13 planar-type clusters 52

- Controlling the nucleophilic properties of cobalt salen complexes for carbon dioxide capture 52
- Average work done in a ground state quantum quench of the Kitaev chain model with variable-range interactions 53
- Ab initio study on the binding of carbon dioxide to cobalt salen complex 53
- Simple techniques for improving deep neural network outcomes on commodity hardware 53
- Integer effects in the entanglement and spin fluctuations of a quantum Hall system with Rashba interaction 54
- Entanglement-fluctuation relation for bipartite pure states 54
- Exact work statistics of quantum quenches in the anisotropic XY model 55
- Effective thermodynamics of isolated entangled squeezed and coherent states 55
- Entanglement spectrum and number fluctuations in the spin-partitioned BCS ground state 56
- Quantum phase transition in a multicomponent anyonic Lieb-Liniger model 56
- Entanglement spectra of q-deformed higher spin VBS states 57
- Entanglement spectra of the q-deformed Affleck-Kennedy-Lieb-Tasaki model and matrix product states 57
- Erratum: Entanglement in bipartite pure states of an interacting boson gas obtained by local projective measurements [Phys. Rev. A 84 , 032330 (2011)] 58
- Perturbative correction to the ground state properties of one-dimensional strongly interacting bosons in a harmonic trap 58
- Quantum quenches in the Dicke model: Statistics of the work done and of other observables 59
- Brownian motion of a charged particle driven internally by correlated noise 59
- Exact moments in a continuous time random walk with complete memory of its history 60

Payot, Betchaida D. …….. 61

Researches

- Bouguer Anomaly of Central Cebu, Philippines 61
- Consumed tectonic plates in Southeast Asia: Markers from the Mesozoic to early Cenozoic stratigraphic units in the northern and central Philippines 62
- Mesozoic rock suites along western Philippines: Exposed proto-South China Sea fragments? 63
- Melt-rock interaction in the sub arc mantle: records from the plagioclase peridotites of the southern Palawan Ophiolite, Philippines 64
- Petrogenesis of ultramafic-mafic clasts in the Dos Hermanos Mélange, Ilocos Norte: Insights to the evolution of western Luzon, Philippines 64
- Petrographic and geochemical characterization of the crustal section of the Pujada Ophiolite, southeastern Mindanao, Philippines: Insights to the tectonic evolution of the northern Molucca Sea Collision Complex 65
- An evolving subduction-related magmatic system in the Masara Gold District, Eastern Mindanao, Philippines 66
- Characterization of the proto-Philippine Sea Plate: Evidence from the emplaced oceanic lithospheric fragments along eastern Philippines 67
- Petrologic nature of the active sub arc crust-mantle boundary: Mixed magmatic-metasomatic processes recorded in xenoliths from Sabtang island, Luzon arc 68
- Slab rollback and microcontinent subduction in the evolution of the Zambales Ophiolite Complex (Philippines): A review 69
- Mantle Evolution from Ocean to Arc: The Record in Spinel Peridotite Xenoliths in Mt. Pinatubo, Philippines 70
- Aqueous fluids and sedimentary melts as agents for mantle wedge metasomatism, as inferred from peridotite xenoliths at Pinatubo and Iraya volcanoes, Luzon arc, Philippines 70
- Alteration and lithogeochemistry in the Masara Gold District, Eastern Mindanao, Philippines, as tools for exploration targeting 71

- Petrological and geochemical characteristics of the Samar Ophiolite ultramafic section: implications on the origins of the ophiolites in Samar and Leyte islands, Philippines 72
- Petrography and geochemistry of Cenozoic sedimentary sequences of the southern Samar Island, Philippines: Clues to the unroofing history of an ancient subduction zone 73
- Arc and backarc geochemical signatures of the proto-Philippine Sea Plate: Insights from the petrography and geochemistry of the Samar Ophiolite volcanic section 74
- Adakitic rocks in the Masara gold-silver mine, Compostela Valley, Mindanao, Philippines: Different places, varying mechanisms? 74
- Geochemical and Geophysical Characteristics of the Balud Ophiolitic Complex (BOC), Masbate Island, Philippines: Implications for its Generation, Evolution and Emplacement 75
- Paleomagnetism of the Samar Ophiolite: Implications for the Cretaceous sub-equatorial position of the Philippine island arc 76
- Podiform chromitite formation in a low-Cr/high-Al system: An example from the Southwest Indian Ridge (SWIR) 76
- Textural Evidence for the Chromite-Oversaturated Character of the Melt Involved in Podiform Chromitite Formation 77
- Lithospheric mantle connection of clinopyroxene inclusions in chromites from the Archean Nuasahi ultramafic-mafic complex (India) 78
- Petrographical and geochemical characteristics of the sheeted dyke-gabbro transition zone in ODP/IODP Hole 1256D 78
- IODP expedition 335: deep sampling in ODP hole 1256D 79
- A chromian spinel-oversaturated melt for podiform chromitite formation: Evidence from well-preserved dunite clots in massive podiform chromitites in the Coto Block, Zambales Ophiolite Complex, Philippines 80
- Abyssal harzburgite veined by silica-oversaturated melt in the Sibuyan Ultramafics, Romblon, Central Philippines 81
- Unusual ultra-depleted dunite from Sibuyan Island (the Philippines): A residue for ultra-depleted MORB? 82
- What underlies the Philippine island arc? Clues from the Calaton Hill, Tablas island, Romblon (Central Philippines) 83

- Geology and Hydrothermal Alteration of the Low Sulfidation 83
- Metasomatic interactions between slab-derived melts and depleted mantle: Insights from xenoliths within Monglo adakite (Luzon arc, Philippines) 84
- Behavior of Major and Trace Elements during Ore Deposition: Example from the Low-Sulfidation Pantingan Gold System, Mount Mariveles, Bataan, Philippines 85
- Temporal Geochemical Evolution of Neogene Magmatism in the Baguio Gold–Copper Mining District (Northern Luzon, Philippines) 86
- The oceanic substratum of Northern Luzon: Evidence from xenoliths within Monglo adakite (the Philippines) 87
- Geology and Hydrothermal Alteration of the Low Sulfidation Pantingan Gold System, Mount Mariveles, Bataan (Luzon), Philippines 87

Reyes, Reinabelle ……. 89

Researches

- Predicting Galaxy Star Formation Rates via the Co-evolution of Galaxies and Halos 89
- The Dark Side of Galaxy Color: evidence from new SDSS measurements of galaxy clustering and lensing 90
- Is LambdaCDM consistent with the Tully-Fisher relation? 91
- Cosmological parameter constraints from galaxy-galaxy lensing and galaxy clustering with the SDSS DR7 92
- Calibrated Tully–Fisher relations for improved estimates of disc rotation velocities 93
- Optical-to-virial velocity ratios of local disk galaxies from combined kinematics and galaxy-galaxy lensing 94
- Photometric redshift requirements for lens galaxies in galaxy-galaxy lensing analyses 95
- Calibrated Tully-fisher Relations For Improved Photometric Estimates Of Disk Rotation Velocities 96
- Confirmation of general relativity on large scales from weak lensing and galaxy velocities 96

- Space Density of Optically Selected Type 2 Quasars 97
- Erratum: "Space Density of optically selected type 2 quasars" (2008, AJ, 136, 2373) 98
- Test of Gravity on Large Scales with Weak Gravitational Lensing and Clustering Measurements of SDSS Luminous Red Galaxies 99
- Improved optical mass tracer for galaxy clusters calibrated using weak lensing measurements 99
- Space Density Of Optically-Selected Type II Quasars From The SDSS 100

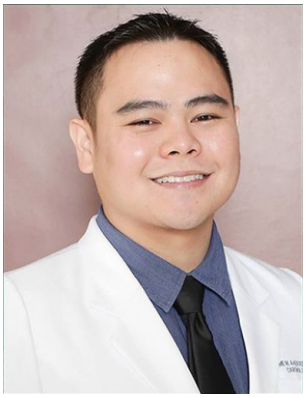

DR. JAIME ALFONSO M. AHERRERA

University of the Philippines Manila

Sex: Male

Education:

University of the Philippines, Philippine General Hospital Fellowship Training in Interventional Cardiology, 2016-2018

University of the Philippines, Philippine General Hospital Fellowship Training in Adult Cardiology, 2013-2016

University of the Philippines, Philippine General Hospital Residency Training in Internal Medicine, 2009-2012

Doctor of Medicine 2004-2008

De La Salle University, BS Human Biology, 2002-2004

Field of Specialization:

Internal Medicine (General Medicine)

Epidemiology

Cardiology

Researches:

Article title: BAG6 Variant rs805303 is Nominally Associated with ACEi-induced Cough Among Filipinos

Authors: Paul Ferdinand M. Reganit, Rody G. Sy, Jezreel L. Taquiso, Charlene F. Agustin, Richard Henry Perlas Tiongco II, Jaime Manalo Aherrera, Elmer Balasico Llanes Felix Eduardo Punzalan, Lauro Lim Abrahan IV

Publication title: Philippine Journal of Science 149 (1) 35-41, March 2020

Abstract:

Cough is a common side effect of angiotensin converting enzyme inhibitor (ACEi) therapy. The incidence of ACEi-induced cough has been shown to correlate with genetic variation among different populations. This study aimed to determine the association of candidate genetic polymorphisms with ACEi-induced cough among Filipinos. Two hundred twenty (220) participants on ACEi therapy pressure-lowering in an unmatched case-control study (82 cases with ACEi-induced cough and 138 controls). Genomic DNA samples were extracted and genotyped for selected genetic variants. The association of genetic variants and clinical factors with ACEi-induced cough was determined using regression analyses. Univariate logistic regression showed that the BAG6 variant rs805303 is nominally associated with ACEi-induced cough among Filipinos, at a per-comparison error rate (PCER) of 0.05 (OR 2.10, p = 0.016). The association of the variant with ACEi cough was statistically significant after multiple regression analysis (adjusted OR 2.09, p = 0.022) while adjusting for confounding clinical factors (sex, alcohol intake, and diastolic blood pressure). Further studies are needed to validate these findings.

Full text link: https://tinyurl.com/y7jrbuh9

Article title: The Klotho Variant rs36217263 Is Associated With Poor Response to Cardioselective Beta-Blocker Therapy Among Filipinos

Authors: Rody G. Sy, Jose B. Nevado, Elmer Balasico Llanes, Jose Donato A. Magno, Deborah Ignacia D. Ona, Felix Eduardo R. Punzalan, Paul Ferdinand M. Reganit, Lourdes Ella G. Santos, Richard Henry Perlas Tiongco II, Jaime Manalo Aherrera, Lauro L. Abrahan, Charlene F.

Agustin, Aimee Yvonne Criselle Landicho Aman, Adrian John P. Bejarin, Eva Maria C. Cutiongco-de la Paz

Publication title: Clinical Pharmacology & Therapeutics 107(1), July 2019

Abstract:

A common drug used for hypertension among Filipinos are beta-blockers. Variable responses to beta-blockers are observed, and genetic predisposition is suggested. This study investigated the association of genetic variants with poor response to beta-blockers among Filipinos. A total of 76 Filipino adult hypertensive participants on beta-blockers were enrolled in an unmatched case-control study. Genotyping was done using DNA from blood samples. Candidate variants were correlated with clinical data using chi-square and logistic regression analysis. The deletion of at least one copy of allele A of rs36217263 near Klotho showed statistically significant association with poor response to beta-blockers [dominant; odds ratio (OR)=3.89, p=0.017)], adjusted for diabetes and dyslipidemia. This association is observed among participants using cardioselective beta-blockers (crude OR=5.60, p=0.008), but not carvedilol (crude OR=2.56, p=0.67). The genetic variant rs36217263 is associated with poor response to cardioselective beta-blockers, which may become a potential marker to aid in the management of hypertension.

Article title: Disease characteristics of takayasu's arteritis among filipino patients seen at rheumatology clinics

Authors: I.E.S. Afos, J.R.L. Hipe, C.M.G. Faustino, Jaime Manalo Aherrera, Lauro Lim Abrahan IV, B.H.M. Reyes

Abstract:

Introduction: Takayasu's arteritis (TA), a large vessel vasculitis has various initial presenting manifestations; making it difficult to diagnose. Hence, the number of those with the disease in the population is underestimated. The study intends to update local data and to describe different presentations of the disease to enhance awareness for TA. Methods: This is a retrospective study done in a tertiary government hospital. Twenty-two out of twenty three charts of patients diagnosed with TA based on the 1990 ACR criteria were reviewed. Demographic profile, initial clinical manifestations, imaging, treatment and outcomes were collected. Descriptive statistics was applied. Institutional Review Board approval was obtained

prior to study initiation. Results: Majority (90.1%) were female; mean age at onset of symptoms and at diagnosis were 30.4 (+12.3)years and 33.2 (+12.0)years respectively. The common reasons for consult were hypertension (26.3%), claudication (21.1%) and abdominal pain (11%). Laboratories showed elevated erythrocyte sedimentation rate (87.5%), leukocytosis (43.8%), anemia (31%) and thrombocytosis (4.5%). Common imaging findings were cardiomegaly (27.3%), aortic regurgitation (27.3%) and carotid stenosis (18.2%). CT angiogram in 90% of cases demonstrated arterial wall narrowing. Other findings were aneurysm (31.8%), contour irregularities (13.6%) and femoral artery occlusion (4.5%). Treatment for active disease were glucocorticoids alone (44%) and combined glucocorticoids and other immunosuppressants (56%). Of the 22 records reviewed, six patients (27%) had stroke. Four (18.2 %) had different surgical procedures; ray amputation of toe for digital ischemia, embolectomy for digital gangrene, balloon angioplasty of the renal artery and renal angioplasty for stenosis. Two (9.1%) who had pregnancies after TA diagnosis had premature deliveries without neonatal complications. No mortality was recorded over the mean follow-up of 49.33 patient-years. Conclusion: Clinicians should be aware of the different initial presenting signs and symptoms of TA since development of collateral circulation may mask other symptoms. Thus, thorough history and physical assessment are essential tools in the diagnosis of TA.
Full text link: https://tinyurl.com/ybfh5qfv

Article title: Clinical Profile and MACE in Patients who Underwent Revascularization for Left Main Coronary Artery and Left Main Equivalent Coronary Artery Disease in UP-PGH
Authors: Jezreel L. Taquiso, Jaime Manalo Aherrera, Richard Henry Perlas Tiongco II, Enqirue, Lii Chua
Publication title: Atherosclerosis Supplements 32: 71-72, June 2018

Abstract:
No available

Article title: Cardiac events occurred commonly among apparently healthy Filipinos with the Brugada ECG pattern in the LIFECARE cohort
Authors: Giselle G. Gervacio, Jaime Manalo Aherrera, Rody G. Sy, Lauro Lim Abrahan IV, Michael Joseph Agbayani, Feliz Eduardo Punzalan, Elmer Balasico Llanes, Paul Ferdinand M.

Reganit, Olivia Sison, E-Shyong Tai, Felicidad V. Velandria, Allan Gumatay, Nina Castillo-Carandang

Publication title: Heart Asia 10(2) May 2018

Abstract:

Background Brugada syndrome is the mechanism for sudden unexplained death. The Brugada ECG pattern is found in 2% of Filipinos. There is a knowledge gap on the clinical outcome of these individuals. The clinical profile and 5-year cardiac event rate of individuals with the Brugada ECG pattern were determined in this cohort. Methods This is a sub-study of LIFECARE (Life Course Study in Cardiovascular Disease Epidemiology), a community based cohort enrolling healthy individuals 20 to 50 years old conducted in 2009–2010. ECGs of all enrollees were screened independently by three cardiologists. The prevalence of the coved Brugada ECG pattern was ascertained, and the 5-year cardiac event rate was determined among those individuals with this pattern. The participants were contacted to determine the occurrence of cardiac events, which included syncope, presyncope, seizures, cardiac arrest and unexplained vehicular accidents. Results A total of 3072 ECGs were reviewed, and 14 subjects (0.4%) with the coved Brugada ECG pattern were identified. Four had a cardiac event on follow-up at 5 years, but all remained alive. Most of these 14 coved Brugada individuals were healthy and asymptomatic at baseline. Conclusion Cardiac events occurred commonly among initially asymptomatic Filipinos with the coved Brugada ECG pattern. Such patients need to be followed up closely.

Article title: "The Sticky LAD": Large Intracoronary Thrombus in an Aneurysmal Left Anterior Descending Artery Presenting as ST-Elevation Myocardial Infarction

Authors: Jaime Manalo Aherrera, Marc Denver Tiongson, Eric Oliver Dizon Sison

Publication title: Journal of medical cases 9(8) 243-245, January 2018

Abstract:

Management of acute coronary syndrome in coronary ectasia and large intracoronary thrombus has been culled from case reports. A 55-year old male sought consult for severe chest pain. On angiography there was note of large burden intracoronary thrombus. Various percutaneous coronary techniques were done. Angiographic success was not achieved, and then he was

maintained on tirofiban. Repeat angiography after 2 weeks revealed dissolution of thrombus with optimal medical therapy. Management of atypical cases should be individualized.
Full text link: https://tinyurl.com/yded5ugt

Article title: "Too Young to Have a Broken Heart": Spontaneous Coronary Artery Dissection Causing ST-Elevation Myocardial Infarction in a Young Adult: A Case Report
Authors: Marc Denver A. Tiongson, Eric Oliver Dizon Sison, Jaime Manalo Aherrera, Dioscoro DC Bayani, Joerelle Mojica, Nashiba Daud, John Daniel Ramos
Publication title: Journal of medical cases 9(6) 164-169, January 2018

Abstract:
ST-elevation myocardial infarction (STEMI) rarely occurs among patients 18 to 34 years old. Spontaneous coronary artery dissection (SCAD) is a rare cause of STEMI and is frequently described among patients in peripartum period. SCAD has a high mortality rate if not recognized and treated immediately. We present a case of SCAD presenting as STEMI in a 19-year-old nonpregnant patient. A 19-year-old female with chronic kidney disease, complained of sudden onset substernal chest pain. Physical examination showed a blood pressure of 140/90 mm Hg, HR of 112 bpm, with note of rales, pedal edema, and cold clammy extremities. Electrocardiogram showed ST-elevation in leads V3 to V6. Cardiac troponin was elevated andechocardiography revealed left ventricular segmental hypokinesia and depressed systolic function. Patient was diagnosed with acute anterolateral wall STEMI. Coronary angiogram revealed total occlusion of the mid-segment of the left anterior descending artery (LAD), while the rest of the coronary arteries were strikingly normal. After
initial balloon angioplasty and stenting of the mid LAD, coronary artery dissection was noted at the distal LAD. A stent was successfully deployed, achieving TIMI flow grade III with no residual stenosis. She remained stable and was discharged improved. STEMI rarely happens in the young adults. Moreover, literature highlights the rarity of STEMI caused by SCAD. SCAD usually occurs among young pregnant patients without risk factors for atherosclerosis. We highlighted the significance of suspecting SCAD among young patients who present with STEMI and prompt treatment with revascularization in clinical situations such as this case. SCAD remains to be a rare cause of STEMI. However, SCAD should be considered among

young individuals with STEMI. Treatment is primarily medical unless there is persistent chest pain and/or ischemic ECG changes, hemodynamic instability, or unstable arrhythmia, where revascularization is necessary.

Full text link: https://tinyurl.com/y9ddvlhg

Article title: Systolic Anterior Motion of Mitral Valve Subchordal Apparatus: A Rare Echocardiographic Pattern in Non-Obstructive Hypertrophic Cardiomyopathy

Authors: Jezreel Taquiso, Stephanie Martha O. Obillos, Joerelle V. Mojica, Lauro Lim Abrahan IV, Elleen C. Cunanan, Jaime Manalo Aherrera, Jose Donato A. Magno

Publication title: Cardiology Research 8(5) 258-264, October 2017

Abstract:

Systolic anterior motion (SAM) of the mitral valve or chordate is one characteristic seen in hypertrophic cardiomyopathy (HCM) either in obstructive or non-obstructive phenotypes. More often than not, the obstruction is caused by valvular rather than chordal SAM. We describe the role of echocardiography in identifying the actual anatomical location of the mitral valve apparatus involved in SAM and in assessing consequent left ventricular outflow tract (LVOT) obstruction in an otherwise asymptomatic patient. We report a case of a 29-year-old male admitted for an elective non-cardiac surgery, presenting with a cardiac murmur and left axis deviation with biventricular hypertrophy on electrocardiogram. On 2D transthoracic echocardiography (TTE), an asymmetrically hypertrophied left ventricle with systolic motion of anterior mitral valve was incidentally seen. Continuous wave Doppler assessment across the LVOT showed some gradient of obstruction (peak gradient: 9 mm Hg). Transesophageal echocardiography (TEE) demonstrated a redundant anterior mitral valve with the subchordal apparatus mainly causing SAM and confirmed the gradient obtained on TTE, with a mild degree, yet non-significant, degree of LVOT obstruction (mean gradient: 10 mm Hg) documented. Because of this finding, patient was cleared for surgery. Management was deemed conservative with emphasis on close surveillance for signs and symptoms attributable to development of significant LVOT obstruction in patients with HCM. To our knowledge, this is the first reported case in our country of an echocardiographic pattern of systolic anterior motion primarily of the subchordal mitral valve apparatus causing some, though non-significant, degree of LVOT obstruction in HCM. Echocardiographic features such as asymmetric left

ventricular hypertrophy and presence of some LVOT obstruction caused primarily by subchordal apparatus could impact management in asymptomatic patients.

Full text link: https://tinyurl.com/y8aqakjr

Article title: A Rare Case of Pneumopericardium in the Setting of Tuberculous Constrictive Pericarditis

Authors: Lauro Lim Abrahan IV, Stephanie Martha O. Obillos, Jaime Manalo Aherrera, Jose Donato A. Magno, Celia Catherine C. Uy-Agbayani, Ulysses King G. Gopez, Jobelle Baldonado

Publication title: Case Reports in Cardiology (12) 1-6, May 2017

Abstract:

A 28-year-old Filipino male was admitted due to high-grade fevers and dyspnea on a background of chronic cough and weight loss. Due to clinical and echocardiographic signs of cardiac tamponade, emergency pericardiocentesis was performed on his first hospital day. Five days after, chest radiographs showed new pockets of radiolucency within the cardiac shadow, indicative of pneumopericardium. On repeat echo, air microbubbles admixed with loculated effusion were visualized in the anterior pericardial space. Constrictive physiology was also supported by a thickened pericardium, septal bounce, exaggerated respiratory variation in AV valve inflow, and IVC plethora. A chest CT scan confirmed the presence of an air-fluid level within the pericardial sac. The patient was started on a quadruple antituberculosis regimen and IV piperacillin-tazobactam to cover for superimposed acute bacterial pericarditis. Pericardiectomy was performed as definitive management, with stripped pericardium measuring 5–7 mm thick and caseous material extracted from the pericardial sac. Histopathology was consistent with tuberculosis. This report highlights pneumopericardium as a rare complication of pericardiocentesis. We focused on the utility of echocardiography for diagnosing and monitoring this condition on a background of tuberculous constrictive pericarditis, ultimately convincing us that pericardiectomy was necessary, instead of the usual conservative measures for pneumopericardium.

Full text link: https://tinyurl.com/ycd3oqzo

Article title: Pulmonary vein mass with extension to the left atrium diagnosed by echocardiography

Authors: Jezreel L. Taquiso, Jaime Manalo Aherrera, Jose Donato Magno, Eric Oliver Dizon Sison

Publication title: BMJ Case Reports, March 2017

Abstract:

We report a case of a man aged 65 years presenting with chronic cough, haemoptysis and intermittent atrial tachyarrhythmias on ECG. On 2D transthoracic echocardiography, an incidental left atrial mass was seen, initially thought to be a thrombus predisposed by intermittent atrial fibrillation. Transoesophageal echocardiography confirmed that this left atrial mass originated from a fixed, non-homogenous, right superior pulmonary vein mass with an extracardiac extension. Because of this finding, a thorough search for a primary focus lead to the discovery of a contiguous posterior mediastinal mass, which was a round cell neoplasm on histology. Management was deemed palliative. Although rare, left-sided cardiac masses should prompt the physician to search for a malignancy in the lung in high-risk patients, as haematogenous spread via the pulmonary vein is a potential mechanism for spread.

Full text link: https://tinyurl.com/y79y2v6x

Article title: PS 08-73 Strange Connections: Case series of Coronary Arterial-Venous Fistulas seen at the Philippine General Hospital

Authors: Christine Train, Jodette Joy Lavente, Elleen Cunanan, Michael Estur, John Daniel Ramos, Jorelle Mojica, Jaime Manalo Aherrera, Eric Oliver Dizon Sison, Jose Donato Magno, Wilfred Dee, John Anonuevo, Elmer Balasico Llanes

Publication title: Journal of Hypertension 34 (Supplement I) September 2016

Abstract: Not available.

Article title: PS 08-01 The Neutrophil-Lymphocyte Ratio (NLR) Predicts Severity of stable Coronary Artery Disease determined by the syntax score

Authors: Jaime Manalo Aherrera, Lowe Chiong, Christine Train, Paul Reganit, Felix Punzalan, John Anonuevo, Ramon Abarquez

Publication title: Journal of Hypertension 34 (Supplement i) September 2016

Abstract:

Objective: The neutrophil-lymphocyte ratio (NLR) is believed to be associated with the complexity of coronary artery disease (CAD). We aim to investigate the association between the NLR and severity of CAD using the SYNTAX scoring system among adult Filipinos. Design and Method: This is a cross-sectional study conducted at a tertiary hospital. The NLR of included patients, taken within 1 week prior to the angiogram, was computed (neutrophil divided by lymphocyte count). After coronary angiogram, the severity of CAD was determined independently, using the SYNTAX scoring system. The primary outcome was presence of severe CAD represented by a SYNTAX score of > 32. Results: A total of 211 patients with a mean age of 57 years were included. Diagnosis after coronary angiogram was 1-Vessel CAD in 64 (30%), 2-Vessel CAD in 34 (16%), and 3-Vessel CAD in 66 (31%). 46 patients (22%) were found to have severe CAD based on a SYNTAX score of > 32. The NLR, neutrophil, and lymphocyte count correlated with SYNTAX score using Pearson's correlation coefficient. The optimal cutoff value of NLR to predict high syntax score is 2.51. On multiple logistic regression, only the NLR (OR 6.98, p < 0.001) and smoking history (5.84, p 0.002) were associated with a SYNTAX score > 32. Conclusions: Among adult Filipinos with angina suspected of CAD, the NLR is a useful, inexpensive tool to predict severity of multi-vessel disease using the SYNTAX scoring system. A cut-off NLR of 2.51 may be used to stratify patients with a high NLR and predict the presence of severe CAD (SYNTAX > 32).

Article title: PS 02-23 Association of the Platelet–Lymphocyte Ratio (PLR) with outcomes in patients admitted for Acute Coronary Syndrome

Authors: Lauro Lim Abrahan IV, Jaime Manalo Aherrera, John Daniel Ramos, Paul Ferdinand Reganit, Felix Eduardo Punzalan

Publication title: Journal of Hypertension 34(3), September 2016,

Abstract:

Introduction: Patients with acute coronary syndrome (ACS) exhibit a wide spectrum of early risk of death (one to 10 percent). High platelet counts may indicate a propensity for platelet-rich thrombi. Lymphocyte counts drop during ACS due to stress-induced cortisol release. Combining these two markers, recent studies have found that the platelet-to-lymphocyte ratio (PLR) is associated with adverse cardiac events among patients with ACS, but local data is

limited. The objective of this study is to determine if an elevated PLR taken on admission is associated with higher rates of adverse cardiac events. Methods: A retrospective cohort of adult patients with ACS admitted at the UP-Philippine General Hospital was analyzed. Leukocyte and platelet counts were measured by an automated hematology analyzer. The PLR values of these patients were computed, and they were stratified into two groups after determining the optimal cut-off from the receiver operating characteristic curve (ROC) curve. The primary outcome was in-hospital mortality. Secondary outcomes included development of heart failure, cardiogenic shock, reinfarction, and significant arrhythmias. Results: A total of 174 Filipinos with ACS were included. In-hospital mortality occurred in 30 patients (17%). These patients had a higher PLR compared to those who were discharged alive (p-value <0.0001). The optimal cutoff value of PLR to predict in-hospital mortality is 165, with a sensitivity of 77% and specificity of 70% (area under the ROC curve of 0.766). On multiple logistic regression analysis, a high PLR was an independent predictor of in-hospital mortality (RR 8.52; p 0.003) after controlling for the effect of other variables. The development of the predetermined secondary outcomes did not correlate with PLR on multivariate analysis. Conclusion: Among Filipino patients with ACS, an elevated PLR taken within 24 hours of admission is a useful marker to predict in-hospital mortality, thus providing vital information for risk stratification and more aggressive management strategies.

Article title: PS 14-78 Renal Artery Stenosis in Takayasu's Arteritis causing early-onset hypertension: a report of four cases at the UP-Philippine General Hospital
Authors: Lauro Lim Abrahan IV, Elleen Cunanan, Percy Jun Prieto, Jaime Manalo Aherrera, Antonio Faltado, Maria Teresa Bacnis Abola
Publication title: Journal of Hypertension 34(Supplement I), September 2016

Abstract: No abstract

Article title: PS 11-26 The "Weekend Effect" among patients presenting with Acute Coronary Syndrome in the Philippine General Hospital
Authors: John Daniel Ramos, Jaime Manalo Aherrera, Felix Eduardo Punzalan
Publication title: Journal of Hypertension 34(3), September 2016

Abstract:

Introduction: Studies have shown that weekend and holiday admissions for patients with acute coronary syndrome (ACS) are associated with higher incidence of in-hospital mortality and major adverse cardiovascular events (MACE). This has been referred to as the "weekend effect." Objectives: We aim to determine whether adults with ACS admitted on weekends have an increased risk for adverse outcomes, primarily in-hospital mortality. Methodology: This is a retrospective cohort observational study. An ACS database of a prospectively collected cohort was reviewed. Participants in this database included patients with a diagnosis of ACS who satisfied pre-defined inclusion and exclusion criteria. Clinical characteristics and admission data (weekend/holiday versus regular day admission) of all patients were collected. Outcomes of interest were in-hospital mortality, severe heart failure, and re-infarction. Analysis: Descriptive analysis was done by obtaining the mean and standard deviation of quantitative variables. Proportions and frequencies were reported for qualitative variables. For quantitative variables, T-test of two independent samples was used to determine if there is a significant difference. For categorical variables, the Z-test was used. Multiple logistic regression was also done to explore the predictors of the weekend effect. Results: A total of 175 patients were included in this study, 59 were admitted on a weekend/holiday and 116 on a regular day. The duration of symptoms prior to admission were longer among those who were admitted during the weekend (40.86±54.11 hrs vs 11.83±8.40 hrs, p=<0.0001). A weekend hospital admission was found to be an independent predictor of in-hospital mortality. Conclusion: For patients with ACS, a weekend admission was associated with increased in-hospital mortality despite similar management approach in both groups. There is a need to further explore the factors that contribute to this "weekend effect" in our setting by a prospective trial.

Article title: PS 17-81 Prognostic Impact of Coronary Collaterals in Acute Coronary Syndrome (ACS): a meta-analysis (PICCACS STUDY)

Authors: John Daniel Ramos, Jaime Manalo Aherrera, Lowe Chiong, Mark Vicente, Felix Eduardo Punzalan

Publication title: Journal of Hypertension 34(supplement I), September 2016

Abstract: No abstract

Full text link: https://tinyurl.com/y8t5j94e

Article title: Prediction of Symptomatic Embolism in Filipinos With Infective Endocarditis Using the Embolic Risk French Calculator

Authors: Jaime Manalo Aherrera, Maria Teresa Bacnis Abola, Maria Margarita O. Balabagno, Lauro Lim Abrahan IV, Jose Donato A. Magno, Paul Ferdinand M. Reganit, Felix Eduardo R. Punzalan

Publication title: Cardiology Research 7(4), August 2016

Abstract:

Background Cardioembolic events are life-threatening complications of infective endocarditis (IE). The embolic risk French calculator estimates the embolic risk in IE computed on admission. Variables in this tool include age, diabetes, atrial fibrillation, prior embolism, vegetation length, and Staphylococcus aureus on culture. A computed risk of > 7% was considered high in the development of this tool. Knowledge of this risk applied in our local setting is important to guide clinicians in preventing such catastrophic complications. Among patients with IE, we aim to determine the efficacy of the embolic risk French calculator, using a computed score of > 7%, in predicting major embolic events. Methods All adults admitted from 2013 to 2016 with definite IE were included. The risk for embolic events was computed on admission. All were monitored for the duration of admission for the occurrence of the primary outcome (any major embolic event: arterial emboli, intracranial hemorrhage, pulmonary infarcts, or aneurysms). Secondary outcomes were: 1) composite of death and embolic events; and 2) death from any cause. Results Eighty-seven adults with definite IE were included. Majority had a valvular heart disease and preserved ejection fraction (EF). The mitral valve was most commonly involved. Embolic events occurred in 25 (29%). Multivariate analysis identified a high embolic score > 7% (relative risk (RR): 15.12, $P < 0.001$), vegetation area ≥ 18 mm^2 (RR: 6.39, $P < 0.01$), and a prior embolism (RR: 5.18, $P = 0.018$) to be independent predictors of embolic events. For the composite of embolic events and death, independent predictors include a high score of > 7% (RR: 13.56, $P < 0.001$) and a prior embolus (RR: 13.75, $P = 0.002$). Independent predictors of death were a high score > 7% (RR: 6.20, $P = 0.003$) and EF ≤ 45% (RR: 9.91, $P = 0.004$). Conclusion Cardioembolic events are more prevalent in our study compared to previous data. The embolic risk French calculator is a useful tool to estimate and predict risk for embolic events

and in-hospital mortality. The risk of developing embolic events should be weighed against the risks of early preventive cardiac surgery, as to institute timely and appropriate management.
Full text link: https://tinyurl.com/yccjraeq

Article title: The Triply Twisted Heart: Cyanosis in an Adult With Situs Inversus, Levocardia, Double Outlet Right Ventricle, and Malposition of the Great Arteries
Authors: Jaime Manalo Aherrera, Jose Donato A. Magno, Celia Catherine C. Uy, Lauro Lim Abrahan IV, Helga F. Sta. Maria, Rodel R. Buitizon, Danny Marcelo Hara
Publication title: Cardiology Research 6(6), August 2015

Abstract:
We present a case of a 19-year-old female presenting with cyanosis since birth. The major anomaly demonstrated was a "triply twisted heart" with a balanced physiology, allowing her to survive into adulthood. Non-invasive imaging was done using 2D and real-time 3D (or 4D) echocardiography with multi-slice imaging from 4D volume datasets. Findings were confirmed using cardiac magnetic resonance imaging (MRI). A segmental approach revealed atrial and visceral situs inversus, levocardia, atrioventricular discordance, and ventriculoarterial discordance. Both the aorta and pulmonary artery were malposed and arise from the right ventricle (double outlet right ventricle or DORV). There was also a complete atrioventricular septal defect (CAVSD) associated with a functional single atrium and a functional univentricle (single ventricle). Other findings include a severe pulmonic stenosis (PS), preserved right and left ventricular systolic function, and a normal pulmonary arterial pressure. She also had a persistent left superior vena cava (SVC) that drains into the morphologic right atrium, while the right-sided SVC drains into the morphologic left atrium. A multidisciplinary team deemed that management be palliative. She is on regular follow-up at our clinics for non-invasive monitoring. To our knowledge, this is the first reported case in an adult with this combination of anomalies.
Full text link: https://tinyurl.com/yborj7ma

Article title: APSC2015-1204 The Platelet-To-Lymphocyte Ratio (PLR) Is a Predictor of In-Hospital Mortality in Filipinos With Acute Coronary Syndrome: A Prospective Cohort

Authors: Lauro Lim Abrahan IV, Jaime Manalo Aherrera, John Daniel Ramos, Paul Ferdinand Reganit, Felix Eduardo Punzalan, Ramon Abarquez Jr.
Publication title: Global Heart 10(2), June 2015

Abstract: No abstract

Article title: APSC2015-1177 The Neutrophil-Lymphocyte Ratio Predicts Severity of Coronary Artery Disease Using the Syntax Score
Authors: Jaime Manalo Aherrea, Lowe Chiong, Christine Train, Marcelyn Fusilero, Paul Ferdinand Reganit, Feliz Eduardo Punzalan, Wilfredo Dee, John Anonuevo, Ramon Abarquez
Publication title: Global Heart 10(2) supplement June 2015

Abstract: No abstract

Article title: APSC2015-1178 Depression and Anxiety in Adult Filipinos With Congenital Heart Disease Using the Validated Filipino Version of the Hospital Anxiety and Depression Score (HADS)
Authors: Jaime Manalo Aherrera, Lauro Lim Abrahan IV, Geraldine Racaza, Christine Train, Danny Marcelo Jara
Publication title: Global Heart 10(2) June 2015

Abstract**:** No abstract

Article title: APSC2015-1176 Risk of Death and Adverse Outcomes in Adult Filipinos Admitted for Infective Endocarditis: A Prospective Cohort
Authors: Jaime Manalo Aherrera, Lauro Lim Abrahan IV, Maria Margarita Balabagno, Antonio Faldato, Paul Ferdinand Reganit, Felix Eduardo Punzalan
Publication title: Global Heart June 10 (2), June 2015

Abstract: No abstract

Article title: Cardiac tamponade as a rare manifestation of systemic lupus erythematosus: A report on four cases in the philippine general hospital

Authors: Jaime Manalo Aherrera, B.H.D. Manapat-Reyes, F.L. Lantion-Ang, Alexander Manguba, Evelyn Salido, F.E. Punzalan, Allan Corpuz, J.R. Magallanes

Publication Title: European Journal of Heart Failure 53(2), April 2015

Abstract:

Synopsis: Cardiac tamponade among systemic lupus erythematosus (SLE) patients is an unusual event. The pericardial effusion may be a consequence of uremia, infections in the pericardium, or the lupus pericarditis itself. We present four atypical cases of cardiac tamponade from pericarditis of connective tissue disease (CTD), all of which were treated with drainage and immunosuppressants. Due to the rarity of this combination, management was a challenge. Clinical Presentation: Four females each sought consult for dyspnea associated with typical manifestations of connective tissue disease such as arthritis, characteristic rashes, serositis, typical laboratory features, and a positive ANA and/or anti-dsDNA. The first three cases fulfilled the criteria for SLE, while the fourth fulfilled the criteria for SLE-dermatomyositis overlap syndrome. Echocardiography was done due to suspicion of pericardial involvement and revealed massive pericardial effusion in tamponade physiology in all cases. Diagnosis: Cardiac tamponade from serositis due to connective tissue disease [SLE (case 1 to 3) or SLE-dermatomyositis overlap (case 4). Other common etiologies of tamponade such as bacterial, tuberculous, malignant, and uremic pericardial effusion were ruled out by clinical and laboratory tools, including Gram stain and culture, cytology, PCR, and biochemical testing. The pericardial fluid of the first case tested positive for lupus erythematosus (LE) cells, indicative of lupus serositis. Treatment and Outcome: All patients underwent pericardial drainage via tube pericardiostomy. They received high dose glucocorticoids after infectious etiologies for the pericardial effusion were ruled out. The fourth case with the overlap syndrome, however, required more immunosuppressants using azathioprine and methotrexate. Resolution of pericardial effusion was noted with this approach. Three of four were discharged improved, however, the third case suffered from worsening nephritis and pulmonary hemorrhage leading to her demise. Significance and Recommendations: Four cases of cardiac tamponade as a manifestation of connective tissue disease were presented. Literature underlines the rarity of this condition anytime during the course of SLE. Despite this, SLE should be considered as one

of the differential diagnosis of cardiac tamponade, especially in patients who manifest with multi-systemic findings. Likewise, massive pericardial effusion should be considered in patients with a connective tissue disease presenting with subtle evidence of pericardial involvement. It requires timely identification and treatment with high dose steroids, after other causes such as infections have been excluded. Immediate drainage through pericardiocentesis or pericardiostomy in combination with immunosuppressants may be life-saving.
Full text link: https://tinyurl.com/yburbof5

Article title: Coarctation of the Aorta and a Parachute Mitral Valve in an Adult With Differential Cyanosis
Authors: Jaime Manalo Aherrera, Maria Teresa Bacnis Abola, Jose Donato A. Magno, Ma. Helga F. Sta. Maria, Lauro Lim Abrahan IV, Richard Henry Perlas Tiongco II, John C. Anonuevo
Publication title: Cardiology Research 6(1) February 2015

Abstract:
Differential cyanosis may occur in Eisenmenger physiology in the presence of a patent ductus arteriosus (PDA). We present a unique case of a 22-year-old male manifesting as cyanosis of the left upper extremity and both lower extremities, but with preservation of the right upper extremity. Work-up revealed multiple congenital defects, reminiscent of the Shone's complex. Survival into adulthood is presumed to be due to a PDA, at the expense of a right-to-left shunt. This report highlights the interplay of multiple anomalies documented on echocardiography and MRI, wherein diagnosis was made non-invasively.
Full text link: https://tinyurl.com/yal67pvk

Article title: GW25-e0613 Clinical profile and predictors of outcomes of patients with mitral stenosis undergoing percutaneous transseptal mitral commissurotomy
Authors: Edgar Timbol, Jaime Manalo Aherrera, Gino Rei Quizon, Wilfredo Dee,
Publication title: Journal of the American College of Cardiology 64(16) October 2014

Abstract: No abstract
Full text link: https://tinyurl.com/y7lxdpnv

Article title: GW25-e0537 Association of the neutrophil–lymphocyte ratio (NLR) with outcomes in patients admitted for an acute coronary syndrome
Authors: Jaime Manalo Aherrera, Lowe Chiong, Paul Ferdinand Reganit, Felix Eduardo Punzalan
Publication title: Journal of the American College of Cardiology 64(16) October 2014

Abstract: No abstract

Article title: "The heart is blind" endogenous endophthalmitis secondary to endocarditis in a patient with systemic lupus erythematosus
Authors: Jaime Manalo Aherrera, J. E. Duya, A. Fausto, J.R. Magallanes
Publication title: European Journal of Heart Failure 16, April 2014

Abstract: No abstract

Article title: PW054 Acquired Arteriovenous Fistula of the Right Common Iliac Artery and Left Common Iliac Vein and Bilateral Lower Extremity Deep Venous Thrombosis in a Woman Presenting as High Output Failure
Authors: Jaime Manalo Aherrera, Edgar Wilson Timbol, Antonio Faltado, Agnes D. Mejia, Mark Vicente
Publication title: Global Heart 9(1) March 2014

Abstract: No abstract

Article title: A Comparison of 12 Lead Electrocardiogram and 2d-Echocardiography Derived Ejection Fraction among Patients with Depressed Ejection Fraction
Authors: Jaime Manalo Aherrera, Paul Ferdinand Reganit, Feliz Eduardo Punzalan, Danny Marcelo Jara, Ramon F. Abarquez
Publication title: Journal of Atherosclerosis and Thrombosis V.21 January 2014

Abstract: No abstract

Article title: "Double Trouble" Wolff Parkinson White Syndrome and Mitral Stenosis Presenting as a Stroke in the Young
Authors: Jaime Manalo Aherrera, Anastasio Manuel Degayo, Lauro Lim Abrahan IV, Michael Joseph Agbayani, Michael Joseph Reyes, Wilfredo Dee
Publication title: Journal of Atherosclerosis and Thrombosis V.21 January 2014

Abstract: No abstract

Article title: When Stemi Is Not Stemi HIV Myocarditis Mimicking St-Elevation Myocardial Infarction on Electrocardiogram: A Case Report
Authors: Jaime Manalo Aherrera, Deonne Thaddeus Vite Gauiran, Agnes D. Mejia
Publication title: Journal of Atherosclerosis and Thrombosis V.21 January 2014

Abstract: No abstract

Article title: Pulmonic Valve Endocarditis with an underlying ventricular septal defect: a report on three cases at the Philippine General Hospital
Authors: Jaime Manalo Aherrera, Michael Joseph T. Reyes, Geraldine O. Floro, Edgar Timbol, Jan Melvin Zapanta, Lauren R. Blanquisco, Kristine D. Tumabiene, Felix Eduardo Punzalan
Publication title: Annual International Conference on Cardiology and Cardiovascular Medicine Research, December 2013

Abstract: No abstract

Article title: An unparsimonious quandary: Mitral stenosis and ventricular septal defect complicating systemic lupus erythematosus and pregnancy
Authors: J.D.A. Magno, M. Barguero, P.I. Pagauitan-Alan, Jaime Manalo Aherrera, F. Eduardo Punzalan

Abstract:
Multiple cardiac defects can significantly affect the course of pregnancy, tilting the hemodynamic balance against the mother and complicating her overall clinical condition. A

29-year-old female presented with heart failure symptoms into her third trimester of pregnancy. After a thorough work up, she was diagnosed with ventricular septal defect (VSD) with eisenmengerization, mitral stenosis (MS), and systemic lupus erythematosus (SLE). After delivery, she developed cyanosis. Management was a challenge, but she was eventually sent home on a calcium blocker, a diuretic and a beta-blocker. The service recommended hemodynamic studies, discussion of management options, antiphospholipid antibody syndrome work-up and advised the patient regarding avoidance of dehydration, high-altitude travels, and avoidance of vasodilators.

Article title: Routine angioplasty after fibrinolytic therapy for ST-segment elevation myocardial infarction: An updated meta-analysis (RAFT-STEMI)

Author: J.D.A. Magno, J.D. Alcover, A.D.C Javier, Jaime Manalo Aherrera, F.E.R. Punzalan, W.G. Dee

Abstract:

Context: The usefulness of a routine invasive strategy has still not yet been fully established among patients with ST-segment elevation myocardial infarction (STEMI) initially treated with fibrinolytic therapy, despite results of previous meta-analyses. Methods: We included newer and larger randomized trials to determine whether routine percutaneous coronary intervention (PCI) after fibrinolysis in STEMI patients was more beneficial than ischemia-guided PCI management in reducing all-cause mortality and reinfarction rates while being safe in terms of occurrence of stroke and major in-hospital bleeding. Using the keywords angioplasty, stent, percutaneous coronary intervention, fibrinolysis, thrombolysis, and myocardial infarction, seven PCI trials were identified, enrolling 2,560 STEMI patients followed up from 30 days to 1 year. Results: A routine invasive strategy did not lead to any significant reduction in mortality (relative risk [RR] 0.79, 95% CI 0.56-1.11; P = 0.18) but showed a significant reduction in reinfarction rates (RR 0.55, 95% CI 0.40-0.77; P = 0.0004) compared with ischemia-guided management. Meanwhile, there were no significant differences in the risk of stroke (RR 0.96, 95% CI 0.40-2.30; P = 0.92) or major bleeding (RR 0.98, 95% CI 0.70-1.36; P = 0.89). Conclusion: Routine PCI after fibrinolytic therapy for STEMI patients is not associated with any significant reduction in mortality but may be considered for its benefit in reducing reinfarction rates, without increasing rates of stroke or major bleeding. These results suggest that an ischemia

guided strategy is still relevant in the management of STEMI patients, especially in situations where catheterization technology is not readily accessible.

Article title: Clinical and Echocardiographic Profile and Outcomes of Peripartum Cardiomyopathy: The Philippine General Hospital Experience
Authors: Vim I. Samonte, Queenie G. Ngalob, Ghea Divina B. Mata, Jaime Manalo Aherrera, Eugenio P. Reyes, Felix Eduardo R. Punzalan
Publication title: Heart Asia 5(1) 245-249, January 2013

Abstract:
Background Peripartum cardiomyopathy (PPCM) is a rare disease entity of unknown aetiology. High rates of mortality or poor overall clinical outcome are reported in women with this condition. Certain characteristics are risk factors for this disease. In Asia, there are limited data, especially in the Southeast Asian region. In the Philippines, no data exist regarding the prevalence or risk factors. Objectives To determine the prevalence, profile and outcomes of PPCM in Philippine General Hospital and to describe their echocardiographic findings. Methods All patients diagnosed with PPCM in the period of 1 January 2009–31 December 2010 were seen and examined. Demographic data and echocardiogram of the patients were reviewed. Results 9 were diagnosed with PPCM during the study period. The prevalence is 1 in 1270 live births. Mean age was 29. 78% presented with moderate to severe heart failure symptoms in the prepartum period. Among purported risk factors for PPCM, obesity, multiparity and pre-eclampsia were seen in most. Conversely, only one patient admitted to having more than a single sexual partner. Only one patient had multifetal pregnancy. None were smokers. 44% underwent caesarean section for maternal indication. No mortality was seen. Fetal outcomes were good with all resulting in live births and most were appropriate for gestational age. Echocardiographic findings showed global wall motion abnormalities in the majority, mean ejection fraction of 34% and mean fractional shortening of 20%. Conclusions PPCM is rare in the Philippines. Compared with international data, our patients are younger with low percentages of promiscuity, multifetal pregnancy, smoking history and tocolytic use. Similar to previous studies, obesity, multiparity and pre-eclampsia were also present in our PPCM patients. Immediate maternal and fetal outcomes were generally good. Adherence to standard heart failure management is high.

Full text link: https://tinyurl.com/yd2jssjb

Article title: Febuxostat versus allopurinol for hyperuricemia and gout: a meta-analysis (Fame study)

Authors:T.E.N. Lo, Jaime Manalo Aherrera, A.Q. Taguba, Ester Gonzales Penserga

Publication title: Annals of the Rheumatic Diseases 70(3) January 2011

Abstract: No Abstract

REMIL LINGGATONG GALAY
University of Philippines Diliman

Sex: Male

Education: Yamaguchi University, Doctor of Philosophy in Veterinary Sciences, April 2011 - March 2015

Field of Specialization:

Zoology
Entomology
Parasitology

Researches:

Article title: Development of a Loop-Mediated Isothermal Amplification (LAMP) Assay Targeting the Citrate Synthase Gene for Detection of Ehrlichia canis in Dogs
Authors: Remil Linggatong Galay, Tetsuya Tanaka
Publication Title: Veterinary Sciences 7(156), October 2020

Abstract:
Canine monocytic ehrlichiosis caused by Ehrlichia canis is one of the leading tick-borne diseases of dogs, particularly in tropical countries. A highly sensitive and specific diagnostic method is essential for early detection to facilitate treatment. This study was conducted to develop E. canis loop-mediated isothermal amplification (LAMP) assay, a highly sensitive yet simple molecular

technique, targeting the citrate synthase (gltA) gene of E. canis. Canine blood samples were subjected to conventional PCR targeting E. canis gltA. After analysis of the sequences of PCR amplicons, LAMP primers were generated. The optimum temperature and time for the LAMP assay were determined using eight samples-after which, the effectiveness and reproducibility of LAMP were verified by testing 40 samples, which included PCR-positive and negative samples. The detection limit was also established. The optimal condition for the assay was 61 • C for 60 min. Compared to PCR, the LAMP assay had a relative sensitivity and specificity of 92.5 and 100%, respectively. Statistical analysis using McNemar's test showed that the E. canis LAMP assay has no significant difference with PCR. Therefore, the LAMP assay developed in this study may be used as an alternative to PCR in the detection of E. canis.
Full text link: https://tinyurl.com/ycvuof26

Article title: Molecular Detection of Rickettsia Spp. and Coxiella Burnetii in Cattle, Water Buffalo, and Rhipicephalus (Boophilus) Microplus Ticks in Luzon Island of the Philippines
Authors: Remil Linggatong Galay, Melbourne R. Talactac, Bea V. Ambita- Salem, Maureen M. Dawn, Chu, Marie O. Lali, Dela Costa, Mae A. Cinnamon, Salangsang, Darwin Kyle, B. Caracas, Florante H. Generoso, Jonathan A. Babelonia, Joenil Vergano, Lena C. Berana, Kristina Andrea C. Sandalo, Billy P. Divina, Cherry Alvarez, Emmanuel R. Mago, Masako Andoh, Tetsuya Tanaka
Publication title: Tropical Medicine of Infectious Diseases 5(2):54, April 2020

Abstract:
Rickettsia and Coxiella burnetii are zoonotic, tick-borne pathogens that can cause febrile illnesses with or without other symptoms in humans, but may cause subclinical infections in animals. There are only a few reports on the occurrence of these pathogens in cattle and water buffalo in Southeast Asia, including the Philippines. In this study, molecular detection of Rickettsia and C. burnetii in the blood and in the Rhipicephalus (Boophilus) microplus ticks of cattle and water buffalo from five provinces in Luzon Island of the Philippines was done. A total of 620 blood samples of cattle and water buffalo and 206 tick samples were collected and subjected to DNA extraction. After successful amplification of control genes, nested PCR was performed to detect gltA of Rickettsia and com1 of C. burnetii. No samples were positive for Rickettsia, while 10 (cattle = 7, water buffaloes = 3), or 1.6% of blood, and five, or 1.8% of tick

samples, were C. burnetii-positive. Sequence analysis of the positive amplicons showed 99-100% similarity to reported C. burnetii isolates. This molecular evidence on the occurrence of C. burnetii in Philippine ruminants and cattle ticks and its zoonotic nature should prompt further investigation and surveillance to facilitate its effective control.

Full text link: https://tinyurl.com/y8p3zyje

Article title: Molecular detection of Anaplasma spp. in blood and milk of dairy cattle in the Philippines

Authors: Remil Linggatong Galay, Kristina Andrea C. Sandalo, Flor Marie Immanuel Rafallo Pilapil-Amante, Tetsuya Tanaka

Publication title: Turkish Journal of Veterinary and Animal Sciences 43(4), July 2019

Abstract:

Anaplasmosis has become a major concern in the cattle industry throughout the world due to its great economic impact. The causative agents, Anaplasma species, are primarily transmitted by ticks, occurring intracellularly within blood cells, with some species being zoonotic. In this study, the presence of Anaplasma spp. was investigated in the blood and milk of dairy cattle in the Philippines. Blood and milk samples were collected from 98 dairy cattle from selected farms in five provinces in the southern part of Luzon Island in the Philippines. After DNA extraction, a conventional PCR for the control gene actin was performed, followed by nested PCR for Anaplasma spp. Selected amplicons were purified and subjected to sequence analysis. It was found that 97 (98.97%) blood samples and 6 (6.12%) milk samples were positive for Anaplasma. Sequence analysis revealed that the positive amplicons from milk samples and their corresponding blood samples shared a high identity (98%–100%) with reported Anaplasma marginale isolates. To the authors' knowledge, this study provides the first molecular evidence of the presence of A. marginale in milk from dairy cattle under field conditions in the Philippines.

Full text link: https://tinyurl.com/y98pd7dd

Article title: Molecular detection of tick-borne pathogens in canine population and Rhipicephalus sanguineus (sensu lato) ticks from southern Metro Manila and Laguna, Philippines

Authors: Remil Linggatong Galay, Anna Angelica L. Manalo, Sidney Lindon Daquioag Dolores, Irene Pearl M. Aguilar, Kristina Andrea C. Sandalo, Kathlyn Cruz, Billy P. Divina, Masako Andoh, Tatsunori Masatani, Tetsuya Tanaka

Publication title: Parasites & Vectors 11(1), December 2018

Abstract:

Background The tropical climate of the Philippines and the high population of dogs, particularly in cities, favors the life-cycle of the brown dog tick, Rhipicephalus sanguineus (sensu lato), a vector of several canine tick-borne pathogens (TBPs) including zoonotic Rickettsia spp. Suspected cases of infections are commonly encountered in veterinary clinics, but the specific TBPs are rarely identified. Furthermore, infection with Rickettsia is not being clinically examined in dogs. In this study, the occurrence of TBPs in blood and ticks collected from household and impounded dogs in highly populated areas of the Philippines, Metro Manila, and the nearby province of Laguna, was examined. Results A total of 248 blood samples and 157 tick samples were subjected to PCR. First, samples were screened using primers for Anaplasma/Ehrlichia spp. and Babesia/Hepatozoon spp. Those that turned positive were further subjected to species-specific PCR. Rickettsia spp. were also detected through a nested PCR. Of the 248 blood samples, 56 (22.6%) were positive for Anaplasma/Ehrlichia spp., while 19 (7.6%) were positive for Babesia/Hepatozoon spp. Species-specific PCR revealed that 61 (23.4%) had a single TBP, with Ehrlichia canis being detected in 39 (15.7%) dogs, while 14 (5.6%) dogs were positive for different combinations of two to four TBPs. Rickettsia infection was detected in 6 (2.4%) dogs. In tick samples, 8 (3.2%) were positive for Ehrlichia/Anaplasma spp., while only 1 (0.63%) was positive for Babesia/Hepatozoon spp. As in the blood samples, E. canis was the most detected, being found in 5 (2%) samples. No tick samples tested positive for Rickettsia spp. Conclusion Ehrlichia canis is the most common TBP affecting dogs in the Philippines. Co-infection with TBPs is quite common, hence testing for multiple TBPs is necessary. Through nested PCR, Rickettsia infection was detected in dogs, and to the authors' knowledge, this study provides the first molecular evidence of Rickettsia infection in dogs in the Philippines.

Article title: Induction of intracellular ferritin expression in embryo-derived Ixodes scapularis cell line (ISE6)

Authors: Emmanuel Hernandez, Kudai Kusakisako, Melbourne R. Talactac, Remil Linggatong Galay, Kentaro Yoshii, Tetsuya Tanaka
Publication title: Scientific Reports 8(1) November 2018

Abstract:
Iron is a very important nutrient for cells; however, it could also cause fatal effects because of its capability to trigger oxidative stress. Due to high exposure to iron from their blood diet, ticks make use of several mechanisms to cope up with oxidative stress. One mechanism is iron sequestration by ferritin and its control protein (IRP). Since the IRP activity is dependent on the ferrous iron concentration, we tried to induce intracellular ferritin (FER1) protein expression by exposing Ixodes scapularis embryo-derived cell line (ISE6) to different concentrations of ferrous sulphate at different time points. We were able to induce FER1 protein after exposure to 2 mM of ferrous sulphate for 48 h, as observed in both Western blotting and indirect immunofluorescent antibody tests. This could indicate that the FER1 produced could be a product of the release of IRPs from the FER1 mRNA leading to its translation. The RNA interference of FER1, through the transfection of dsRNA, led to an increase in mortality and decrease in the cellular proliferation of ISE6 cells. Overall, ISE6 cells could be a good tool in further understanding the mechanism of FER1 action, not just in Ixodes ticks but in other tick species as well.
Full text link: https://tinyurl.com/yajqvaf9

Article title: Glutathione S-transferases play a role in the detoxification of flumethrin and chlorpyrifos in Haemaphysalis longicornis
Authors: Emmanuel Hernandez, Kudai Kusakisako, Melbourne R. Talactac, Remil Linggatong Galay, Takeshi Hatta, Kozo Fujisaki, Naotoshi Tsuji, Tetsuya Tanaka
Publication title: Parasites & Vectors 11(1) August 2018

Abstract:
Background: Haemaphysalis longicornis is a tick of importance to health, as it serves as a vector of several pathogens, including Theileria orientalis, Babesia ovata, Rickettsia japonica and the severe fever with thrombocytopenia syndrome virus (SFTSV). Presently, the major method of control for this tick is the use of chemical acaricides. The glutathione S-transferase (GST) system

is one mechanism through which the tick metabolizes these acaricides. Two GSTs from H. longicornis (HlGST and HlGST2) have been previously identified. Results: Enzyme kinetic studies were performed to determine the interaction of acaricides with recombinant H. longicornis GSTs. Recombinant HlGST activity was inhibited by flumethrin and cypermethrin, while recombinant HlGST2 activity was inhibited by chlorpyrifos and cypermethrin. Using real-time RT-PCR, the upregulation of the HlGST gene was observed upon exposure to sublethal doses of flumethrin, while the HlGST2 gene was upregulated when exposed to sublethal doses of chlorpyrifos. Sex and strain dependencies in the induction of GST gene expression by flumethrin were also observed. Knockdown of the HlGST gene resulted in the increased susceptibility of larvae and adult male ticks to sublethal doses of flumethrin and the susceptibility of larvae against sublethal doses of chlorpyrifos was increased upon knockdown of HlGST2. Conclusions: HlGST could be vital for the metabolism of flumethrin in larvae and adult male ticks, while HlGST2 is important in the detoxification of chlorpyrifos in larval ticks.
Full text available: https://tinyurl.com/y753toe6

Article title: Hemolymph defensin from the hard tick Haemaphysalis longicornis attacks Gram-positive bacteria
Authors: Yurika Yada, Emmanuel Hernandez, Kudai Kusakisako, Melbourne R. Talactac, Remil Linggatong Galay, Masako Andoh, Kozo Fujisaki, Tetsuya Tanaka
Publication title: Journal of Invertebrate Pathology 156, July 2018

Abstract:
Ticks are key vectors of some important diseases of humans and animals. Although they are carriers of disease agents, the viability and development of ticks are not harmed by the infectious agents due to their innate immunity. Antimicrobial peptides directly protect hosts against pathogenic agents such as viruses, bacteria, and parasites. Among the identified and characterized antimicrobial peptides, defensins have been considerably well studied. Defensins are commonly found among fungi, plants, invertebrates, and vertebrates. The sequence of the tick hemolymph defensin (HEdefensin) gene from the hard tick Haemaphysalis longicornis was analyzed after identification and cloning from a cDNA library. HEdefensin has a predicted molecular mass of 8.15 kDa including signal peptides and a theoretical isoelectric point of 9.48. Six cysteine residues were also identified in the amino acids. The synthetic HEdefensin peptide

only showed antibacterial activity against Gram-positive bacteria such as Micrococcus luteus. A fluorescence propidium iodide exclusion assay also showed that HEdefensin increased the membrane permeability of M. luteus. Additionally, an indirect fluorescent antibody test showed that HEdefensin binds to M. luteus. These results suggested that HEdefensin strongly affects the innate immunity of ticks against Gram-positive bacteria.
Full text link: https://tinyurl.com/y7yghmm3

Article title: Vector competence of Haemaphysalis longicornis ticks for a Japanese isolate of the Thogoto virus
Authors: Melbourne R. Talactac, Kentaro Yoshii, Emmanuel Hernandez, Kudai Kusakisako, Remil Linggatong Galay, Kozo Fujisaki, Masami Mochizuki, Tetsuya Tanaka
Publication title: Scientific Reports 8(1), June 2018

Abstract:
Thogoto virus (THOV), a tick-borne arbovirus not previously reported in East Asia, was recently isolated from Haemaphysalis longicornis in Kyoto, Japan. In this study, we investigated the vector competence of H. longicornis ticks for a Japanese isolate of the Thogoto virus using anal pore microinjection and experimental virus acquisition. Our results showed that anal pore microinjection can readily infect adult ticks, and THOV-infected ticks can successfully transmit the virus to mice. Blood feeding was also critical in the distribution of the virus in tick organs, most especially in the salivary glands. Furthermore, co-feeding between an infected adult and naïve nymphs can also produce infected molted adults that can horizontally transmit THOV to mice. Altogether, our results suggest that H. longicornis is a competent vector for the Japanese THOV isolate and could be the primary tick vector of the virus in Japan.
Full text link: https://tinyurl.com/y8s9ne33

Article title: Characterization and expression analysis of a newly identified glutathione S-transferase of the hard tick Haemaphysalis longicornis during blood-feeding
Authors: Emmanuel Hernandez, Kudai Kusakisako, Melbourne R. Talactac, Remil Linggatong Galay, Takeshi Hatta, Tomohide Matsuo, Kozo Fujisaki, Naotoshi Tsuji, Tetsuya Tanaka
Publication title: Parasites & Vectors 11(1), February 2018

Abstract:

Background: Ticks are obligate hematophagous parasites important economically and to health. Ticks consume large amounts of blood for their survival and reproduction; however, large amounts of iron in blood could lead to oxidative stress. Ticks use several molecules such as glutathione S-transferases (GSTs), ferritins, and peroxiredoxins to cope with oxidative stress. This study aimed to identify and characterize the GSTs of the hard tick Haemaphysalis longicornis in order to determine if they have a role in coping with oxidative stress. Methods: Genes encoding GSTs of H. longicornis were isolated from the midgut CDNA library. Genes have been cloned and recombinant GSTs have been expressed. The enzymatic activities, enzyme kinetic constants, and optimal pH of the recombinant GSTs toward 1-chloro-2,4-dinitrobenzene (CDNB) were determined. The gene transcription and protein expression profiles were determined in the whole ticks and internal organs, and developmental stages using real time RT-PCR and Western blotting during blood feeding. The localization of GST proteins in organs was also observed using immunofluorescent antibody test (IFAT). Results: We have isolated two genes encoding GSTs (HlGST and HlGST2). The enzymatic activity toward CDNB is 9.75 ± 3.04 units/mg protein for recombinant HlGST and 11.63 ± 4.08 units/mg protein for recombinant HlGST2. Kinetic analysis of recombinant HlGST showed K m values of 0.82 ± 0.14 mM and 0.64 ± 0.32 mM for the function of CDNB and GSH, respectively. Meanwhile, recombinant HlGST2 has K m values of 0.61 ± 0.20 mM and 0.53 ± 0.02 mM for the function of CDNB and GSH, respectively. The optimum pH of recombinant HlGST and recombinant HlGST2 activity was 7.5-8.0. Transcription of both GSTs increases in different developmental stages and organs during blood-feeding. GST proteins are upregulated during blood-feeding but decreased upon engorgement in whole ticks and in some organs, such as the midgut and hemocytes. Interestingly, salivary glands, ovaries, and fat bodies showed decreasing protein expression during blood-feeding to engorgement. Varying localization of GSTs in the midgut, salivary glands, fat bodies, ovaries, and hemocytes was observed depending on the feeding state, especially in the midgut and salivary glands. Conclusions: In summary, a novel GST of H. longicornis has been identified. Characterization of the GSTs showed that GSTs have positive correlation with the degree and localization of oxidative stress during blood-feeding. This could indicate their protective role during oxidative stress.

Full text link: https://tinyurl.com/yc2n8hrv

Article title: Evaluation of vaccine potential of 2-Cys peroxiredoxin from the hard tick Haemaphysalis longicornis

Authors: Kodai Kusakisako, Takeshi Miyata, Masashi Tsujio, Remil Linggatong Galay, Melbourne R. Talactac, Emmanuel Hernandez, Kozo Fujisaki, Tetsuya Tanaka

Publication title: Experimental and Applied Acarology, 74(1), January 2018

Abstract:

Ticks require blood feeding on vertebrate animals throughout their life cycle, and also concentrate the iron-containing blood, resulting in a high concentration of hydrogen peroxide (H2O2). High concentrations of H2O2 are harmful to organisms, due to their serious damage of macromolecules. Ticks have antioxidant enzymes, such as peroxiredoxins (Prxs), that scavenge H2O2. Prxs may have important roles in regulating the H2O2 concentration in ticks during blood feeding and oviposition. Moreover, Prxs are considered potential vaccine candidates in other parasites, such as Leishmania and Fasciola. In the present study, the efficacy of a tick Prx (HlPrx2) as a vaccine candidate antigen was evaluated. First, recombinant HlPrx2 (rHlPrx2) was expressed in Escherichia coli, and then, its purity and endotoxin levels were confirmed prior to administration. The rHlPrx2 proteins were of high purity with acceptably low endotoxin levels. Second, the ability of rHlPrx2 administration to stimulate mouse immunity was evaluated. The rHlPrx2 protein, with or without an adjuvant, could stimulate immunity in mice, especially the IgG1 of Th2 immune response. Using Western blot analysis, we also observed whether rHlPrx2-immunized mice sera could recognize native HlPrx2 protein in crude tick midgut proteins. Western blot analysis demonstrated that rHlPrx2-administrated mouse sera could detect the native HlPrx2. Finally, the effects of rHlPrx2 immunization in mice were studied using nymphal ticks. Although the challenged ticks were not affected by rHlPrx2 immunization, rHlPrx2 still might be considered as a vaccine candidate against ticks because of its high immunogenicity.

Full text link: https://tinyurl.com/y9qgbdgt

Article title: Immunofluorescent detection in the ovary of host antibodies against a secretory ferritin injected into female Haemaphysalis longicornis ticks

Authors: Remil Linggatong Galay, Tomohide Matsuo, Emmanuel Hernandez, Melbourne R. Talactac, Kudai Kusakisako, Rika Omemiya-Shirafuji, Masami Mochizuki, Kozo Fujisaki, Tetsuya Tanaka
Publication title: Parasitology International 67(2), October 2017

Abstract:

Due to the continuous threat of ticks and tick-borne diseases to human and animal health worldwide, and the drawbacks of chemical acaricide application, many researchers are exploring vaccination as an alternative tick control method. Earlier studies have shown that host antibodies can circulate in the ticks, but it has not been confirmed whether these antibodies can be passed on to the eggs. We previously reported that ticks infesting rabbits immunized with a recombinant secretory ferritin of Haemaphysalis longicornis (HlFER2) had reduced egg production and hatching. Here we attempted to detect the presence of antibodies against HlFER2 in the ovary and eggs of female ticks through immunofluorescent visualization. Purified anti-HlFER2 antibodies or rabbit IgG for control was directly injected to engorged female H. longicornis. Ovaries and eggs after oviposition were collected and prepared for an indirect immunofluorescent antibody test. Positive fluorescence was detected in ovaries one day post-injection of anti-HlFER2 antibodies. Through silencing of Hlfer2 gene, we also determined whether the injected antibodies can specifically bind to native HlFER2. Immunofluorescence was observed in the oocytes of dsLuciferase control ticks injected with anti-HlFER2 antibodies, but not in the oocytes of Hlfer2-silenced ticks also injected with anti-HlFER2 antibodies. Our current findings suggest that host antibodies can be passed on to the oocytes, which is significant in formulating a vaccine that can disrupt tick reproduction.

Article title: Synchronous Langat Virus Infection of Haemaphysalis longicornis Using Anal Pore Microinjection
Authors: Melbourne R. Talactac, Kentaro Yoshii, Emmanuel Hernandez, Kodai Kusakisako, Remil Lingggatong Galay, Kozo Fujisaki, Masami Mochizuki, Tetsuya Tanaka
Publication title: Viruses 9(7): 189, July 2017

Abstract:

The tick-borne encephalitis virus (TBEV) serocomplex of flaviviruses consists of arboviruses that cause important diseases in animals and humans. The transmission of this group of viruses is commonly associated with tick species such as Ixodes spp., Dermacentor spp., and Hyalomma spp. In the case of Haemaphysalis longicornis, the detection and isolation of flaviviruses have been previously reported. However, studies showing survival dynamics of any tick-borne flavivirus in H. longicornis are still lacking. In this study, an anal pore microinjection method was used to infect adult H. longicornis with Langat virus (LGTV), a naturally attenuated member of the TBEV serocomplex. LGTV detection in ticks was done by real-time PCR, virus isolation, and indirect immunofluorescent antibody test. The maximum viral titer was recorded at 28 days post-inoculation, and midgut cells were shown to be the primary replication site. The tick can also harbor the virus for at least 120 days and can successfully transmit LGTV to susceptible mice as confirmed by detection of LGTV antibodies. However, no transovarial transmission was observed from the egg and larval samples. Taken together, our results highly suggest that anal pore microinjection can be an effective method in infecting adult H. longicornis, which can greatly assist in our efforts to study tick and virus interactions.

Full text link: https://tinyurl.com/y97efeaj

Article title: Ticks' antioxidant complex: A defense stronghold and a potential target for their control

Authors: Remil Linggatong Galay, Emmanuel Hernandez, Kodai Kusakisako, Melbourne R. Talactac, K. Fujisaki, Tetsuya Tanaka

Abstract:

The parasitic blood-sucking lifestyle of ticks makes them efficient transmitters of various diseases in humans and animals worldwide. All developmental stages of ticks exclusively feed on blood, and female hard ticks in particular can ingest large volume of blood relative to their unfed size. Their nutritional dependence for blood is extraordinary because it is potentially toxic, with blood containing high iron and pro-oxidant content. Iron and pro-oxidants may react and produce reactive oxygen species that in high levels may cause oxidative stress. To counteract the negative effects that may result from consumption of blood, ticks are armed with

a complex antioxidant system. Several components of their antioxidant defense have been already identified and characterized using various molecular biological techniques. These antioxidant molecules were found to have significant roles in various physiological processes such as blood feeding and reproduction. Others were found to be involved in detoxification mechanisms against environmental toxins including chemical acaricides. A few studies also demonstrated the significant role of tick antioxidant molecules in microbial population and pathogen transmission. This chapter will review our current understanding of tick antioxidant defense with emphasis on its potential as a target for tick and tick-borne pathogen control.
Full text link: https://tinyurl.com/y9ogmumt

Article title: Characterization and antiviral activity of a newly identified defensin-like peptide, HEdefensin, in the hard tick Haemaphysalis longicornis
Authors: Melbourne R. Talactac, Yurika Yada, Kentaro Yoshii, Emmanuel Hernandez, Kodai Kusakisako, Maeda Hiroki, Remil Linggatong Galay, Kozo Fujisaki, Masami Mochizuki, Tetsuya Tanaka
Publication title: Developmental and comparative immunology v68, November 2016

Abstract:
Tick defensins are antimicrobial peptides that play a major role in the innate immunity of ticks by providing a direct antimicrobial defense. In this study, we identified and characterized a defensin-like encoding gene, HEdefensin, from the expressed sequence tags (EST) database of hemolymph from the hard tick Haemaphysalis longicornis. Expression of the gene in whole adult ticks and in different organs was upregulated during blood feeding, though not after Langat virus (LGTV) challenge. A synthetic HEdefensin peptide demonstrated significant virucidal activity against LGTV but not against an adenovirus in co-incubation virucidal assays. Moreover, the RNAi-mediated gene silencing of HEdefensin did not significantly affect the virus titer as compared to the control group. The data reported here have established the in vitro virucidal activity of the peptide against LGTV. However, its role in the innate antiviral immunity of H. longicornis remains to be explored, and further studies are needed to fully evaluate the potential biological activities of the peptide against bacteria, fungi or parasites.

Article title: 2-Cys peroxiredoxin is required in successful blood-feeding, reproduction, and antioxidant response in the hard tick Haemaphysalis longicornis

Authors: Kodai Kusakisako, Remil Linggatong Galay, Rika Umemiya-Shirafuji, Emmanuel Hernandez, Hiroki Maeda, Melbourne R. Talactac, Naotoshi Tsuji, Masami Mochizuki, Kozo Fujisaki, Tetsuka Tanaka

Publication title: Parasites & Vectors 9(1): 457, August 2016

Abstract:

Background Ticks are obligate hematophagous arthropods that feed on vertebrate blood that contains iron. Ticks also concentrate host blood with iron; this concentration of the blood leads to high levels of iron in ticks. The host-derived iron reacts with oxygen in the tick body and this may generate high levels of reactive oxygen species, including hydrogen peroxide (H2O2). High levels of H2O2 cause oxidative stress in organisms and therefore, antioxidant responses are necessary to regulate H2O2. Here, we focused on peroxiredoxin (Prx), an H2O2-scavenging enzyme in the hard tick Haemaphysalis longicornis. Methods The mRNA and protein expression profiles of 2-Cys peroxiredoxin (HlPrx2) in H. longicornis were investigated in whole ticks and internal organs, and developmental stages, using real-time PCR and Western blot analysis during blood-feeding. The localization of HlPrx2 proteins in tick tissues was also observed by immunostaining. Moreover, knockdown experiments of HlPrx2 were performed using RNA interference to evaluate its function in ticks. ResultsReal-time PCR showed that HlPrx2 gene expression in whole ticks and internal organs was significantly upregulated by blood-feeding. However, protein expression, except in the midgut, was constant throughout blood-feeding. Knockdown of the HlPrx2 gene caused significant differences in the engorged body weight, egg weight and hatching rate for larvae as compared to the control group. Finally, detection of H2O2 after knockdown of HlPrxs in ticks showed that the concentration of H2O2 significantly increased before and after blood-feeding. Conclusion Therefore, HlPrx2 can be considered important for successful blood-feeding and reproduction through the regulation of H2O2 concentrations in ticks before and after blood-feeding. This study contributes to the search for a candidate target for tick control and further understanding of the tick's oxidative stress coping mechanism during blood-feeding.

Full text link: https://tinyurl.com/y7yvxr3j

Article title: Host Immunization with Recombinant Proteins to Screen Antigens for Tick Control
Authors: Remil Linggatong Galay, Takeshi Miyata, Rika Umemiya-Shirafuji, Masami Mochizuki, Kozo Fujisaki, Tetsuya Tanaka
Publication title: Methods in microbiology 1404: 261-273, April 2016

Abstract:
Ticks (Parasitiformes: Ixodida) are known for their obligate blood feeding habit and their role in transmitting pathogens to various vertebrate hosts. Tick control using chemical acaricides is extensively used particularly in livestock management, but several disadvantages arise from resistance development of many tick species, and concerns on animal product and environmental contamination. Vaccination offers better protection and more cost-effective alternative to application of chemical acaricides, addressing their disadvantages. However, an ideal anti-tick vaccine targeting multiple tick species and all the tick stages is still wanting. Here, we describe the procedures involved in the evaluation of a vaccine candidate antigen against ticks at the laboratory level, from the preparation of recombinant proteins, administration to the rabbit host and monitoring of antibody titer, to tick infestation challenge and determination of the effects of immunization to ticks.

Article title: RNA Interference — A Powerful Functional Analysis Tool for Studying Tick Biology and its Control
Authors: Remil Linggatong Galay, Rika Umemiya-Shirafuji, Masami Mochizuki, Kozo Fujisaki, Tetsuya Tanaka
Publication title: RNA Interference

Abstract:
Ticks (Acari: Ixodida) are blood-sucking arthropods globally recognized as vectors of numerous diseases. They are primarily responsible for the transmission of various pathogens, including viruses, rickettsiae, and blood parasites of animals. Ticks are second to mosquitoes in terms of disease transmission to humans. The continuous emergence of tick-borne diseases and acaricide resistance of ticks necessitates the development of new and more effective control agents and strategies; therefore, understanding of different aspects of tick biology and their interaction with pathogens is very crucial in developing effective control strategies. RNA interference (RNAi)

has been widely used in the area of tick research as a versatile reverse genetic tool to elucidate the functions of various tick proteins. During the past decade, numerous studies on ticks utilized RNAi to evaluate potentially key tick proteins involved in blood feeding, reproduction, evasion of host immune response, interaction with pathogens, and pathogen transmission that may be targeted for tick and pathogen control. This chapter reviewed the application of RNAi in tick research over the past decade, focusing on the impact of this technique in the advancement of knowledge on tick and pathogen biology.

Full text link: https://tinyurl.com/yd42xjku

Article title: Induction of gene silencing in Haemaphysalis longicornis ticks through immersion in double-stranded RNA

Authors: Remil Linggatong Galay, Emmanuel Hernandez, Melbourne Talactac, Hiroki Maeda, Kodai Kusakisako, Rika-Umemiya Shirafuji Masami Mochizuki, Kozo Fujisaki, Tetsuya Tanaka

Publication title: Tick and tick-borne diseases 7(5), April 2016

Abstract:

The Continuous Emergence of tick-borne diseases and chemical acaricide-resistant tick strains necessitates the development of new and more effective control strategies. RNA interference through the injection of double-stranded RNA (dsRNA) has been a very useful tool in tick research for evaluating gene function. However, this technique can be sophisticated due to the required equipment and technique. Here we studied the feasibility of an immersion technique to induce gene silencing in Haemaphysalis longicornis ticks. We targeted the Hlfer1 gene, previously shown to be crucial in successful blood feeding and reproduction. Larval, nymphal, and adult female H. longicornis ticks were immersed in Hlfer1 or Luciferase dsRNA for control. The dsRNA dissolving medium, incubation temperature and time were varied to establish the optimum conditions. RT-PCR was performed to confirm gene silencing.It was found that immersing the ticks in dsRNA dissolved in nuclease-free water at 15 ◦ C for 12h resulted in clear gene silencing. The phenotypes of adult ticks immersed in dsRNA were then compared with those of adult ticks injected with dsRNA. Similar to dsRNA injection, the post–blood meal weight of ticks immersed in Hlfer1 dsRNA was significantly lower than the control group. Moreover, high post–blood meal mortality and low egg output was observed both from ticks injected with and immersed in Hlfer1 dsRNA. Our results here suggest that Immersion in

dsRNA can effectively induce gene silencing and not only offers an alternative method to dsRNA injection but also opens the possibility of applying dsRNA for tick control

Article title: Virucidal activity of Haemaphysalis longicornis longicin P4 peptide against tick-borne encephalitis virus surrogate Langat virus
Authors: Melbourne R. Talactac, Kentaro Yoshii, Hiroki Maeda, Kodai Kusakisako, Emmanuel Hernandez, Naotoshi Tsuji, Kozo Fujisaki, Remil Linggatong Galay, Tetsuya Tanaka, Masami Mochizuki
Publication title: Parasites & Vectors 9(1), February 2016

Abstract:
Longicin is a defensin-like peptide, identified from the midgut epithelium of hard tick Haemaphysalis longicornis. Several studies have already shown the antimicrobial and parasiticidal activities of longicin peptide and one of its synthetic partial analogs, longicin P4. In this study, longicin peptides were tested for potential antiviral activity against Langat virus (LGTV), a tick-borne flavivirus. Longicin P1 and P4 peptides were chemically synthesized. Antiviral activity of the longicin peptides against LGTV was evaluated through in vitro virucidal assays, wherein the antiviral efficacy was determined by reduction in number of viral foci and virus yield. Additionally, longicin P4 was also tested for its activity against human adenovirus, a non-enveloped virus. Lastly, to assess the importance of longicin on the innate antiviral immunity of H. longicornis ticks, gene silencing through RNAi was performed. Longicin P4 produced significant viral foci reduction and lower virus yield against LGTV, while longicin P1 failed to demonstrate the same results. Conversely, both longicin partial analogs (P1 and P4) did not show significant antiviral activity when tested on adenovirus. In addition, longicin-silenced ticks showed significantly higher virus titer after 7 days post-infection but a significantly lower titer was detected after an additional 14 days of observation as compared to the Luc dsRNA-injected ticks. Mortality in both groups did not show any significant difference. Our results suggest that longicin P4 has in vitro antiviral activity against LGTV but not against a non-enveloped virus such as adenovirus. Likewise, though most cationic antimicrobial peptides like longicin act directly on target membranes, the exact mechanism of membrane targeting of longicin P4 in enveloped viruses, such as LGTV, requires further investigation. Lastly, while the in vitro virucidal capacity of longicin P4 was confirmed in this study, the role of the endogenous

tick longicin in the antiviral defense of H. longicornis against LGTV still remains to be demonstrated.

Full text link: https://tinyurl.com/y8p3nsdk

Article title: Impaired cellular immune response to injected bacteria after knockdown of ferritin genes in the hard tick Haemaphysalis longicornis

Authors: Remil Linggatong Galay, Rie Takechi, Rika Umemiya-Shirafuji, Melbourne R. Talactac, Hiroki Maeda, Kodai Kusakisako, Masami Mochizuki, Kozo Fujisaki, Tetsuya Tanaka

Publication title: Parasitology International 65(3), January 2016

Abstract: No abstract

Article title: A novel C-type lectin with triple carbohydrate recognition domains has critical roles for the hard tick Haemaphysalis longicornis against Gram-negative bacteria

Authors: Hiroki Maeda, Takeshi Miyata, Kodai Kusakisako, Remil Linggatong Galay, Melbourne R. Talactac, Rika Umemiya-Shirafuji, Masami Mochizuki, Kozo Fujisaki, Tetsuya Tanaka

Publication title: Developmental and comparative Immunology 57, December 2015

Abstract:

C-type lectins (CLecs) play an important role in innate immunity against invaders. In this study, a novel CLec was identified from *Haemaphysalis longicornis* ticks (HlCLec). HlCLec contains a signal peptide and a transmembrane region. Interestingly, HlCLec possesses three dissimilar carbohydrate recognition domains (CRDs). Each CRD contains the mutated motif of Ca2+-binding site 2. *HlCLec* mRNA was up-regulated during blood feeding, and had highest expression in the midgut and ovary. HlCLec localization was also confirmed by immunofluorescent antibody test (IFAT). HlCLec was found on the cell membrane and basal lamina of midgut and ovary. In addition, the recombinant HlCLec and individual CRDs demonstrated direct binding activity to *Escherichia coli* and *Staphylococcus aureus*; however, no growth inhibition activity was observed. Furthermore, *E. coli* injection after silencing of *HlCLec* caused drastic reduction in survival rate of ticks. These results strongly suggest the key role of HlCLec in tick innate immunity against Gram-negative bacteria.

Article title: Functional analysis of recombinant 2-Cys peroxiredoxin from the hard tick Haemaphysalis longicornis

Authors: Kodai Kusakisako, Tatsutori Masatani, T Miyata, Remil Linggatong Galay, H. Maeda, Melbourne R. Talactac, N. Tsuji, Masami Mochizuki, F. Fujisaki, Tetsuya Tanaka

Publication title: Insect Molecular Biology, 25(1) October 2015

Abstract:

Ticks are obligate haematophagous arthropods that feed on vertebrate blood containing high levels of iron. The host-derived iron reacts to oxygen in the tick's body, and then high levels of reactive oxygen species, including hydrogen peroxide (H2 O2), may be generated. High levels of H2 O2 cause oxidative stress to aerobic organisms. Therefore, antioxidant responses are necessary to control H2 O2 . We focused on peroxiredoxins (Prxs), H2 O2 -scavenging enzymes. The sequence of Haemaphysalis longicornis 2-Cys Prx (HlPrx2) was identified from fat body cDNA libraries of this tick and recombinant HlPrx2 was then prepared using Escherichia coli. By comparison with the 2-Cys Prxs of other organisms, we found two conserved cysteines in HlPrx2, Cys51 and Cys172. We examined the antioxidant activity of HlPrx2 and mutant proteins produced by a single base substitution, converting one or both of these cysteines into serines. The assays revealed that proteins containing Cys51 showed antioxidant activity when H2 O2 was removed. Sodium dodecyl sulphate polyacrylamide gel electrophoresis and size-exclusion chromatography demonstrated that only the wild-type HlPrx2 formed homodimers and that all of the proteins that we made had a high molecular weight peak. These results indicate that both Cys51 and Cys172 are essential for the dimerization of HlPrx2, whereas only the Cys51 residue is necessary for antioxidant activity.

Article title: Ticks and Tick-borne Diseases

Authors: Rie Takechi, Remil Linggatong Galay, Tomohide Matsuo, Hiroki Maeda, Kudai Kusakisako, Melbourne R. Talactac, Masami Mochizuki, Kozo Fujisaki, Tetsuya Tanaka

Publication title: Ticks and tick-borne diseases 7(1), August 2015

Abstract: no abstract

Article title: Identification of the Babesia-responsive leucine-rich repeat domain-containing protein from the hard tick Haemaphysalis longicornis

Authors: Hiroki Maeda, Koshi Kurisu, Takeshi Miyata, Kodai Kusakisako, Remil Linggatong Galay, Melbourne R. Talactac, Masami Mochizuki, Kozo Fujisaki, Tetsuya Tanaka
Publication title: Parasitology Research 114(5), February 2015

Abstract:
Haemaphysalis longicornis is a tick known for transmitting Babesia parasites, including Babesia gibsoni, in East Asian countries. The vector tick must have strategies to control Babesia parasites, while Babesia parasites are also considered to establish an evasive mechanism from the tick's innate immunity. Due to this mutual tolerance, H. longicornis is considered to be a vector of Babesia parasites. Recent studies have shown the important roles of leucine-rich repeat (LRR) domain-containing proteins in innate immunity in many living organisms. Some LRR domain-containing proteins were identified in ticks; however, their functions are still unknown. In this study, a novel LRR domain-containing protein was identified from H. longicornis (HlLRR). HlLRR contains two LRR domains, and the expression levels of mRNA and proteins were upregulated during blood feeding, particularly in the salivary glands and midgut. In addition, recombinant HlLRR (rHlLRR) demonstrated growth inhibition activity against B. gibsoni in vitro without a hemolytic effect at any concentration used. Moreover, the diameters of Babesia merozoites treated with rHlLRR were significantly larger than those of the control group. These results strongly indicate the key roles of HlLRR in the tick's innate immunity against Babesia parasites. Furthermore, HlLRR might be a potential alternative drug to treat babesiosis.

Article title: Iron metabolism in hard ticks (Acari: Ixodidae): The antidote to their toxic diet
Authors: Remil Linggatong Galay, Rika Umemiya-Shirafuji, Masami Mochizuki, Kozo Fujisaki, Tetsuya Tanaka
Publication title: Parasitology International 64(2), December 2014

Abstract: No Abstract

Article title: Evaluation and comparison of the potential of two ferritins as anti-tick vaccines against Haemaphysalis longicornis
Authors: Remil Linggatong Galay, Takeshi Miyata, Rika Umemiya-Shirafuji, Hiroki Maeda, Kodai Kusakisako, Naotoshi Tsuji, Masami Mochizuki, Kozo Fujisaki, Tetsuya Tanaka

Publication title: Parasites & Vectors 7(1): 482, October 2014

Abstract:

Background Tick control is an essential aspect of controlling the spread of tick-borne diseases affecting humans and animals, but it presently faces several challenges. Development of an anti-tick vaccine is aimed at designing cost-effective and environmentally friendly protection against ticks and tick-borne diseases as an alternative to the use of chemical acaricides. A single vaccine from the tick midgut protein Bm86 is currently available for field applications, but its efficacy is limited to only some tick species. Identification of candidate vaccine antigens that can affect multiple tick species is highly desirable. The hard tick Haemaphysalis longicornis has two kinds of the iron-binding protein ferritin (HlFER), an intracellular HlFER1 and a secretory HlFER2, and RNA interference experiments showed that these are physiologically important in blood feeding and reproduction and in protection against oxidative stress. Here we investigated the potential of targeting HlFERs for tick control by immunizing the host with recombinant HlFERs (rHlFER1 and rHlFER2).Methods Rabbits were immunized with rHlFERs three times subcutaneously at two-week intervals. Antisera were collected before the first immunization and a week after each immunization to confirm the antigen-specific serum antibody titer by serum ELISA. Two weeks after the final immunization, the rabbits were challenged with tick infestation. After dropping, tick feeding and reproduction parameters were evaluated to determine vaccine efficacy. To demonstrate the effects of antibodies, oxidative stress was detected in the eggs and larvae.ResultsThe antibody titer of rHlFER-immunized rabbits greatly increased after the second immunization. Antibodies exhibited cross-reactivity with rHlFERs and reacted with tick native HlFERs in Western blot analysis. Significantly lower bodyweight was observed in the ticks infested from the rHlFER2-immunized rabbit compared to those from the control rabbit. Reduced oviposition and hatching rate were observed in both rHlFER-immunized groups. rHlFER2 showed a higher vaccine efficacy. The antibodies against rHlFERs were detected in the eggs, and higher levels of oxidative stress biomarkers in the eggs and larvae, of ticks from rHlFER vaccinated rabbits.Conclusion Collectively, these results showed that HlFER2 has a good potential as an anti-tick vaccine antigen that may affect multiple tick species.

Full text link: https://tinyurl.com/y9nz35xu

Article title: Two Kinds of Ferritin Protect Ixodid Ticks from Iron Overload and Consequent Oxidative Stress

Authors: Remil Linggatong Galay, Rika Umemiya-Shirafuji, Eugene T. Bacolod, Hiroki Maeda, Hiroki Maeda, Kodai Kusakisako, Jiro Koyama, Naotoshi Tsuji, Masami Mochizuki, Kozo Fujisaki, Tetsuya Tanaka

Publication title: PLoS ONE 9(3):e90661, March 2014

Abstract:

Ticks are obligate hematophagous parasites that have successfully developed counteractive means against their hosts' immune and hemostatic mechanisms, but their ability to cope with potentially toxic molecules in the blood remains unclear. Iron is important in various physiological processes but can be toxic to living cells when in excess. We previously reported that the hard tick Haemaphysalis longicornis has an intracellular (HlFER1) and a secretory (HlFER2) ferritin, and both are crucial in successful blood feeding and reproduction. Ferritin gene silencing by RNA interference caused reduced feeding capacity, low body weight and high mortality after blood meal, decreased fecundity and morphological abnormalities in the midgut cells. Similar findings were also previously reported after silencing of ferritin genes in another hard tick, Ixodes ricinus. Here we demonstrated the role of ferritin in protecting the hard ticks from oxidative stress. Evaluation of oxidative stress in Hlfer-silenced ticks was performed after blood feeding or injection of ferric ammonium citrate (FAC) through detection of the lipid peroxidation product, malondialdehyde (MDA) and protein oxidation product, protein carbonyl. FAC injection in Hlfer-silenced ticks resulted in high mortality. Higher levels of MDA and protein carbonyl were detected in Hlfer-silenced ticks compared to Luciferase-injected (control) ticks both after blood feeding and FAC injection. Ferric iron accumulation demonstrated by increased staining on native HlFER was observed from 72 h after iron injection in both the whole tick and the midgut. Furthermore, weak iron staining was observed after Hlfer knockdown. Taken together, these results show that tick ferritins are crucial antioxidant molecules that protect the hard tick from iron-mediated oxidative stress during blood feeding.

Full text link: https://tinyurl.com/y7c445ow

Article title: Expression analysis of autophagy-related genes in the hard tick Haemaphysalis longicornis

Authors: Rika Umemoya-Shirafuji, Remil Linggatong Galay, Hiroki Maeda, Suguro Kawano, Tetsuya Tanaka, Shinya Fukumoto, Hiroshi Suzuki, Naotoshi Tsuji, Kozo Fukisaki
Publication title: Veterinary Parasitology 201(1-2), February 2014

Abstract: No abstract

Article title: Inhibitory effect of cyclophilin A from the hard tick Haemaphysalis longicornis on the growth of Babesia bovis and Babesia bigemina
Authors: Hiroki Maeda, Damdinsuren Boldbaatar, Koda Kusakisako, Remil Linggatong Galay, Kyaw Min Aung, Rika Umemiya-Shirafuji, Masami Mochizuki, Kozo Fujisaki, Tetsuya Tanaka
Publication title: Parasitology Research 112(6), March 2013

Abstract:
Haemaphysalis longicornis is known as one of the most important ticks transmitting Babesia parasites in East Asian countries, including Babesia ovata and Babesia gibsoni, as well as Theileria parasites. H. longicornis is not the natural vector of Babesia bovis and Babesia bigemina. Vector ticks and transmitted parasites are thought to have established unique host-parasite interaction for their survival, meaning that vector ticks may have defensive molecules for the growth control of parasites in their bodies. However, the precise adaptation mechanism of tick-Babesia parasites is still unknown. Recently, cyclophilin A (CyPA) was reported to be important for the development of Babesia parasites in ticks. To reveal a part of their adaptation mechanism, the current study was conducted. An injection of B. bovis-infected RBCs into adult female H. longicornis ticks was found to upregulate the expression profiles of the gene and protein of CyPA in H. longicornis (HlCyPA). In addition, recombinant HlCyPA (rHlCyPA) purified from Escherichia coli exhibited significant inhibitory growth effects on B. bovis and B. bigemina cultivated in vitro, without any hemolytic effect on bovine RBCs at all concentrations used. In conclusion, our results suggest that HlCyPA might play an important role in the growth regulation of Babesia parasites in H. longicornis ticks, during natural acquisition from an infected host. Furthermore, rHlCyPA may be a potential alternative chemotherapeutic agent against babesiosis.

Article title: Multiple ferritins are vital to successful blood feeding and reproduction of the hard tick Haemaphysalis longicornis

Authors: Remil Linggatong Galay, Kyaw Min Aung, Rika Umemiya-Shirafuji, Hiroki Maeda, Tomohide Matsuo, Hiroaki Kawaguchi, Niroaki Miyoshi, Hiroshi Suzuki, Xuenan Xuan, Masami Mochizuki, Kozo Fujisaki, Tetsuya Tanaka

Publication title: Journal of experimental Biology 216(10), February 2013

Abstract:

Ticks are obligate hematophagous parasites and important vectors of diseases. The large amount of blood they consume contains great quantities of iron, an essential but also toxic element. The function of ferritin, an iron storage protein, and iron metabolism in ticks need to be further elucidated. Here, we investigated the function a newly identified secreted ferritin from the hard tick Haemaphysalis longicornis (HlFER2), together with the previously identified intracellular ferritin (HlFER1). Recombinant ferritins, expressed in Escherichia coli, were used for anti-serum preparation and also assayed for iron-binding activity. RT-PCR and Western blot analyses of different organs and developmental stages of the tick during blood feeding were performed. The localization of ferritins in different organs was demonstrated through an indirect immunofluorescent antibody test. RNA interference (RNAi) was performed to evaluate the importance of ferritin on blood feeding and reproduction of ticks. The midgut was also examined after RNAi using light and transmission electron microscopy (TEM). RT-PCR showed differences in gene expression in some organs and developmental stages. Interestingly, only HlFER2 was detected in the ovary during oviposition and in egg despite the low mRNA transcript. RNAi induced reduced post-blood meal body weight, high mortality, and decreased fecundity. The expression of vitellogenin genes were affected by silencing of ferritin. Abnormalities in digestive cells, including disrupted microvilli, and alteration of digestive activity were also observed. Taken altogether, our results showed that the iron storage and protective functions of ferritin are critical to successful blood feeding and reproduction of H. longicornis.

Article title: Host-derived transferrin is maintained and transferred from midgut to ovary in Haemaphysalis longicornis ticks

Authors: Hiroyuki Mori, Remil Linggatong Galay, Hiroki Maeda, Tomohide Matsuo, Rika Umemiya-Shirafuji, Masami Mochizuki, Kozo Fujisaki, Tetsuya Tanaka
Publication title: Ticks and ticke-borne diseases 5(2), January 2013

Abstract: No abstract

Article title: Target of rapamycin (TOR) controls vitellogenesis via activation of the S6 kinase in the fat body of the tick, Haemaphysalis longicornis
Authors: Rika Umemiya-Shirafuji, Damdinsuren Boldbaatar, Min Liao, Battur Banzragch, Morshedur Rahman, Thasaneeya Kuboki, Remil Linggatong Galay, Tetsuya Tanaka, Kozo Fujisaki
Publication title: International Journal of Parasitology 42(11), September 2012

Abstract:
Vitellogenin (Vg) synthesis, vitellogenesis, is an essential process for the development and reproduction of ticks. Our previous finding led to the hypothesis that target of rapamycin (TOR) pathway is important for vitellogenesis in the hard tick, Haemaphysalis longicornis. The TOR pathway controls cellular activity according to nutrient availability in eukaryotes. TOR, a member of the phosphatidylinositol 3-kinase family, is a central player in this pathway. Here, we present preliminary evidence that H. longicornis TOR (HlTOR) controls vitellogenesis via activation of S6 kinase (S6K) in the fat body. RNA interference (RNAi)-mediated gene silencing of HlTOR was undertaken to elucidate the involvement of HlTOR in the vitellogenesis of the tick. HlTOR-RNAi caused inhibition of S6K phosphorylation in the fat body. HlTOR-RNAi also altered not only the expression levels of GATA mRNA and protein but also the intracellular localisation of GATA in the fat body. The expression levels of Vg mRNA and protein in the fat body of HlTOR-RNAi ticks were significantly lower than those in control ticks. In the pre-ovipositional stage, the ovaries of control ticks had brown oocytes developing, but those of HlTOR-RNAi ticks were white and immature. The haemolymph colour indicated that the amount of Vg was lower in HlTOR-RNAi ticks than in the controls. Furthermore, rapamycin inhibited S6K phosphorylation and reduced the expression levels of Vg mRNA and protein in the fat bodies. Vg proteins were not detected in rapamycin-treated fat bodies in the presence of

20-hydroxyecdysone. These results suggest that HlTOR activity is critical for vitellogenesis stimulated by 20-hydroxyecdysone.

Article title: HlSRB, a Class B Scavenger Receptor, Is Key to the Granulocyte-Mediated Microbial Phagocytosis in Ticks

Authors: Kyaw Min Aung, Damdinsure Boldbaatar, Rika Umemiya-Shirafuji, Min Liao, Naotoshi Tsuji, Xuan Xuenan, Hiroshi Suzuki, Aiko Kume, Remil Linggatong Galay, Tetsuya Tanaka, Kozo Fujisaki

Publication title: PLoS ONE 7(3): E33504 March 2012

Abstract:

Ixodid ticks transmit various pathogens of deadly diseases to humans and animals. However, the specific molecule that functions in the recognition and control of pathogens inside ticks is not yet to be identified. Class B scavenger receptor CD36 (SRB) participates in internalization of apoptotic cells, certain bacterial and fungal pathogens, and modified low-density lipoproteins. Recently, we have reported on recombinant HlSRB, a 50-kDa protein with one hydrophobic SRB domain from the hard tick, Haemaphysalis longicornis. Here, we show that HlSRB plays vital roles in granulocyte-mediated phagocytosis to invading Escherichia coli and contributes to the first-line host defense against various pathogens. Data clearly revealed that granulocytes that up-regulated the expression of cell surface HlSRB are almost exclusively involved in hemocyte-mediated phagocytosis for E. coli in ticks, and post-transcriptional silencing of the HlSRB-specific gene ablated the granulocytes' ability to phagocytose E. coli and resulted in the mortality of ticks due to high bacteremia. This is the first report demonstrating that a scavenger receptor molecule contributes to hemocyte-mediated phagocytosis against exogenous pathogens, isolated and characterized from hematophagous arthropods.

Full text link: https://tinyurl.com/yd4wktbb

Article title: Scavenger Receptor Mediates Systemic RNA Interference in Ticks

Authors: Kyaw Min Aung, Damdinsuren Boldbaatar, Rika Umemiya-Shirafuji, Min Liao, Xuan Xuenan, Hiroshi Suzuki, Remil Linggatong Galay, Tetsuya Tanaka, Kozo Fujisaki

Publication title: PLoS ONE 6(12): E28407 December 2011

Abstract:

RNA interference is an efficient method to silence gene and protein expressions. Here, the class B scavenger receptor CD36 (SRB) mediated the uptake of exogenous dsRNAs in the induction of the RNAi responses in ticks. Unfed female Haemaphysalis longicornis ticks were injected with a single or a combination of H. longicornis SRB (HlSRB) dsRNA, vitellogenin-1 (HlVg-1) dsRNA, and vitellogenin receptor (HlVgR) dsRNA. We found that specific and systemic silencing of the HlSRB, HlVg-1, and HlVgR genes was achieved in ticks injected with a single dsRNA of HlSRB, HlVg-1, and HlVgR. In ticks injected first with HlVg-1 or HlVgR dsRNA followed 96 hours later with HlSRB dsRNA (HlVg-1/HlSRB or HlVgR/HlSRB), gene silencing of HlSRB was achieved in addition to first knockdown in HlVg-1 or HlVgR, and prominent phenotypic changes were observed in engorgement, mortality, and hatchability, indicating that a systemic and specific double knockdown of target genes had been simultaneously attained in these ticks. However, in ticks injected with HlSRB dsRNA followed 96 hours later with HlVg-1 or HlVgR dsRNAs, silencing of HlSRB was achieved, but no subsequent knockdown in HlVgR or HlVg-1 was observed. The Westernblot and immunohistochemical examinations revealed that the endogenous HlSRB protein was fully abolished in midguts of ticks injected with HlSRB/HlVg-1 dsRNAs but HlVg-1 was normally expressed in midguts, suggesting that HlVg-1 dsRNA-mediated RNAi was fully inhibited by the first knockdown of HlSRB. Similarly, the abolished localization of HlSRB protein was recognized in ovaries of ticks injected with HlSRB/HlVgR, while normal localization of HlVgR was observed in ovaries, suggesting that the failure to knock-down HlVgR could be attributed to the first knockdown of HlSRB. In summary, we demonstrated for the first time that SRB may not only mediate the effective knock-down of gene expression by RNAi but also play essential roles for systemic RNAi of ticks.

Full text link: https://tinyurl.com/ycze5r57

Article title: Anti-babesial activity of a potent peptide fragment derived from longicin of Haemaphysalis longicornis

Authors: Remil Linggatong Galay, Hiroki Maeda, Kyaw Min Aung, Rika Umemiya Shirafuji, Xuenan Xuan, Ikuo Igarashi, Naotoshi Tsuji, Tetsuya Tanaka, Kozo Fujisaki

Publication title: Tropical Animal Health and Production 44(2): 343-8, November 2011

Abstract:

Babesiosis is one of the most important tick-borne diseases affecting livestock that can cause major economic losses worldwide particularly in the tropics. Control relies on controlling both the protozoan parasite and the tick vector. Antiprotozoal drugs are most commonly used for treatment, but problems on emergence of resistant strains and food residues are encountered. Longicin, a defensin-like peptide identified from the hard tick, Haemapysalis longicornis, as well as one of its synthetic partial analogs (P4), were previously reported to exert antimicrobial, fungicidal, and parasiticidal activity. Both longicin and P4 showed babesiacidal activity, in vitro and in vivo. Here, peptide fragments of P4 were studied for in vitro activity against bovine Babesia parasites. One of the peptide fragments, antimicrobial peptide 1 (AMP1), reduced the parasitemia of Babesia bigemina. No peptide had significant effect on Babesia bovis. The sequence of AMP1 corresponded to the longicin sequence which is associated with antiparasitic activity. Although AMP1 caused reduction in parasitemia of B. bigemina, the difference in morphology of the parasite compared with the control group was not statistically significant. However, the percentage occurrence of piroplasms decreased, whereas the abnormal pycnotic form increased. The results demonstrated that this shorter peptide retained the anti-babesial activity of the parent peptide, exerting an antiparasitic effect against a bovine Babesia species. Therefore, this short peptide can be considered for chemical synthesis as an alternative therapeutic agent for babesiosis.

Article title: Tick Longicin Implicated in the Arthropod Transmission of Toxoplasma Gondii
Authors: Tetsuya Tanaka, Remil Linggatong Galay, Rika Umemiya-Shirafuji, Hiroshi Suzuki
Publication title: Journal of Veterinary Science and Technology 3(2), January 2011

Abstract:

Antimicrobial peptides are major components of host innate immunity, a well-conserved evolutionarily ancient defensive mechanism. Infectious disease-bearing vector ticks are thought to have evolved to produce specific defense peptides implicated in controlling the infection and transmission of various pathogens. Longicin, a defensin peptide identified from the hard tick, Haemaphysalis longicornis , is known to have a significant deadly effect against both Gram-negative and Gram-positive bacteria and other microorganisms. In this study, female H. longicornis ticks were experimentally injected with Toxoplasma gondii tachyzoite parasites, and

the transcription profiles of longicin in ticks demonstrating the amplification of T. gondii B-1 gene fragments were examined to determine whether and how ticks may respond immunologically in controlling T. gondii infections. As a result, 10 days after parasite injection, ticks indicated the upregulation of the longicin gene, consistently with the presence of T. gondii The effects of recombinant longicin on the morphology of T. gondii tachyzoites were also examined in vitro . Tachyzoite parasites incubated with recombinant longicin induced pathological changes in cell morphology followed by a marked reduction in the number of parasites. These findings suggested that recombinant longicin could impair parasite membranes, leading to the destruction of Toxoplasma parasites.

Full text link: https://tinyurl.com/ycfr683h

FRANCIS NORMAN C. PARAAN
University of the Philippine Diliman

Sex: Male

Education:

Doctor of Philosophy in Physics, Stony Brook University, New York

Field of Specialization:

Quantum Physics

Computational Physics

Condensed Matter Physics

Researches:

Article title: Selective capture of CO2 over N2 and CH4: B clusters and their size effects
Authors: Alexandra B Santos-Putungan, Nataša Stojić, Nadia Binggeli, Francis NC Paraan
Publication title: Materials Today Communications 22:100712, March 2020

Abstract:
Using density-functional theory (DFT), we investigate the selectivity of adsorption of CO2 over N2 and CH4 on planar-type B clusters, based on our previous finding of strong chemisorption of CO2 on the B10−13 planar and quasiplanar clusters. We consider the prototype B8 and B12 planar-type clusters and perform a comparative study of the adsorption of the three molecules on these clusters. We find that, at room temperature, CO2 can be separated from N2 by selective binding to the B12 cluster and not to the B8 cluster. Selective adsorption of CO2 over CH4 at

room temperature is possible for both clusters. Based on our DFT-adsorption data (including also a semi-infinite Boron sheet) and the available literature-adsorption value for N2 on the planar-type B36 cluster, we discuss the selectivity trend of CO2 adsorption over N2 and CH4 with planar-cluster size, showing that it extends over sizes including B10-13 clusters and significantly larger.

Article title: Strong chemisorption of CO2 on B10-B13 planar-type clusters
Authors: Alexandra B Santos-Putungan, Nataša Stojić, Nadia Binggeli, Francis NC Paraan
Publication title: Journal of Physics: Condensed Matter 31:14, January 2019

Abstract:
An ab initio density functional study was performed investigating the adsorption of CO$_2$ on the neutral boron B$_{n}$ ($n = 10-13$) clusters, characterized by planar and quasiplanar ground-state atomic structures. For all four clusters, we found strong chemisorption energy of CO$_2$ reaching 1.6 eV for B$_{12}$ at the cluster edge sites with the adsorbed molecule in the plane of the cluster. A configuration with chemisorbed dissociated CO$_2$ molecule also exists for B$_{11}$ and B$_{13}$ clusters. The strong adsorption is due to the bending of the CO$_2$ molecule, which provides energetically accessible fully in-plane frontier molecular orbitals matching the edge states of the clusters. At the same time, the intrinsic dipole moment of a bent CO$_2$ molecule facilitates the transfer of excess electronic charge from the cluster edges to the molecule.

Article title: Controlling the nucleophilic properties of cobalt salen complexes for carbon dioxide capture
Authors: Meliton R Chiong, Francis NC Paraan
Publication title: RSC advances 9(40): 23254-23260, January 2019

Abstract:
The nucleophilic properties of cobalt salen complexes are examined using density functional theory to investigate its carbon fixing capacity.
Full text link : https://tinyurl.com/y72u3qqq

Article title: Average work done in a ground state quantum quench of the Kitaev chain model with variable-range interactions

Authors: Francis N. C. Paraan, Raymart Jay Canoy

Conference title: 36th Samahang Pisika ng Pilipinas Physics Conference and Annual Meeting

At: Puerto Princesa City, Palawan, Philippine

Abstract:

We study the average work done associated with a ground state quantum quench of the Kitaev chain model with variable-range interactions. We do this by initially preparing an isolated quantum system in the ground state of the initial Hamiltonian at zero temperature. We, then, abruptly change the relative chemical potential parameter. The average work done on the system, which is defined as the difference between the measured energies before and after the quench, is derived and shown to have inflection points at the critical values of the relative chemical potential of the initial Hamiltonian.

Full text link: https://tinyurl.com/y7etbfyb

Article title: Ab initio study on the binding of carbon dioxide to cobalt salen complex

Authors: Meliton Chiong III, Francis N. C. Paraan

Conference title: 35th Samahang Pisika ng Pilipinas Physics Conference and Annual Meeting

At: Cebu City

Abstract:

Metal-organic complexes, such as metal-Schiff bases, can function as catalysts for electrochemical reduction. In this work we present first principles electronic structure calculations for the adduct formation involving carbon dioxide (CO2) and cobalt salen [Co(salen)] complex. Binding energy calculations show that carbon dioxide forms a stable adduct with [Co(salen)] −1 complex. The bonding between carbon dioxide and the cobalt metal center involves back-bonding mainly between the metal d z 2 orbital and the π * orbital of CO2. An accompanying partial charge transfer from Co to CO2 was observed. This study can be used as a preliminary result to further study the structure and stability of other cobalt-carbon complexes.

Article title: Simple techniques for improving deep neural network outcomes on commodity hardware

Authors: Nicholas Christopher A. Colina, Carlos E. Perez, Francis N. C. Paraan

Conference title: STRUCTURE, FUNCTION AND DYNAMICS FROM NM TO GM: Proceedings of the 8th Jagna International Workshop

Abstract:

We benchmark improvements in the performance of deep neural networks (DNN) on the MNIST data test upon imple-menting two simple modifications to the algorithm that have little overhead computational cost. First is GPU parallelization on a commodity graphics card, and second is initializing the DNN with random orthogonal weight matrices prior to optimization. Eigenspectra analysis of the weight matrices reveal that the initially orthogonal matrices remain nearly orthogonal after training. The probability distributions from which these orthogonal matrices are drawn are also shown to significantly affect the performance of these deep neural networks.

Article title: Integer effects in the entanglement and spin fluctuations of a quantum Hall system with Rashba interactions

Authors: Rona Barbarona, Francis N. C. Paraan

Publication title: Journal of Statistical Mechanics: Theory and Experiment 2016(5): 053104, May 2016

Abstract:

We report distinct nonanalytic signatures in the spin-orbit entanglement of a 2D electron gas with Rashba interactions at integer values of the filling factor and at certain level crossings. The accompanying sharp changes in the bulk spin-orbit entanglement entropy can be probed by measuring the fluctuation in the transverse spin polarization of the electron gas.

Article title: Entanglement-fluctuation relation for bipartite pure states

Authors: Aura Mae B Villaruel, Francis NC Paraan

Publication title: Physical Review A 94(2): 022323, December 2015

Abstract:

We identify a subsystem fluctuation (variance) that measures entanglement in an arbitrary bipartite pure state. This fluctuation is of an observable that generalizes the notion of

polarization to an arbitrary N-level subsystem. We express this polarization fluctuation in terms of the order-2 Renyi entanglement entropy and a generalized concurrence. The fluctuation-entanglement relation presented here establishes a framework for experimentally measuring entanglement using Stern-Gerlach-type state selectors.
Full text link: https://arxiv.org/pdf/1512.05551.pdf

Article title: Exact work statistics of quantum quenches in the anisotropic XY model
Authors: Francis A Bayocboc Jr, Francis NC Paraan
Publication title: Physical Review E 92(3): 032142, September 2015

Abstract:
We derive exact analytic expressions for the average work done and work fluctuations in instantaneous quenches of the ground and thermal states of a one-dimensional anisotropic XY model. The average work and a quantum fluctuation relation is used to determine the amount of irreversible entropy produced during the quench, eventually revealing how the closing of the excitation gap leads to increased dissipated work. The work fluctuation is calculated and shown to exhibit non-analytic behavior as the pre-quench anisotropy parameter and transverse field are tuned across quantum critical points. Exact compact formulas for the average work and work fluctuation in ground state quenches of the transverse field Ising model allow us to calculate the first singular derivative at the critical field values.

Article title: Effective thermodynamics of isolated entangled squeezed and coherent states
Authors: King Karl R Seroje, Rafael S. dela Rosa, Francis NC Paraan
Publication title: European Journal of Physics 36(5): 0550551, August 2015

Abstract:
The R\'enyi entanglement entropy is calculated exactly for mode-partitioned isolated systems such as the two-mode squeezed state and the multi-mode Silbey-Harris polaron ansatz state. Effective thermodynamic descriptions of the correlated partitions are constructed to present quantum information theory concepts in the language of thermodynamics. Boltzmann weights are obtained from the entanglement spectrum by deriving the exact relationship between an

effective temperature and the physical entanglement parameters. The partition function of the resulting effective thermal theory can be obtained directly from the single-copy entanglement.
Full text link: https://tinyurl.com/y9cfktv4

Article title: Entanglement spectrum and number fluctuations in the spin-partitioned BCS ground state
Authors: Xavier M Puspus, Kristian Hauser Villegas, Francis NC Paraan
Publication title: Physical Review B 90(15): 155123, October 2014

Abstract:
We study entanglement between the spin components of the Bardeen-Cooper-Schrieffer (BCS) ground state by calculating the full entanglement spectrum and the corresponding von Neumann entanglement entropy. The entanglement spectrum is effectively modeled by a generalized Gibbs ensemble (GGE) of non-interacting electrons, which may be approximated by a canonical ensemble at the BCS critical temperature. We further demonstrate that the entanglement entropy is jointly proportional to the pairing energy and to the number of electrons about the Fermi surface (an area law). Furthermore, the entanglement entropy is also proportional to the number fluctuations of either spin component in the BCS state.
Full text link: https://tinyurl.com/y9ggn7b6

Article title: Quantum phase transition in a multicomponent anyonic Lieb-Liniger model
Authors: Raul A Santos, Francis NC Paraan, Vladimir E Korepin
Publication title: Physical Review B 86(4), April 2012

Abstract:
We study a one-dimensional multicomponent anyon model that reduces to a multicomponent Lieb-Liniger gas of impenetrable bosons (Tonks-Girardeau gas) for vanishing statistics parameter. At fixed component densities, the coordinate Bethe ansatz gives a family of quantum phase transitions at special values of the statistics parameter. We show that the ground state energy changes extensively between different phases. Special regimes are studied and a general classification for the transition points is given. An interpretation in terms of statistics of composite particles is proposed.

Full text link: https://tinyurl.com/y8j7zt8v

Article title: Entanglement spectra of q-deformed higher spin VBS states
Authors: Raul A Santos, Francis NC Paraan, Vladimir E Korepin, Andreas Klümper
Publication title: Journal of Physics A: Mathematical and Theoretical 45(17), January 2012

Abstract:
We calculate the reduced density matrix of a block of integer spin-S's in a q-deformed valence-bond-solid (VBS) state. This matrix is diagonalized exactly for an infinitely long block in an infinitely long chain. We construct an effective Hamiltonian with the same spectrum as the logarithm of the density matrix. We also derive analytic expressions for the von Neumann and R\'enyi entanglement entropies. For blocks of finite length, we calculate the eigenvalues of the reduced density matrix by perturbation theory and numerical diagonalization. These results enable us to describe the effects of finite-size corrections on the entanglement spectrum and entropy in this generalized VBS model.
Full text link: https://tinyurl.com/yavqtfer

Article title: Entanglement spectra of the q-deformed Affleck-Kennedy-Lieb-Tasaki model and matrix product states
Authors: RA Santos, FNC Paraan, VE Korepin, A Klümper
Publication title: EPL (Europhysics Letters) 98(3): 37005, December 2011

Abstract:
We exactly calculate the reduced density matrix of matrix product states (MPS). Our compact result enables one to perform analytic studies of entanglement in MPS. In particular, we consider the MPS ground states of two anisotropic spin chains. One is a q-deformed Affleck-Kennedy-Lieb-Tasaki (AKLT) model and the other is a general spin-1 quantum antiferromagnet with nearest-neighbor interactions. Our analysis shows how anisotropy affects entanglement on different continuous parameter manifolds. We also construct an effective boundary spin model that describes a block of spins in the ground state of the q-deformed AKLT Hamiltonian. The temperature of this effective model is given in terms of the deformation parameter q.

Full text link: https://tinyurl.com/ydzbcmxc

Article title: Erratum: Entanglement in bipartite pure states of an interacting boson gas obtained by local projective measurements [Phys. Rev. A 84 , 032330 (2011)]
Authors: Francis NC Paraan, Javier Molina-Vilaplana, Vladimir E Korepin, Sougato Bose
Publication title: Physical Review A 86(4): 049901, September 2011

Abstract:
We quantify the extractable entanglement of excited states of a Lieb-Liniger gas that are obtained from coarse-grained measurements on the ground state in which the boson number in one of two complementary contiguous partitions of the gas is determined. Numerically exact results obtained from the coordinate Bethe ansatz show that the von Neumann entropy of the resulting bipartite pure state increases monotonically with the strength of repulsive interactions and saturates to the impenetrable-boson limiting value. We also present evidence indicating that the largest amount of entanglement can be extracted from the most probable projected state having half the number of bosons in a given partition. Our study points to a fundamental difference between the nature of the entanglement in free-bosonic and free-fermionic systems, with the entanglement in the former being zero after projection, while that in the latter (corresponding to the impenetrable-boson limit) being nonzero.
Full text link: https://tinyurl.com/y6w8n3ks

Article title: Perturbative correction to the ground state properties of one-dimensional strongly interacting bosons in a harmonic trap
Authors: Francis NC Paraan, Vladimir E Korepin
Publication title: Physical Review A 82(6) November 2010

Abstract:
We calculate the first-order perturbation correction to the ground state energy and chemical potential of a harmonically trapped boson gas with contact interactions about the infinite repulsion Tonks-Girardeau limit. With c denoting the interaction strength, we find that for a large number of particles N the $1/c$ correction to the ground state energy increases as $N^{5/2}$, in contrast to the unperturbed Tonks-Girardeau value that is proportional to N^2.

We describe a thermodynamic scaling limit for the trapping frequency that yields an extensive ground state energy and reproduces the zero temperature thermodynamics obtained by a local density approximation.
Full text link: https://tinyurl.com/ycwrdz4e

Article title: Quantum quenches in the Dicke model: Statistics of the work done and of other observables
Authors: Francis NC Paraan, Alessandro Silva
Publication title: Physical Review E 80(6), December 2009

Abstract:
We study the statistics of the work done in a zero temperature quench of the coupling constant in the Dicke model describing the interaction between an ensemble of two level systems and a single bosonic mode. When either the final or the initial coupling constants approach the critical coupling lambdac that separates the normal and superradiant phases of the system, the probability distribution of the work done displays singular behavior. The average work tends to diverge as the initial coupling parameter is brought closer to the critical value lambdac. In contrast, for quenches ending close to criticality, the distribution of work has finite moments but displays a sequence of edge singularities. This contrasting behavior is related to the difference between the processes of compression and expansion of a particle subject to a sudden change in its confining potential. We confirm this by studying in detail the time-dependent statistics of other observables, such as the quadratures of the photons and the total occupation of the bosonic modes.
Full text link: https://tinyurl.com/y7h5pnnk

Article title: Brownian motion of a charged particle driven internally by correlated noise
Authors: Francis NC Paraan, Mikhail P Solon, JP Esguerra
Publication title: Physical Review E 77(2), March 2008

Abstract:
We give an exact solution to the generalized Langevin equation of motion of a charged Brownian particle in a uniform magnetic field that is driven internally by an exponentially

correlated stochastic force. A strong dissipation regime is described in which the ensemble-averaged fluctuations of the velocity exhibit transient oscillations that arise from memory effects. Also, we calculate generalized diffusion coefficients describing the transport of these particles and briefly discuss how they are affected by the magnetic field strength and correlation time. Our asymptotic results are extended to the general case of internal driving by correlated Gaussian stochastic forces with finite autocorrelation times.

Full text link: https://tinyurl.com/yathf6pz

Article title: Exact moments in a continuous time random walk with complete memory of its history

Authors: Francis NC Paraan, JP Esguerra

Publication title: Physical Review E 74(3), October 2006

Abstract:

We present a continuous time generalization of a random walk with complete memory of its history [Phys. Rev. E 70, 045101(R) (2004)] and derive exact expressions for the first four moments of the distribution of displacement when the number of steps is Poisson distributed. We analyze the asymptotic behavior of the normalized third and fourth cumulants and identify new transitions in a parameter regime where the random walk exhibits superdiffusion. These transitions, which are also present in the discrete time case, arise from the memory of the process and are not reproduced by Fokker-Planck approximations to the evolution equation of this random walk.

Full text link: https://tinyurl.com/y88oj3dd

BETCHAIDA D. PAYOT

University of the Philippines Diliman

Sex: Female

Education: Doctor of Philosophy in Geology, Kanazawa University Japan, 2009
Master of Science in Geology, University of the Philippines, 2006
Bachelor of Science in Geology, University of the Philippines, 2002

Field of Specialization:

Igneous Petrology and Geochemistry

Researches:

Article title: Bouguer Anomaly of Central Cebu, Philippines

Authors: Lt. Armada, Carla B. Dimalanta, Nathaniel Parcutela, Rurik Austria, Jenielyn Padrones, Betchaida Payot, Karlo L. Queaño, Graciano P. Yumul, Jr.

Publication title: Journal of Maps 16(2) 577-584, December 2020

Abstract:

Cebu Island in Central Philippines consists of a Cretaceous basement complex capped by mostly Tertiary sedimentary units. Recent mapping conducted in Central Cebu revealed limited exposures of lithologies, especially those comprising the basement complex. The gravity method was utilized to generate Bouguer anomaly maps for Central Cebu. These geophysical maps provide the first images of the subsurface extent of the basement units. A prominent

nearly circular gravity anomaly high is consistently observed in the Bouguer anomaly maps coinciding with the location of dense basement and intrusive rocks. However, field mapping revealed the very limited surface exposure of these units. The gravity highs recognized in the residual anomaly maps may correspond to the larger extent of the intrusive units at depth. The broad gravity high observed in the regional anomaly map may define the extent of the subsurface distribution of the Cretaceous basement complex.

Full text link: https://tinyurl.com/y9grn454

Article title: Consumed tectonic plates in Southeast Asia: Markers from the Mesozoic to early Cenozoic stratigraphic units in the northern and central Philippines

Authors: Karlo L Queaño, Graciano P Yumul Jr, Edanjarlo J Marquez, Jillian A Gabo-Ratio, Betchaida D Payot, Carla B Dimalanta

Publication title: Journal of Asian Earth Sciences: X, September 2020

Abstract:

Tectonic reconstruction models of Southeast Asia all invoke in the early Cenozoic the collision of Mesozoic oceanic plates, which have been fragmented, consumed along subduction zones or emplaced onto the overriding plate. However, with marked variations in these models, we reinvestigate the tectonic evolutionary landscape of Southeast Asia through the lens of Philippine geology. In particular, we present revisions to the more recent models by adopting the unique approach of integrating data that we have gathered for the past 17 years from the Upper Mesozoic to Lower Cenozoic stratigraphic formations in northern and central Philippines. These formations, which resulted mainly from submarine mass transport processes, evolved in response to early arc-related processes of oblique subduction, frontal wedge deformation, terrane accretion and strike slip faulting. Additional key constraints for the revisions include: (1) the timing of early Cenozoic magmatism in eastern Luzon; (2) the spatial distribution of the Upper Mesozoic to Lower Cenozoic sedimentary formations with respect to other key features (e.g. distribution of Mesozoic ophiolite fragment and continent-derived rocks) in the Philippine arc; (3) the paleolatitudinal position of Luzon and surrounding regions and; (4) the movement of the surrounding plates since the Late Mesozoic. In revising previous models, a subduction zone (proto-East Luzon Trough) separating Benham Plateau and the Philippine arc was placed to explain the spatial distribution of Eocene arc-related formational

units and Mesozoic ophiolite materials comprising the accretionary complex east of Luzon at ~40 Ma period. During this time, Luzon was modeled at the southern margin of the East Asia Sea or the proto-Philippine Sea Plate. Mesozoic ophiolitic complexes that line the eastern Philippine arc as well as the ophiolitic and pelagic limestone and chert fragments included in the arc-derived, Eocene formations in Luzon could very well be traces of the now consumed East Asia Sea-proto-Philippine Sea Plate. Within the same period, we modified the Palawan Microcontinental Block (PCB), positioned at the trailing edge of the proto-South China Sea to include the whole Mindoro island and the Romblon Island Group in Central Philippines. Pieces of the consumed Izanagi Plate, the proto-South China Sea and continental-derived sediments from Asia mainland are reflected in the Mesozoic metamorphic rocks and the Eocene sedimentary formation in western Mindoro. Finally, we model Cebu, Bohol and Negros islands in Central Philippines as being at the leading oceanic edge of the Indo-Australian Plate during the early Cenozoic. With the northward movement of the Indo-Australian plate and the trench roll back of the southern margins of the Philippine Sea Plate, the accretion of the Cretaceous arc-related rocks of Cebu, Bohol and Negros onto the Philippine arc by the end of Eocene or early Oligocene becomes a possibility.

Full text link: https://tinyurl.com/y9qscp5f

Article title: Mesozoic rock suites along western Philippines: Exposed proto-South China Sea fragments?

Authors: Graciano P Yumul Jr, Carla B Dimalanta, Jillian A Gabo-Ratio, Karlo L Queaño, Leo T Armada, Jenielyn T Padrones, Decibel V Faustino-Eslava, Betchaida D Payot, Edanjarlo J Marquez

Publication Title: Journal of Asian Earth Sciences: X, May 2020

Abstract:

An ancient oceanic crustal leading edge east of mainland Asia, the proto-South China Sea crust, must have existed during the Mesozoic based on tectonic reconstructions that accounted for the presence of subducted slabs in the lower mantle and the exposed oceanic lithospheric fragments strewn in the Philippine and Bornean regions. Along the western seaboard of the Philippine archipelago, numerous Mesozoic ophiolites and associated lithologies do not appear to be genetically associated with the younger Paleogene-Neogene ocean basins that currently

surround the islands. New sedimentological, paleomagnetic, paleontological, and isotopic age data that we generated are presented here, in combination with our previous results and those of others, to reassess the geological make-up of the western Philippine island arc system. We believe that the oceanic lithospheric fragments, associated melanges, and sedimentary rocks in this region are exhumed slivers of the proto-South China Sea ocean plate.
Full text link: https://tinyurl.com/y92rnhgq

Article title: Melt-rock interaction in the subarc mantle: records from the plagioclase peridotites of the southern Palawan Ophiolite, Philippines
Authors: Florence Annette Labis, Betchaida D. Payot, Gabriel Theopilus Vinalay Valera, Julius Pasco, Jesley Mei A. Dycoco, Akihiro Tamura, Tomoaki Morishita, Shoji Arai
Publication title: International Geology Review, April 2020

Abstract:
The interaction between migrating melts and the upper mantle largely affects the composition of the ascending melt and residual peridotites. In island arcs, melt-rock interactions and products which involved highly depleted mantle peridotites are still largely undocumented despite their petrological importance. In this contribution, the petrographic and geochemical signatures of refractory and refertilized peridotites comprising the mantle section of the southern Palawan Ophiolite, Philippines are investigated. The peridotites are dominantly comprised of residual spinel harzburgites with minor dunite and plagioclase peridotites. Spinel harzburgites are similar to other highly depleted residual mantle materials of other suprasubduction zone ophiolites. Plagioclase peridotites, which are cut by gabbroic intrusions, preserve distinct petrological characteristics indicating melt-rock interaction. The melts preserved as gabbroic dikes have signatures transitional between mid-ocean ridge and island arc, and are comparable to back-arc basin lavas. We therefore propose that the plagioclase peridotites were formed due to the reaction between highly depleted mantle peridotites beneath an intraoceanic arc and migrating BABB-like magmas possibly during the incipient stages of back-arc rifting.

Article title: Petrogenesis of ultramafic-mafic clasts in the Dos Hermanos Mélange, Ilocos Norte: Insights to the evolution of western Luzon, Philippines

Authors: Julius Pasco, Jesley Mei A. Dycoco, Gabriel Theopilus Vinalay Valera, Betchaida D. Payot, John Dave B. Pillejera, Frances Aleksis Anika E. Uy, Lt. Armada, Carla B. Dimalanta
Publication title: Journal of Asian Earth Sciences 184, August 2019

Abstract:

The clasts of ophiolitic mélanges formed in orogenic margins reflect the tectonomagmatic history of a region and record the petrological signatures of oceanic lithospheres that interacted in the past. Exposed at the northwestern edge of Luzon, Philippines, the highly deformed Dos Hermanos Mélange (DHM) provides new insights on the complex history of western Luzon island. The DHM is a tectonic mélange composed predominantly of ultramafic-mafic clasts set in a sheared serpentinite matrix. The ultramafic clasts are mostly harzburgites with rare occurrences of lherzolite, dunite and chromitite. Petrographic (e.g. protogranular to equigranular texture) and geochemical characteristics (e.g. spinel Cr# = 0.17–0.60, olivine Fo content = 87–91) of the peridotites typify residual mantle peridotites which underwent low to moderately high degrees of partial melting. Mineral chemistry of some dunite and harzburgite samples (e.g. high spinel TiO2 = 0.01–0.64 wt%) further record subsequent modification of the depleted mantle material by arc-related processes (e.g. metasomatism). Most of the mafic clasts classify as gabbros and are composed of highly anorthitic plagioclase (An88–99) and Ti-poor pyroxenes which suggest derivation from arc-related melts. One troctolite clast, however, records the distinct petrographic (e.g. ophitic texture) and geochemical (e.g. low An content of plagioclase = 73–80) signatures of primitive MOR-related magma. These contrasting petrologic signatures in the ultramafic-mafic clasts of the DHM are similar to those observed in the crustal and mantle sections of the Eocene Zambales Ophiolite Complex (ZOC). This suggests that the DHM, like the ZOC, records the complex history of the convergence and emplacement of an ancient oceanic crust onto the Philippine Mobile Belt. Later tectonic processes in the region, which occurred after the emplacement of the ZOC, resulted to the extensive dissection and translation of ophiolitic blocks northwards transforming them into the DHM.

Article title: Petrographic and geochemical characterization of the crustal section of the Pujada Ophiolite, southeastern Mindanao, Philippines: Insights to the tectonic evolution of the northern Molucca Sea Collision Complex

Authors: Valerie Shayne V Olfindo, Betchaida D Payot, Gabriel Theophilus V Valera, Efren G Gadot Jr, Barbie Ross B Villaplaza, Kenichiro Tani, Carla B Dimalanta, Graciano P Yumul Jr.
Publication title: Journal of Asian Earth Sciences 184, October 2019

Abstract:
The Molucca Sea Collision Complex (MSCC) preserves the complex interaction between the Eurasian, Philippine Sea and the completely subducted Molucca Sea Plates. Petrological studies of obducted arc and ophiolitic materials in this region thus provide a unique opportunity to elucidate the tectono-magmatic evolution of the area. In this study, we present new petrographic and geochemical data on the crustal section of the Pujada Ophiolite which is extensively exposed in southeastern Mindanao, Philippines. Our work reveals that this ophiolite is a remnant of an oceanic lithosphere with backarc affinity. U-Pb dating of zircons from the isotropic gabbros further constrains the age of the Pujada Ophiolite to Late Cretaceous (90 Ma). This age is consistent with the inferred age of the proto-Molucca Sea Plate based on tectonic reconstructions and tomography. Exposed to the north of the Pujada Ophiolite and separated by a NE-SW trending thrust fault is the Iba Formation. This unit originally purported to be the carapace of the Pujada Ophiolite records an IA (island arc) affinity. The geochemical signature of the Iba Formation suggests derivation from an enriched mantle source affected by slab-derived components related to the East Mindanao-Halmahera Arc. We therefore interpret the Pujada Ophiolite as a trapped fragment of the proto-Molucca Sea Plate that was thrust onto the Halmahera Arc possibly during the waning stages of the collision between the Sangihe and Halmahera Arcs.

Article title: An evolving subduction-related magmatic system in the Masara Gold District, Eastern Mindanao, Philippines
Authors: Alfred Elmer Buena, Barbie Ross B Villaplaza, Betchaida D Payot, Jillian Aira S Gabo-Ratio, Noelynna T Ramos, Decibel V Faustino-Eslava, Karlo L Queaño, Carla B Dimalanta, Jenielyn T Padrones, Kenichiro Tani, Walter W Brown, Graciano P Yumul Jr
Publication title: Journal of Asian Earth Sciences: X, June 2019

Abstract:

The Masara Gold District in Eastern Mindanao, Philippines, is one of the most prolific gold provinces in the Philippines. Recent district-scale mineral exploration makes it possible to undertake geologic and geochemical studies and thus to yield better insights about the mineralization environment of the Masara Gold District. In the Masara Gold District, mineralization is hosted in andesitic rocks and multiple stocks of diorite intrusions. New U-Pb and whole rock K-Ar age dating of these host rocks reveal Eocene to Plio-Pleistocene ages for the magmatic suites. A new lithologic unit is proposed to accommodate the composite diorite phases associated with mineralization. Major and trace element geochemistry of these host rocks show that the Eocene magmatic suite exhibits a tholeiitic character while the diorite and subvolcanic andesite pulses of the Miocene are calc-alkaline in composition. Adakitic rocks were emplaced during the Late Miocene and Plio-Pleistocene. Mineralization in eastern Mindanao is associated with several intrusive events formed during the Oligocene to the Pliocene. The majority of these mineralization events is associated with calc-alkaline magmatic suites. Based on this study, epithermal gold mineralization in the Masara Gold District is closely related to the Late Miocene magmatic rocks which exhibit calc-alkaline and adakitic signatures.

Full text link: https://tinyurl.com/ybgutyyx

Article title: Characterization of the proto-Philippine Sea Plate: Evidence from the emplaced oceanic lithospheric fragments along eastern Philippines

Authors: Carla B Dimalanta, Decibel V Faustino-Eslava, Jillian Aira S Gabo-Ratio, Edanjarlo J Marquez, Jenielyn T Padrones, Betchaida D Payot, Karlo L Queano, Noelynna T Ramos, Graciano P Yumul Jr

Publication title: Geoscience Frontiers 11(1): 3-21, February 2019

Abstract:

The proto-Philippine Sea Plate (pPSP) has been proposed by several authors to account for the origin of the Mesozoic supra-subduction ophiolites along the Philippine archipelago. In this paper, a comprehensive review of the ophiolites in the eastern portion of the Philippines is undertaken. Available data on the geology, ages and geochemical signatures of the oceanic lithospheric fragments in Luzon (Isabela, Lagonoy in Camarines Norte, and Rapu-Rapu island), Central Philippines (Samar, Tacloban, Malitbog and Southeast Bohol), and eastern Mindanao

(Dinagat and Pujada) are presented. Characteristics of the Halmahera Ophiolite to the south of the Philippines are also reviewed for comparison. Nearly all of the crust-mantle sequences preserved along the eastern Philippines share Early to Late Cretaceous ages. The geochemical signatures of mantle and crustal sections reflect both mid-oceanic ridge and supra-subduction signatures. Although paleomagnetic information is currently limited to the Samar Ophiolite, results indicate a near-equatorial Mesozoic supra-subduction zone origin. In general, correlation of the crust-mantle sequences along the eastern edge of the Philippines reveal that they likely are fragments of the Mesozoic pPSP. © 2019 China University of Geosciences (Beijing) and Peking University.

Full text link: https://tinyurl.com/yaoyou7o

Article title: Petrologic nature of the active subarc crust-mantle boundary: Mixed magmatic-metasomatic processes recorded in xenoliths from Sabtang island, Luzon arc

Authors: Gabriel Theophilus V Valera, Betchaida D Payot, Shoji Arai, Miyuki Takeuchi, Satoko Ishimaru, Akihiro Tamura

Publication title: Journal of Volcanology and Geothermal Research 374, pp80-99, April 2019

Abstract:

Some arc magmas reside in the uppermost mantle and the lower crust. Their deep-seated behavior determines the composition of magmas that erupt at the surface. Mafic-ultramafic xenoliths newly found in Sabtang island, Batanes group of islands of the Luzon arc record subarc processes. The xenolith suite is comprised mainly of dunites, orthopyroxenites, clinopyroxenites, hornblendites, and gabbros, all hosted in basaltic to andesitic lavas. Petrographic characteristics suggest the metasomatic formation of orthopyroxenites and hornblendites from dunites and clinopyroxenites, respectively. The apparently primary minerals are homogeneous in composition. Olivine is relatively magnesian (Fo 82–90) and chromian spinel is rich in Cr# (=Cr/[Cr + Al], around 0.7) in dunites. Clinopyroxene is relatively magnesian (Mg# = Mg/[Mg + Fe^{2+}] = 0.73–0.93) in clinopyroxenites and gabbros, and plagioclase is highly anorthitic (An 89–98) in the gabbros. The primary mineral assemblage reflects crystallization of olivine and spinel followed by clinopyroxene all occurring in the uppermost mantle and lower crust of the Luzon arc. The orthopyroxenes and amphiboles were metasomatically produced at the expense of olivine and clinopyroxene, respectively.

Clinopyroxene in the xenoliths is in equilibrium with the magmas that formed the Sabtang volcanics. They have relatively elevated contents of large-ion lithophile elements and light-rare-earth elements, which suggest derivation from an enriched mantle. The Sabtang xenoliths evidence the very active modification of the subarc mantle-crust boundary zone by mantle-derived magmas and slab-derived melts/fluids so that the mineral assemblage of the resultant rocks is similar to that of the predominant recent magma.

Article title: Slab rollback and microcontinent subduction in the evolution of the Zambales Ophiolite Complex (Philippines): A review

Authors: Graciano P Yumul Jr, Carla B Dimalanta, Ricky C Salapare, Karlo L Queano, Decibel V Faustino-Eslava, Edanjarlo J Marquez, Noelynna T Ramos, Betchaida D Payot, Juan Miguel R Guotana, Jillian Aira S Gabo-Ratio, Leo T Armada, Jenielyn T Padrones, Keisuke Ishida, Shigeyuki Suzuki

Publication title: Geoscience Frontiers 11(1):23-26, February 2019

Abstract:

New radiolarian ages show that the island arc-related Acoje block of the Zambales Ophiolite Complex is possibly of Late Jurassic to Early Cretaceous age. Radiometric dating of its plutonic and volcanic-hypabyssal rocks yielded middle Eocene ages. On the other hand, the paleontological dating of the sedimentary carapace of the transitional mid-ocean ridge – island arc affiliated Coto block of the ophiolite complex, together with isotopic age datings of its dikes and mafic cumulate rocks, also yielded Eocene ages. This offers the possibility that the Zambales Ophiolite Complex could have: (1) evolved from a Mesozoic arc (Acoje block) that split to form a Cenozoic back-arc basin (Coto block), (2) through faulting, structurally juxtaposed a Mesozoic oceanic crust with a younger Cenozoic lithospheric fragment or (3) through the interplay of slab rollback, slab break-off and, at a later time, collision with a microcontinent fragment, caused the formation of an island arc-related ophiolite block (Acoje) that migrated trench-ward resulting into the generation of a back-arc basin (Coto block) with a limited subduction signature. This Meso-Cenozoic ophiolite complex is compared with the other oceanic lithosphere fragments along the western seaboard of the Philippines in the context of their evolution in terms of their recognized environments of generation.

Full text link: https://tinyurl.com/yd3r8ozr

Article title: Mantle Evolution from Ocean to Arc: The Record in Spinel Peridotite Xenoliths in Mt. Pinatubo, Philippines

Authors: Betchaida D Payot, Shoji Arai, Masako Yoshikawa, Akihiro Tamura, Mitsuru Okuno, Danikko John V Rivera

Publication title: Minerals 8(11): pp515 November 2018

Abstract:

A suite of peridotite xenoliths were collected from lahar flow deposits located close to the summit of Mt. Pinatubo. Spinel harzburgite is the most dominant lithology among dunites, pyroxenites and websterites. A rare spinel lherzolite xenolith (P12-7) is also present in this suite. The spinel lherzolite has well-preserved protogranular texture with very minimal presence of secondary amphibole, low Cr# in the chromian spinel, and depleted and hump shaped patterns of chondrite-normalized rare earth element (REE) patterns for the clinopyroxenes. In contrast, the spinel harzburgites contain abundant secondary amphiboles and orthopyroxenes, higher Cr# in the spinel, and slightly elevated patterns for the chondrite-normalized REE patterns for the amphiboles. The spinel lherzolite also exhibits higher olivine Fo content for a given spinel Cr# compared to the spinel harzburgites. The spinel lherzolite is interpreted as a typical residue from partial melting of abyssal peridotites whereas the spinel harzburgites may have formed via partial melting with subsequent modification during the influx of fluids in the mantle wedge. Our results suggest that fragments of MOR-derived lithosphere exist in the mantle wedge beneath the Philippine island arc. This work provides evidence for the conversion of abyssal to arc peridotites in the mantle wedge.

Full text link: https://tinyurl.com/ycsw6hqv

Article title: Aqueous fluids and sedimentary melts as agents for mantle wedge metasomatism, as inferred from peridotite xenoliths at Pinatubo and Iraya volcanoes, Luzon arc, Philippines

Authors: Masako Yoshikawa, Akihiro Tamura, Shoji Arai, Tatsuhiko Kawamoto, Betchaida D Payot, Danikko John Rivera, Ericson B Bariso, Ma Hannah T Mirabueno, Mitsuru Okuno, Tetsuo Kobayashi

Publication title: Lithos 262: 355-368, October 2017

Abstract:

Mantle xenoliths entrained in subduction-zone magmas often record metasomatic signature of the mantle wedge. Such xenoliths occur in magmas from Iraya and Pinatubo volcanoes, located at the volcanic front of the Luzon arc in the Philippines. In this study, we present the major element compositions of the main minerals, trace element abundances in pyroxenes and amphiboles, and Nd–Sr isotopic compositions of amphiboles in the peridotite xenoliths form Pinatubo volcano. These data indicate enrichment in fluid-mobile elements, such as Rb, Ba, U, Pb, and Sr, and Nd-Sr isotopic ratios relative to those of mantle. The results are considered in terms of mixing of asthenospheric mantle and subducting oceanic crustal components. The enrichments observed in the Pinatubo mantle xenoliths are much less pronounced than those reported for the Iraya mantle xenoliths. This disparity suggests differences in the metasomatic agents contributing to the two suites; i.e., aqueous fluids infiltrated the mantle wedge beneath the Pinatubo volcano, whereas aqueous fluids and sediment-derived melts infiltrated the mantle wedge beneath the Iraya volcano.

Article title: Alteration and lithogeochemistry in the Masara Gold District, Eastern Mindanao, Philippines, as tools for exploration targeting

Authors: Barbie Ross B Villaplaza, Alfred Elmer Buena, Nichole Anthony D Pacle, Betchaida D Payot, Jillian Aira S Gabo-Ratio, Noelynna T Ramos, Carla B Dimalanta, Decibel V Faustino-Eslava, Karlo L Queaño, Graciano P Yumul Jr, Kotaro Yonezu

Publication title: Ore Geology Reviews 91: 530-540, September 2017

Abstract:

The intermediate to low sulfidation epithermal gold deposit in Masara, Compostela Valley, Eastern Mindanao, Philippines, is associated with a diorite porphyry from the Late Miocene Lamingag Intrusive Complex. Detailed mineralogical investigation of the host rocks in the deposit reveals five major alteration zones and at least two mineralizing events. A potassic alteration zone characterized by stockwork magnetite veins, secondary biotite and magnetite and an early-stage chlorite-sericite alteration composed of quartz+chlorite+illite+sericite+pyrite±biotite±magnetite±calcite assemblages are interpreted to be linked with an earlier porphyry copper system in the area. These were overprinted by

late-stage chlorite-sericite alteration consisting of quartz+chlorite+illite+sericite+pyrite±adularia±magnetite±epidote and sericite assemblages which generally contain quartz+illite+sericite+pyrite. These alteration overprints are inferred to be related to a younger low to intermediate-sulfidation epithermal gold mineralization which involved near-neutral fluids. Advanced argillic alteration comprising quartz+kaolinite+magnetite+dickite±illite±calcite was also observed in the area. Isocon analysis shows that alteration zones associated with epithermal mineralization are generally characterized by enrichment in SiO2 and K2O and depletion of CaO and Na2O as well as additions of Au, Cu, Zn and Pb. Pearce Element Ratio (PER) analysis indicates high degrees of sericitization in the altered diorite porphyry, tuff and quartz diorite units. At least three major alteration centers are defined based on the spatial distribution of the Alteration Index of surface samples calculated from the PER analysis. The results of this study support the use of whole-rock geochemistry as a complement to traditional techniques in exploration geochemistry.

Article title: Petrological and geochemical characteristics of the Samar Ophiolite ultramafic section: implications on the origins of the ophiolites in Samar and Leyte islands, Philippines
Authors: JMR Guotana, BD Payot, CB Dimalanta, NT Ramos, DV Faustino-Eslava, KL Queaño, GP Yumul Jr
Publication title: International Geology Review 60(30):1-17, July 2017

Abstract:
Cretaceous ophiolites and ophiolitic fragments occur in the Samar and Leyte islands in eastern central Philippines. The Samar Ophiolite is a complete crust–mantle sequence exposed in southern Samar, whereas the Tacloban and Malitbog ophiolite complexes are, respectively, located in the northeastern and southwestern portions of the nearby Leyte island. Despite the close proximity of these islands, the genetic relationship of these ophiolites and ophiolitic complexes, if any, remains to be elucidated. We present here new petrographic and geochemical data on the harzburgites and dunites of the ultramafic section of the Samar Ophiolite. These mantle peridotites are highly depleted residues which have low modal pyroxene content, high spinel Cr# (=0.62–0.79), and slightly enriched light rare earth element abundance with depletion in Zr and Ti. Such characteristics are typical of supra-subduction zone peridotites and strongly

contrast with the abyssal signatures of the Tacloban and Malitbog ophiolite complexes. The absence of a structure between these adjacent ophiolite fragments initially hints that they form a single oceanic crust. However, with our new results, we suggest other possible mechanisms that could explain the relationship of these ophiolites.

Article title: Petrography and geochemistry of Cenozoic sedimentary sequences of the southern Samar Island, Philippines: Clues to the unroofing history of an ancient subduction zone
Authors: Nichole Anthony D Pacle, Carla B Dimalanta, Noelynna T Ramos, Betchaida D Payot, Decibel V Faustino-Eslava, Karlo L Queaño, Graciano P Yumul Jr
Publication title: Journal of Asian Earth Sciences 142: 3-19, August 2016

Abstract:

The Cenozoic sedimentary sequences of southern Samar Island in eastern Philippines were examined to understand the unroofing history of an ancient arc terrane. Petrographic and geochemical data reveal varying degrees of inputs from the ophiolite basement and differences in modal compositions. The sedimentary units are mostly made up of lithic fragments. The Late Oligocene to Early Miocene Daram Formation contains more chert and volcanic fragments whereas the Late Miocene to Early Pliocene Catbalogan Formation is dominantly composed of ultramafic components. These variances are correspondingly reflected in the geochemical signatures of these two sedimentary formations. The Catbalogan Formation clastic rocks have higher volatile-free MgO and Fe2O3 values (average: 8.4% for both oxides) compared to the Daram Formation samples (average: 5.1 and 6.3%, respectively). Geochemical variations are also reflected in the Co, Cr and Ni values: the Catbalogan Formation samples reflect higher concentrations (Co: 15-57 ppm; Cr: 231-1094 ppm; Ni: 84-484 ppm) compared to the Daram Formation samples (Co: 24-32 ppm; Cr: 234-418 ppm; Ni: 212-323 ppm). These observations suggest that the Daram Formation eroded and transported more of the crustal portions of the ophiolite, while the younger Catbalogan Formation represents a later exhumation and subsequent erosion of the ultramafic section. An oceanic island arc (OIA) setting is proposed for the two formations based on several tectonic discrimination diagrams (e.g. Th-La-Sc, La vs. Th). The OIA signature is further supported by their smooth chondrite-normalized rare earth element (REE) patterns with no obvious Eu anomaly as well as LREE enrichment which are typical of sediments deposited in OIA setting. Based on the dominantly ophiolitic provenance

of the Daram and Catbalogan Formations, the post-emplacement history of the nearby Samar Ophiolite is constrained during the Late Oligocene to Early Pliocene period.

Article title: Arc and backarc geochemical signatures of the proto-Philippine Sea Plate: Insights from the petrography and geochemistry of the Samar Ophiolite volcanic section
Authors: Juan Miguel R Guotana, Betchaida D Payot, Carla B Dimalanta, Noelynna T Ramos, Decibel V Faustino-Eslava, Karlo L Queaño, Graciano P Yumul Jr
Publication title: Journal of Asian Earth Sciences 142: 77-92, July 2016

Abstract:
Remnants of a Cretaceous lithosphere are found at the peripheries of the West Philippine Basin. These Mesozoic fragments preserve arc affinity and include the Amami Plateau, the East Halmahera Ophiolite and the ophiolites along the eastern margin of the Philippine archipelago. The eastern margin of the Philippines is composed of Early to Late Cretaceous ophiolites and ophiolitic complexes that exhibit strong subduction imprints. The early Late Cretaceous Samar Ophiolite in the central Philippines forms part of this eastern belt. Recent surveys in southern Samar revealed the presence of peridotites, gabbros, and massive and pillowed flows of the Samar Ophiolite. Major, trace and rare earth element signatures of the volcanic rock samples indicate moderate to strong subduction-related influences and formation in an island arc setting. In contrast to other similarly-aged ophiolites along the eastern margin of the archipelago, those to the north of Samar Island exhibit weak to almost mid-oceanic ridge characteristics. These differences in the geochemical signatures of the ophiolites and ophiolitic complexes along eastern Philippines require a re-evaluation of a previous model suggesting that these ophiolites originated from a single oceanic lithosphere, possibly the proto-Philippine Sea Plate.

Article title: Adakitic rocks in the Masara gold-silver mine, Compostela Valley, Mindanao, Philippines: Different places, varying mechanisms?
Authors: Graciano P Yumul Jr, Walter W Brown, Carla B Dimalanta, Carlito A Ausa, Decibel V Faustino-Eslava, Betchaida D Payot, Noelynna T Ramos, Adrian Nicol L Lizada, Alfred Elmer Buena, Barbie Ross B Villaplaza, Pearlyn C Manalo, Karlo L Queaño, Juan Miguel R Guotana, Nichole Anthony D Pacle

Publication title: Journal of Asian Earth Sciences 142:45-55, June 2016

Abstract:

The presence of adakites has been used as an indicator for the occurrence of gold mineralization in many mineral prospecting works. Traditionally, the unique geodynamic controls to adakite formation, particularly the high temperature gradient and other slab-melting requirements, have been taken as key elements that must be present during their formation. However, several studies have suggested alternative mechanisms. This paper presents fractional crystallization as the most viable mechanism for the generation of adakitic rocks in the Masara gold-silver mine in Eastern Mindanao, Philippines. Furthermore, this paper also argues that the occurrence of adakitic rocks does not necessarily indicate the presence of mineralization. Depending on the scale, their occurrence may be an exploration marker at a regional or district level, but at the mine-level, other more localized parameters will have to be considered.

Article title: Geochemical and Geophysical Characteristics of the Balud Ophiolitic Complex (BOC), Masbate Island, Philippines: Implications for its Generation, Evolution and Emplacement

Authors: Pearlyn C Manalo, Carla B Dimalanta, Decibel V Faustino-Eslava, Betchaida D Payot, Noelynna T Ramos, Karlo L Queaño, Americus DC Perez, Graciano P Yumul Jr

Publication title: Terrestrial, Atmospheric & Oceanic Sciences 26 (6), December 2015

Abstract:

This paper presents the first field, geochemical and geophysical information on the recently recognized Early Cretaceous Balud Ophiolitic Complex (BOC) in the island of Masbate in the Central Philippines. Mapping of the western limb of the island revealed that only the upper crustal section of the BOC is exposed in this area. Geochemically, the pillow basalts are characterized by transitional mid-oceanic ridge basalt-island arc tholeiitic compositions. Gravity surveys yielded low Bouguer anomaly values that are consistent with the highly dismembered nature of the BOC. Short wavelength, high amplitude magnetic anomalies registered across the study area are attributed to shallow magnetic sources. This is taken to support the model that the ophiolitic complex occurs as thin crustal slivers that are not deeply-rooted in the mantle. Comparing BOC with other ophiolites in the Central Philippines, such as those in the islands of

Sibuyan, Leyte and Bohol, suggests the possibility of a common or contiguous source for similarly-aged and geochemically composed crust-mantle sequences in the region.
Full text link: https://tinyurl.com/y9mr6qdh

Article title: Paleomagnetism of the Samar Ophiolite: Implications for the Cretaceous sub-equatorial position of the Philippine island arc
Authors: Hertz G Balmater, Pearlyn C Manalo, Decibel V Faustino-Eslava, Karlo L Queaño, Carla B Dimalanta, Juan Miguel R Guotana, Noelynna T Ramos, Betchaida D Payot, Graciano P Yumul Jr
Publication title: Tectonophysics: 664, October 2015

Abstract:
Samar island in the eastern part of Central Philippines is underlain by a complete ophiolite suite, the Samar Ophiolite. We present the first geochronological and paleomagnetic data for the Samar Ophiolite. Whole rock K-Ar dating of two basalt samples yielded an age of 100.2 ± 2.7 Ma and 97.9 ± 2.8 Ma. Thirteen sites in four localities yielded characteristic remanent magnetization with in situ direction of D = 340°, I = - 24°, k = 15, α95 = 11° and tilt-corrected direction of D = 342°, I = - 27°, k = 15, α95 = 11°. These values suggest that the ophiolitic basement rocks of Samar formed in the Late Cretaceous at a paleolatitude of 14°S ± 6°. The paleolatitude is several degrees south of the sub-equatorial positions calculated for the three other Mesozoic ophiolites of the Philippine Mobile Belt (PMB) whose paleomagnetism had been previously studied. The PMB ophiolites in eastern and central Philippines share a common age, geochemistry and paleolatitude with the Halmahera Ophiolite, suggesting that they originated from a Mesozoic supra-subduction zone that spanned a few degrees north of the equator to around 15°S.

Article title: Podiform chromitite formation in a low-Cr/high-Al system: An example from the Southwest Indian Ridge (SWIR)
Authors: Betchaida D Payot, Shoji Arai, Henry JB Dick, Natsue Abe, Yuji Ichiyama
Publication title: Mineralogy and Petrology 108(4): 533-549, August 2013

Abstract:

Recent reassessment of abyssal peridotites obtained during the dredging of the oblique supersegment and the easternmost subsection of the Southwest Indian Ridge by the R/V Knorr Cruise 162 and the R/V Yokosuka YK98-07 revealed the occurrence of dunites containing podiform chromitites and dunites with variable chromite concentration closely associated with lherzolite and harzburgite. The size of the chromitite pods varies from a few mm to 2 cm in width. Chromites in the podifom chromitites have very low Cr# (=0.22–0.23) and low TiO2 (<0.17 wt%). They are almost free of silicate inclusions except for a few euhedral sulfide grains which occur far from cracks and lamellae and are considered primary in origin. The lherzolite which possibly represents the wallrock hosting the dunites with podiform chromitites also show low spinel Cr#(=0.16) and low Cr# in the clinopyroxenes (=0.09–0.10) and orthopyroxenes (=0.07–0.09). The small size of the SWIR podiform chromitites is strongly controlled by the low Cr/Al available in the wallrock and the invading melt. The presence of sulfide inclusions and the absence of PGEs further attest to the low Cr/Al (i.e. low refractoriness) in the system involved in the genesis of the SWIR podiform chromitites. Lastly, the discovery of podiform chromitites in the SWIR implies that the formation of podiform chromitite at mid-oceanic ridges, regardless of its spreading rate, is highly possible.

Full text link: https://tinyurl.com/ycsxqnjc

Article title: Textural Evidence for the Chromite-Oversaturated Character of the Melt Involved in Podiform Chromitite Formation

Authors: Betchaida D Payot, Shoji Arai, Rodolfo A Tamayo Jr, Graciano P Yumul Jr

Publication title: Resource Geology 63(3): 313-319, July 2013

Abstract:

Well-preserved oval-shaped dunite clots occur within the exceptionally fresh massive podiform chromitites from the Coto Block of the Zambales Ophiolite Complex, the Philippines. The dunite/chromitite boundary shows an interlocking texture; olivine inclusions in chromites in the podiform chromitites show the same optical extinction with larger adjacent olivines in the dunite clots. This texture was formed by the reaction between chromite-oversaturated melt and its dunite inclusions. The existence of such type of melt was previously only hypothesized to explain the origin of layered and podiform chromitites but is now confirmed by this discovery.

Full text link: https://tinyurl.com/y9s8mvwm

Article title: Lithospheric mantle connection of clinopyroxene inclusions in chromites from the Archean Nuasahi ultramafic-mafic complex (India)
Authors: Sisir Mondal, Shoji Arai, Betchaida D. Payot, Akihiro Tamura
Conference title: GOLDSCHMIDT 2013, Florence Italy

Abstract: No abstract

Article title: Petrographical and geochemical characteristics of the sheeted dyke-gabbro transition zone in ODP/IODP Hole 1256D
Authors: Marie Phyton, Lyderic France, Benedicte Abily, Natsue Abe, J. C. Alt, Marguerite Godard, Benoit Ildefonse, Jurgen Koepke, M. D. Kurtz, R. Oizumi, B. D. Payot
Conference title: EGU General Assembly 2012

Abstract:
During IODP Expedition 335, high grade granoblastic hornfels were extensively recovered as drilling cuttings at the gabbro-sheeted dyke transition zone of ODP Hole 1256D (East Pacific Rise, 6°44.163'N, 91°56.061'W). This lithology probably results from high-temperature metamorphism of previously hydrothermally altered diabases and/or basalts; the heat source likely stems from the melt lens located at the top of the magmatic chambers imaged along present-day fast-spreading ridges. This lithology, associated with gabbroic bodies, characterises the transition zone between the sheeted dyke complex and the uppermost gabbroic section, and represents the interface between magmatic and hydrothermal convecting systems in an oceanic crust formed at fast-spreading ridges. In this study, 14 samples from the junk basket (cuttings) and 2 samples from cores obtained during Expedition 335 were observed and analysed. The petrological and chemical characteristics of 5 granoblastic samples collected during Expedition 312 at the root of the sheeted dyke complex and between two gabbroic horizons were also acquired for comparison. Samples collected during IODP Expedition 335 are mainly fine grained oxide grabbronorites composed of two pyroxenes, plagioclases and oxides (ilmenite, magnetite) with more or less amphiboles, sulphides, quartz and accessory minerals. Orthopyroxene Shape (roundish or anhedral), the amount of oxide inclusions in clinopyroxene

and plagioclase morphology (laths or triple-junction mosaic) indicate various recrystallisation degrees. Plagioclases show a strong zoning in the less recrystallised samples, which tend to disappear with increasing recrystallisation degree. Samples show usually low alteration (less than 10%) with moderate transformation of pyroxenes into talc or actinolite. Samples from Expedition 312 show finer grains, higher degree of alteration (up to 30%), and weaker recrystallisation. They are mainly composed of plagioclases, amphibole and oxides (ilmenite, magnetite) with more or less pyroxenes, quartz and alteration phases. Samples from the higher stratigraphic level (root of the sheeted dyke complex above the shallowest gabbro) are virtually free of pyroxenes while the strongly recrystallised samples from the bottom of the hole (i.e. closer to the gabbroic section) contain only episodic amphibole and are rich in pyroxenes. The composition of plagioclase ranges from An12 to An85, with higher anorthite contents observed in the most recrystallised samples. Pyroxenes composition ranges from Wo37En46Fs17 to Wo46En38Fs16 for Cpx and Wo4En59Fs37 to Wo2En65Fs33 for Opx, and does not show any significant variation with the recrystallisation degree. Temperatures of recrystallisation were estimated between 902 and 980°C using the two-pyroxenes geothermometer. Heating and probable partial melting resulting from magmatic activity below hydrothermally altered sheeted dyke complex would lead to metamorphism and recrystallisation associated with light elements migration. This process would lead to variations in the modal composition of the rock and in the chemical composition of the minerals stable in hydrothermal and magmatic conditions.

Article title: IODP expedition 335: deep sampling in ODP hole 1256D

Authors: Damon AH Teagle, Benoit Ildefonse, Henry J. B. Dick, Daisuke Endo, E. C. Ferre, Lyderic France, Marguerite Godard, Gilles Guerin, Michelle Harris, Yoom-Mi Kim, Juergen H. Koepke, Mark Kurz, Peter Blum, Johan Lissenberg, Sumyo Miyashita, Antony Morris, Ryo Oizumi, Betchaida D. Payot

Publication title: Scientific Drilling 13: 28-34 April 2012

Abstract:

Observations of the gabbroic layers of untectonized ocean crust are essential to test theoretical models of the accretion of new crust at mid-ocean ridges. Integrated Ocean Drilling Program (IODP) Expedition 335 ("Superfast Spreading Rate Crust 4") returned to Ocean Drilling Program

(ODP) Hole 1256D with the intention of deepening this reference penetration of intact ocean crust a significant distance (~350 m) into cumulate gabbros. Three earlier cruises to Hole 1256D (ODP 206, IODP 309/312) have drilled through the sediments, lavas, and dikes and 100 m into a complex dike-gabbro transition zone. Operations on IODP Expedition 335 proved challenging throughout, with almost three weeks spent re-opening and securing unstable sections of the hole. When coring commenced, the comprehensive destruction of the coring bit required further remedial operations to remove junk and huge volumes of accumulated drill cuttings. Hole-cleaning operations using junk baskets were successful, and they recovered large irregular samples that document a hitherto unseen sequence of evolving geological conditions and the intimate coupling between temporally and spatially intercalated intrusive, hydrothermal, contact-metamorphic, partial melting, and retrogressive processes. Hole 1256D is now clean of junk, and it has been thoroughly cleared of the drill cuttings that hampered operations during this and previous expeditions. At the end of Expedition 335, we briefly resumed coring before undertaking cementing operations to secure problematic intervals. To ensure the greatest scientific return from the huge efforts to stabilize this primary ocean lithosphere reference site, it would be prudent to resume the deepening of Hole 1256D in the nearest possible future while it is open to full depth.

Full text link: https://tinyurl.com/ydxnuc82

Article title: A chromian spinel-oversaturated melt for podiform chromitite formation: Evidence from well-preserved dunite clots in massive podiform chromitites in the Coto Block, Zambales Ophiolite Complex, Philippines

Authors: BD Payot, S Arai, RA Tamayo Jr, GP Yumul Jr

Publication Title: EGUGA pp5858, April 2012

Abstract:

Oval-shaped dunite clots occur within massive podiform chromitites in the Coto Block of the Zambales Ophiolite Complex, Philippines. The size of the well-preserved dunite clots ranges from 3-4 cm in length and 1.5-2 cm in width. These dunite clots are composed mainly of olivine, spinel and very minor amounts of serpentine. Olivines are mostly subhedral and coarse-grained reaching up to 3 mm across. Compared to the spinels in the massive podiform chromitites, the dark brown spinels in dunite are anhedral to subhedral and are generally smaller (<0.5 mm).

The massive podiform chromitites hosting the dunite clots are primarily composed of spinel (95%) with olivine, plagioclase, serpentine and chlorite as the interstitial silicate matrix (5%). The reddish brown spinels are subhedral to euhedral and are coarse-grained reaching up to 5 mm across. The contact between the massive podiform chromitites and the dunite is very ragged and irregular. Near the contact, rounded to lobate olivine grains (<0.5 mm in diameter) occur as inclusions within the spinels in the massive podiform chromitites. These olivine inclusions show the same/continuous optical extinction as the adjacent and large olivines in the dunite. The Cr# of chromian spinel in the dunite clots and the massive podiform chromitites falls within a very narrow range (Cr#=0.42-0.52). However, the Cr# of the chromian spinel in the dunite clots (Cr#=0.47-0.52) is slightly higher than the massive podiform chromitites (Cr#=0.46-0.0.48). The former similarly shows higher Fe3+ content than the latter. TiO2 content of the chromian spinels in the dunite clots and the massive podiform chromitites is generally low (<0.11 wt%). Olivines in the dunite clots show slightly lower Fo content (=93-95) than the olivines in the interstices of the massive podiform chromitites (=95-96). The former similarly have lower NiO contents (=0.40-0.59 wt%) compared to the latter (=0.50-0.84 wt%). The occurrence of the well-preserved dunite clots in the massive podiform chromitites possibly provide us with evidence to indicate the chromian spinel-oversaturated character of the melt involved in the formation of podiform chromitite. The existence of such type of melt was only hypothesized by Irvine (1977) based on the interpretation of stratiform chromitite genesis.

Article title: Abyssal harzburgite veined by silica-oversaturated melt in the Sibuyan Ultramafics, Romblon, Central Philippines

Authors: Betchaida D Payot, Shoji Arai, Rodolfo A Tamayo Jr

Publication title: Journal of Mineralogical and Petrological Sciences 106(3): 175-180, June 2011

Abstract:

Thin discordant gabbronorite veins (~0.5 mm to 3 cm in width) occur within remarkably fresh harzburgite boulders of the Sibuyan Ultrarnafics. The harzburgite host rock displays protogranular to porphyroclastic textures and is dominantly composed of olivine. orthopyroxene with minor amounts of clinopyroxene, spinel and am-plubole. The mineral chemistry of the harzburgite is comparable to depleted abyssal perklotites as shown by the Fo content of the ohvine (= 90-91) and Cr# of the spinel (= 0.40-0.52). The gabbronorites are

coarse-grained adcumulates and comprised of orthopyroxene, plagioclase and amphibole. Plagioclase hi the gabbronorites shows high An content whereas both oithopyroxene and amphibole show variable Mg# almost similar to reported values from arc gabbros. The contact between the harzburgite and the gabbronorite veins is demarcated by the foimation of secondary orthopyroxene with low Cr2O3 and CaO contents. Clinopyroxetie in the harzbur-gite shows strong enrichment in light rare earth elements (LREEs). Amphibole rimming the clinopyroxene in the harzburgite has similar patterns as the clinopyroxene but with much higher REE abundance. The amphibole in the gabbronorites also shows enrichment in LREEs, Rb, Ba and Ti. We propose that the harzburgite-gab-bronorite occurrence in the Sibuyan Ultrarnafics is a product of mantle-melt reaction. The metasornatic agent is a silicate melt enriched in Si, Cr, Fe and LREEs. At a bigger scale, the harzburgite-gabbionoiite connection observed in the Sibuyan Ultramafics possibly documents early stage modification and conversion of abyssal peri-dotites to ophiolitic peridotites by SSZ-related melts.

Full text link: https://tinyurl.com/ybaanaf9

Article title: Unusual ultra-depleted dunite from Sibuyan Island (the Philippines): A residue for ultra-depleted MORB?

Authors: Betchaida D Payot, Shoji Arai, Akihiro Tamura, Satoko Ishimaru, Rodolfo A Tamayo Jr

Publication title: Journal of mineralogical and petrological sciences, January 2010

Abstract:

Ultra-depleted dunites from the Sibuyan Island, Romblon (Central Philippines) are primarily composed of olivine, orthopyroxene (<5%), trace clinopyroxene and chromian spinel and are totally free of hydrous Minerals and plagioclase. Mineral chemistry shows very refractory compositions (olivine Fo = 92-94; spinel Cr# > 0.75). Rare clinopyroxene preserved in the Ultra-depleted dunites is anhedral and interstitial to olivine grains. They are neither subsolidus exsolution products from orthopyroxene nor metasomatic in origin. Clinopyroxene has high Mg# = 0.94-0.97 and low Al2O3 Contents (<0.85 wt%). They are also very depleted in trace elements with only selected heavy rare earth elements detected during the LA-ICP-MS analysis. Light to middle REEs and LILEs were hardly detected, which is indicative of the very depleted character of the melt that precipitated the clinopyroxene. The calculated melts in equilibrium

with the clinopyroxene have heavy REE contents similar to olivine-hosted ultra-depleted melts of MORB affinity from the East Pacific Rise and the Mid-Atlantic Ridge. The formation of the Sibuyan Ultra-depleted dunites is being attributed to extremely high degree of dry melting below a mid-oceanic ridge.

Full text link: https://tinyurl.com/yccom9fj

Article title: What underlies the Philippine island arc? Clues from the Calaton Hill, Tablas island, Romblon (Central Philippines)

Authors: BD Payot, S Arai, RA Tamayo Jr, GP Yumul Jr.

Publication title: Journal of Asian Earth Sciences 36 (4-5): 371-389, October 2009

Abstract:

We report here for the first time the occurrence of a high-temperature metamorphic/plutonic complex (amphibolites, metagabbros, hornblende pyroxenites and hornblendites) in Calaton Hill, Tablas island, Romblon, Central Philippines. The mineral assemblages and relic magmatic textures in these rocks imply apparent derivation from arc-related protoliths. Major element and trace element data are also comparable to those of gabbroic rocks in arc-related setting. Subsolidus re-equilibration under granulite to amphibolite facies is documented by the triple junctions between mineral phases in the different lithologies, the recrystallization of plagioclase and the presence of coronas around olivine with mineral assemblage of orthopyroxene + amphibole ± green spinel. The formation of hornblendite and the pervasive occurrence of amphiboles in the different lithologies are being attributed to the infiltration of a younger hydrous arc magma which also caused metamorphism and hybridization on the surrounding rocks. The characteristics of the Calaton Hill samples are comparable with those of the well-studied xenoliths from Ichinomegata, NE Honshu arc, Japan. We therefore interpret the Calaton Hill metamorphic/plutonic complex as representative of the lower crust underlying the Philippine island arc.

Article title: Geology and Hydrothermal Alteration of the Low Sulfidation

Authors: Betchaida D Payot, Victor B Maglambayan, Carla B Dimalanta, Graciano P Yumul, Rodolfo A Tamayo, Toshihiko Matsuda, Shigeyuki Suzuki, Herve Bellon

Publication title: Resource Geology 55(3): 155-162, November 2008

Abstract:

The Pantingan Gold System (PGS) is a vein-type epithermal prospect exposed within the summit caldera of Mount Mariveles, Bagac, Bataan (Luzon), Philippines. It consists of nine major veins, eight of which trend NW-WNW and distributed in an en echelon array. The eastern tips of these veins appear to terminate near the NE-NNE trending Vein 1, which is located in the easternmost portion of the prospect. Metal assay results on vein and wall rock samples indicate concentrations of 0.01 to 1.1 g/ton Au, trace to 34 g/ton Ag and 0.003 to 0.02 % Cu. Andesite lava flow deposits host the PGS. Potassium-Argon isotopic dating of these andesites yields a narrow age range of 0.88± 0.13 to 1.13 ± 0.17 Ma. The surface exposures of the veins (up to 5 m wide) are encountered at different levels between 590–740 masl. These commonly display a massive texture although banding prominently occurs in Vein 1. The veins consist of gray to cream-colored crystalline and chalcedonic quartz and amorphous silica. Pyrite is the most ubiquitous sulfide mineral. It occurs either as fine-grained disseminations and aggregates in quartz or as infillings in vugs. Calcite, marcasite and bornite are also occasionally noted in the deposit. The prospect shows silicic, argillic, propylitic and advanced argillic alteration zones. Silicic and argillic alterations are confined in the immediate wall rocks of the quartz veins. Argillic alteration grades to a propylitic zone farther away from the veins. The advanced argillic alteration zone, indicated by a suite of acidic clay minerals that include kaolin-ite, dickite, pyrophyllite and alunite, might have been imprinted during the late stages of gold deposition. As a whole, the PGS displays geological and mineralogical features typical of gold mineralization in a low sulfidation, epithermal environment. It is also representative of a young, tectonically undisturbed gold deposit.

Article title: Metasomatic interactions between slab-derived melts and depleted mantle: Insights from xenoliths within Monglo adakite (Luzon arc, Philippines)

Authors: M Grégoire, Sébastien Jégo, RC Maury, Mireille Polvé, B Payot, RA Tamayo Jr, GP Yumul Jr

Publication title: Lithos 103 (3-4): 415-430, July 2008

Abstract:

The Monglo adakite contains mafic and ultramafic xenoliths, which probably originated from the mantle section of an Early Cretaceous supra-subduction zone ophiolitic complex located within the Luzon arc crust. Spinel-bearing dunites are dominant among this xenolith collection and display evidence for three episodes of subduction-related melt percolation. The first one is evidenced by an undeformed clinopyroxene characterized by convex-upwards REE pattern. This clinopyroxene crystallized from a calc-alkaline basaltic magma, likely formed in the Cretaceous supra-subduction setting of the ophiolite. Then, two metasomatic events, evidenced by orthopyroxene-rich and amphibole-rich secondary parageneses, respectively, affected most of the spinel dunites. The opx-rich paragenesis is related to the circulation within the dunitic upper mantle of hydrous slab-derived melts similar to those affecting the mantle peridotite xenoliths from Papua New Guinea and Kamchatka. Finally the amphibole-rich veins are related to the interaction between the studied dunite xenoliths and the host adakite or an adakitic melt similar to it.

Full text link: https://tinyurl.com/ya4vxkg7

Article title: Behavior of Major and Trace Elements during Ore Deposition: Example from the Low-Sulfidation Pantingan Gold System, Mount Mariveles, Bataan, Philippines

Authors: Betchaida D Payot, Rodolfo A Tamayo Jr, Victor B Maglambayan, Carla B Dimalanta, Graciano P Yumul Jr, Shigeyuki Suzuki, Mei-Fu Zhou

Publication title: Resource geology 57 (2): 180-196, June 2007

Abstract:

The evaluation of the relatively fresh host rock and altered rock samples associated with the Pantingan Gold System exposed in Mount Mariveles, Bataan yield several notable observations that are useful in pinpointing potential gold pathfinder elements. Geochemical and petrologic analysis showed that the altered rocks can be subdivided into rocks that underwent propylitic alteration (group 1), argillized rocks with silica contents similar to those of the fresh host rocks (group 2), argillized but not strongly silicified rocks (group 3) and argillized and strongly silicified rocks (group 4). Selected element ratio patterns in the altered rocks and gold concentrations in gold-bearing quartz veins vary between the rock groups. Moreover, mass balance calculation also reflected the geochemical observations pertaining to the gains and losses of SiO2, Fe2O3+ MgO, CaO + Na2O and K2O, which are believed to be chemical

reactions (i.e. breakdown of plagioclase, silica inundation or leaching, sulfide and calcite formation) caused by the influx of hydrothermal fluids.

Article title: Temporal Geochemical Evolution of Neogene Magmatism in the Baguio Gold–Copper Mining District (Northern Luzon, Philippines)
Authors: Mireille Polvé, Rene C Maury, Sebastien Jego, Hervé Bellon, Ahmed Margoum, Graciano P Yumul Jr, Betchaida D Payot, Rodolfo A Tamayo Jr, Joseph Cotten
Publication title: Resource Geology 57(2): 197-218, June 2007

Abstract:
Baguio, in the Central Cordillera of Northern Luzon, is a district that displays porphyry copper and epithermal gold mineralization, associated with Early Miocene–Pliocene–Quaternary calc-alkaline and adakitic intrusions. Systematic sampling, K-Ar dating, major and trace elements, and Sr, Nd, Pb isotopic analyses of fresh magmatic rocks indicate three magmatic pulses: an Early Miocene phase (21.2–18.7 Ma), a Middle–Late Miocene phase (15.3–8 Ma) and finally a Pliocene–Quaternary event (3–1 Ma). The first phase emplaced evolved calc-alkaline magmas, essentially within the Agno Batholith complex, and is thought to be related to the westward-dipping subduction of the West Philippine Basin. After a quiescence period during which the Kennon limestone was deposited, magmatic activity resumed at 15.3 Ma, in connection with the start of the subduction of the South China Sea along the Manila Trench. It emplaced first petrogenetically related and relatively unradiogenic low-K calc-alkaline lavas and intermediate adakites. Temporal geochemical patterns observed from 15.3 to 1 Ma include progressive enrichment in K and other large ion lithophile elements, increase in radiogenic Sr and Pb and corresponding decrease in radiogenic Nd. These features are thought to reflect the progressive addition to the Luzon arc mantle wedge of incompatible elements largely inherited from South China Sea sediments. The origin of the long quiescence period, from 8 to 3 Ma, remains problematic. It might represent a local consequence of the docking of the Zambales ophiolitic terrane to Northern Luzon. Then, magmatic activity resumed at 3 Ma, emplacing chemically diversified rocks ranging from low K to high K and including a large proportion of adakites, especially during the Quaternary (dacitic plugs). The authors tentatively relate this diversity to the development of a slab tear linked with the subduction of the fossil South China Sea ridge beneath the Baguio area.

Full text link: https://tinyurl.com/yc2smofh

Article title: The oceanic substratum of Northern Luzon: Evidence from xenoliths within Monglo adakite (the Philippines)

Authors: Betchaida D Payot, Sebastien Jego, Rene C Maury, Mireille Polve, Michel Gregoire, Georges Ceuleneer, Rodolfo A Tamayo Jr, Graciano P Yumul Jr, Herve Bellon, Joseph Cotten

Publication title: Island Arc 16(2): 276-290, February 2007

Abstract:

A 8.65 Ma adakitic intrusive sheet exposed near Monglo village in the Baguio District of Northern Luzon contains a suite of ultramafic and mafic xenoliths including in order of abundance: spinel dunites showing typical mantle-related textures, mineral and bulk rock compositions, and serpentinites derived from them; amphibole-rich gabbros displaying incompatible element patterns similar to those of flat or moderately enriched back-arc basin basalt magmas; and amphibolites derived from metabasalts and/or metagabbros of identical affinity. A single quartz diorite xenolith carrying a similar subduction-related geochemical signature has also been sampled. One amphibolite xenolith provided a whole-rock K-Ar age of 115.6 Ma (Barremian). We attribute the origin of this suite to the sampling by ascending adakitic magmas of a Lower Cretaceous ophiolitic complex located at a depth within the 30-35 km thick Luzon crust. It could represent an equivalent of the Isabela-Aurora and Pugo-Lepanto ophiolitic massifs exposed in Northern Luzon.

Full text link: https://tinyurl.com/ycrzxrme

Article title: Geology and Hydrothermal Alteration of the Low Sulfidation Pantingan Gold System, Mount Mariveles, Bataan (Luzon), Philippines

Authors: Betchaida D Payot, Victor B Maglambayan, Carla B Dimalanta, Graciano P Yumul, Rodolfo A Tamayo, Toshihiko Matsuda, Shigeyuki Suzuki, Herve Bellon

Publication title: Resource Geology 55(3): 155-162, January 2005

Abstract:

The Pantingan Gold System (PGS) is a vein-type epithermal prospect exposed within the summit caldera of Mount Mariveles, Bagac, Bataan (Luzon), Philippines. It consists of nine

major veins, eight of which trend NW-WNW and distributed in an en echelon array. The eastern tips of these veins appear to terminate near the NE-NNE trending Vein 1, which is located in the easternmost portion of the prospect. Metal assay results on vein and wall rock samples indicate concentrations of 0.01 to 1.1 g/ton Au, trace to 34 g/ton Ag and 0.003 to 0.02 % Cu. Andesite lava flow deposits host the PGS. Potassium-Argon isotopic dating of these andesites yields a narrow age range of 0.88 +/- 0.13 to 1.13 +/- 0.17 Ma. The surface exposures of the veins (up to 5 m wide) are encountered at different levels between 590-740 masl. These commonly display a massive texture although banding prominently occurs in Vein 1. The veins consist of gray to cream-colored crystalline and chalcedonic quartz and amorphous silica. Pyrite is the most ubiquitous sulfide mineral. It occurs either as fine-grained disseminations and aggregates in quartz or as infillings in vugs. Calcite, marcasite and bornite are also occasionally noted in the deposit. The prospect shows silicic, argillic, propylitic and advanced argillic alteration zones. Silicic and argillic alterations are confined in the immediate wall rocks of the quartz veins. Argillic alteration grades to a propylitic zone farther away from the veins. The advanced argillic alteration zone, indicated by a suite of acidic clay minerals that include kaolinite, dickite, pyrophyllite and alunite, might have been imprinted during the late stages of gold deposition. As a whole, the PGS displays geological and mineralogical features typical of gold mineralization in a low sulfidation, epithermal environment. It is also representative of a young, tectonically undisturbed gold deposit.

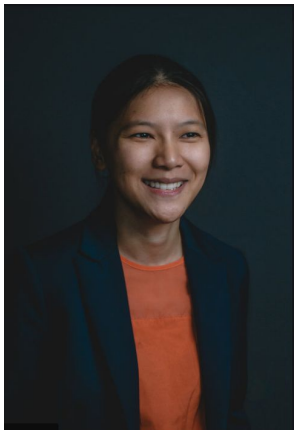

REINABELLE REYES
University of the Philippines

Sex: Female

Education:

Princeton University, Doctor of Philosophy Astrophysics, 2006-2011

Abdus Salam International Center for Theoretical Physics, Diploma in High Energy Physics, 2005-2006

Ateneo de Manila University, Bachelor of Science in Physics, 2001-2005

Field of Specialization

Data Science

Data Analytics

Physics

Researches:

Article Title: Predicting Galaxy Star Formation Rates via the Co-evolution of Galaxies and Halos

Authors: Douglas F. Watson, Andrew P. Hearin, Andreas A. Berlind, Matthew A. Becker, Peter S. Behroozi, Ramin A. Skibba, Reinabelle Reyes, Andrew R. Zentner,

Publication title: Monthly Notices of the Royal Astronomical Society 446(1), March 2014

Abstract:

In this paper, we test the age matching hypothesis that the star formation rate (SFR) of a galaxy of fixed stellar mass is determined by its dark matter halo formation history, e.g. more quiescent galaxies reside in older haloes. We present new Sloan Digital Sky Survey measurements of the galaxy two-point correlation function and galaxy–galaxy lensing as a function of stellar mass and SFR, separated into quenched and star-forming galaxy samples to test this simple model. We find that our age matching model is in excellent agreement with these new measurements. We also find that our model is able to predict: (1) the relative SFRs of central and satellite galaxies, (2) the SFR dependence of the radial distribution of satellite galaxy populations within galaxy groups, rich groups, and clusters and their surrounding larger scale environments, and (3) the interesting feature that the satellite quenched fraction as a function of projected radial distance from the central galaxy exhibits an ~r−.15 slope, independent of environment. These accurate predictions are intriguing given that we do not explicitly model satellite-specific processes after infall, and that in our model the virial radius does not mark a special transition region in the evolution of a satellite. The success of the model suggests that present-day galaxy SFR is strongly correlated with halo mass assembly history.

Full text link: https://tinyurl.com/yamz34wv

Article title: The Dark Side of Galaxy Color: evidence from new SDSS measurements of galaxy clustering and lensing

Authors: Andrew P. Hearin, Douglas F. Watson, Matthew R. Becker, Reinabelle Reyes, Andreas A. Berlind, Andrew R. Zentner

Publication title: Monthly Notices of the Royal Astronomical Society 444(1), October 2013

Abstract

The age-matching model has recently been shown to predict correctly the luminosity L and g − r colour of galaxies residing within dark matter haloes. The central tenet of the model is intuitive: older haloes tend to host galaxies with older stellar populations. In this paper, we demonstrate that age matching also correctly predicts the g − r colour trends exhibited in a wide variety of statistics of the galaxy distribution for stellar mass M* threshold samples. In particular, we

present new Sloan Digital Sky Survey (SDSS) measurements of galaxy clustering and the galaxy–galaxy lensing signal ΔΣ as a function of M* and g − r colour, and show that age matching exhibits remarkable agreement with these and other statistics of low-redshift galaxies. In so doing, we also demonstrate good agreement between the galaxy–galaxy lensing observed by SDSS and the ΔΣ signal predicted by abundance matching, a new success of this model. We describe how age matching is a specific example of a larger class of conditional abundance matching models (CAM), a theoretical framework we introduce here for the first time. CAM provides a general formalism to study correlations at fixed mass between any galaxy property and any halo property. The striking success of our simple implementation of CAM suggests that this technique has the potential to describe the same set of data as alternative models, but with a dramatic reduction in the required number of parameters. CAM achieves this reduction by exploiting the capability of contemporary N-body simulations to determine dark matter halo properties other than mass alone, which distinguishes our model from conventional approaches to the galaxy–halo connection.

Full text link: https://tinyurl.com/yb85jwdx

Article title: Is LambdaCDM consistent with the Tully-Fisher relation?

Author: Reinabelle Reyes, Gunn, J.E., Mandelbaum, R.

Publication title : Probes of Dark Matter on Galaxy Scales, AAS Topical Conference Series Vol. 1. (Proceedings of the conference held 14-19 July 2013 in Monterey, CA. Bulletin of the American Astronomical Society, Vol. 45, #7, #403.04)

Abstract:

We consider the question of the origin of the Tully-Fisher relation in LambdaCDM cosmology. Reproducing the observed tight relation between stellar masses and rotation velocities of disk galaxies presents a challenge for semi-analytical models and hydrodynamic simulations of galaxy formation. Here, our goal is to construct a suite of galaxy mass models that is fully consistent with observations, and that also reproduces the observed Tully-Fisher relation. We take advantage of a well-defined sample of disk galaxies in SDSS with measured rotation velocities (from long-slit spectroscopy of H-alpha), stellar bulge and disk profiles (from fits to SDSS images), and average dark matter halo masses (from stacked weak lensing of a larger, similarly-selected sample). The primary remaining freedom in the mass models come from the

final dark matter halo profile (after contraction from baryon infall and, possibly, feedback) and the stellar IMF. We find that the observed velocities are reproduced by models with Kroupa IMF and NFW (i.e., unmodified) dark matter haloes for galaxies with stellar masses 10^9-10^10 M_sun. For higher stellar masses, models with contracted NFW haloes are favored. A scenario in which the amount of halo contraction varies with stellar mass is able to reproduce the observed Tully-Fisher relation over the full stellar mass range of our sample from 10^9 to 10^11 M_sun. We present this as a proof-of-concept for consistency between LambdaCDM and the Tully-Fisher relation.

Article title: Cosmological parameter constraints from galaxy-galaxy lensing and galaxy clustering with the SDSS DR7

Authors: Rachel Mandelbaum, Anze Slosar, Tobias Baldauf, Uros Seljak, Christopher Hirata, Reinabelle Reyes, Robert E. Smith

Publication title: Monthly Notices of the Royal Astronomical Society 432(2,) July 2012

Abstract

Recent studies have shown that the cross-correlation coefficient between galaxies and dark matter is very close to unity on scales outside a few virial radii of galaxy haloes, independent of the details of how galaxies populate dark matter haloes. This finding makes it possible to determine the dark matter clustering from measurements of galaxy–galaxy weak lensing and galaxy clustering. We present new cosmological parameter constraints based on large-scale measurements of spectroscopic galaxy samples from the Sloan Digital Sky Survey (SDSS) data release 7. We generalize the approach of Baldauf et al. to remove small-scale information (below 2 and 4 h−1 Mpc for lensing and clustering measurements, respectively), where the cross-correlation coefficient differs from unity. We derive constraints for three galaxy samples covering 7131 deg2, containing 69 150, 62 150 and 35 088 galaxies with mean redshifts of 0.11, 0.28 and 0.40. We clearly detect scale-dependent galaxy bias for the more luminous galaxy samples, at a level consistent with theoretical expectations. When we vary both σ8 and Ωm (and marginalize over non-linear galaxy bias) in a flat Λ cold dark matter model, the best-constrained quantity is σ8(Ωm/0.25)0.57 = 0.80 ± 0.05 (1σ, stat. + sys.), where statistical and systematic errors (photometric redshift and shear calibration) have comparable contributions, and we have fixed ns = 0.96 and h = 0.7. These strong constraints on the matter clustering suggest that this method

is competitive with cosmic shear in current data, while having very complementary and in some ways less serious systematics. We therefore expect that this method will play a prominent role in future weak lensing surveys. When we combine these data with Wilkinson Microwave Anisotropy Probe 7-year (WMAP7) cosmic microwave background (CMB) data, constraints on σ8, Ωm, H0, wde and ∑mν become 30–80 per cent tighter than with CMB data alone, since our data break several parameter degeneracies.

Article title: Calibrated Tully–Fisher relations for improved estimates of disc rotation velocities
Authors: Reinabelle Reyes, R. Mandelbaum, J. E. Gunn, J. Pizagno, Claire N. Lacker
Publication title: Monthly Notices of the Royal Astronomical Society 417(3), November 2011

Abstract:

In this paper, we derive scaling relations between photometric observable quantities and disc galaxy rotation velocity Vrot or Tully–Fisher relations (TFRs). Our methodology is dictated by our purpose of obtaining purely photometric, minimal-scatter estimators of Vrot applicable to large galaxy samples from imaging surveys. To achieve this goal, we have constructed a sample of 189 disc galaxies at redshifts $z < 0.1$ with long-slit Hα spectroscopy from Pizagno et al. and new observations. By construction, this sample is a fair subsample of a large, well-defined parent disc sample of ~170 000 galaxies selected from the Sloan Digital Sky Survey Data Release 7 (SDSS DR7). The optimal photometric estimator of Vrot we find is stellar mass M★ from Bell et al., based on the linear combination of a luminosity and a colour. Assuming a Kroupa initial mass function (IMF), we find: $\log [V80/(\mathrm{km\ s^{-1}})] = (2.142 \pm 0.004) + (0.278 \pm 0.010)[\log (M★/M_\odot) - 10.10]$, where V80 is the rotation velocity measured at the radius R80 containing 80 per cent of the i-band galaxy light. This relation has an intrinsic Gaussian scatter dex and a measured scatter σmeas= 0.056 dex in log V80. For a fixed IMF, we find that the dynamical-to-stellar mass ratios within R80, (Mdyn/M★)(R80), decrease from approximately 10 to 3, as stellar mass increases from M★≈ 109 to 1011 M⊙. At a fixed stellar mass, (Mdyn/M★)(R80) increases with disc size, so that it correlates more tightly with stellar surface density than with stellar mass or disc size alone. We interpret the observed variation in (Mdyn/M★)(R80) with disc size as a reflection of the fact that disc size dictates the radius at which Mdyn/M★ is measured, and consequently, the fraction of the dark matter 'seen' by the gas at that radius. For the lowest M★ galaxies, we find a positive correlation between TFR

residuals and disc sizes, indicating that the total density profile is dominated by dark matter on these scales. For the highest M★ galaxies, we find instead a weak negative correlation, indicating a larger contribution of stars to the total density profile. This change in the sense of the correlation (from positive to negative) is consistent with the decreasing trend in (Mdyn/M★)(R80) with stellar mass. In future work, we will use these results to study disc galaxy formation and evolution and perform a fair, statistical analysis of the dynamics and masses of a photometrically selected sample of disc galaxies.

Article title: Optical-to-virial velocity ratios of local disk galaxies from combined kinematics and galaxy-galaxy lensing

Authors: Reinabelle Reyes, Rachel Mandelbaum, James E. Gunn, Reiko Nakajima, Uros Seljak, Chris M. Hirata

Publication Title: Monthly Notices of the Royal Astronomical Society 425(4), October 2011

Abstract:

In this paper, we measure the optical-to-virial velocity ratios Vopt/V200c of disk galaxies in the Sloan Digital Sky Survey (SDSS) at a mean redshift of = 0.07 and with stellar masses 10^9 M_sun < M_* < 10^11 M_sun. Vopt/V200c, the ratio of the circular velocity measured at the virial radius of the dark matter halo (\sim150 kpc) to that at the optical radius of the disk (\sim10 kpc), is a powerful observational constraint on disk galaxy formation. It links galaxies to their dark matter haloes dynamically and constrains the total mass profile of disk galaxies over an order of magnitude in length scale. For this measurement, we combine Vopt derived from the Tully-Fisher relation (TFR) from Reyes et al. with V200c derived from halo masses measured with galaxy-galaxy lensing. In anticipation of this combination, we use similarly-selected galaxy samples for both the lensing and TFR analysis. For three M_* bins with lensing-weighted mean stellar masses of 0.6, 2.7, and 6.5 x 10^10 M_sun, we find halo-to-stellar mass ratios M_vir/M_* = 41, 23, and 26, with 1-sigma statistical uncertainties of around 0.1 dex, and Vopt/V200c = 1.27\pm0.08, 1.39\pm0.06, 1.27\pm0.08 (1{\sigma}). Our results suggest that the dark matter and baryonic contributions to the mass within the optical radius are comparable, if the dark matter halo profile has not been significantly modified by baryons. The results obtained in this work will serve as inputs to and constraints on disk galaxy formation

models, which will be explored in future work. Finally, we note that this paper presents a new and improved galaxy shape catalogue for weak lensing that covers the full SDSS DR7 footprint.

Full text link: https://tinyurl.com/y7qvyxov

Article title: Photometric redshift requirements for lens galaxies in galaxy-galaxy lensing analyses

Authors: Reiko Nakahima, R. Mandelbaum, U. Seljak, J.D. Cohn, Reinabelle Reyes, Richard J. Cool

Publication Title: Monthly Notices of the Royal Astronomical Society 420(4), July 2011

Abstract:

Weak gravitational lensing is a valuable probe of galaxy formation and cosmology. Here we quantify the effects of using photometric redshifts (photo-z) in galaxy-galaxy lensing, for both sources and lenses, both for the immediate goal of using galaxies with photo-z as lenses in the Sloan Digital Sky Survey (SDSS) and as a demonstration of methodology for large, upcoming weak lensing surveys that will by necessity be dominated by lens samples with photo-z. We calculate the bias in the lensing mass calibration as well as consequences for absolute magnitude (i.e. k-corrections) and stellar mass estimates for a large sample of SDSS Data Release 8 (DR8) galaxies. The redshifts are obtained with the template-based photo-z code ZEBRA on the SDSS DR8 ugriz photometry. We assemble and characterize the calibration samples (˜9000 spectroscopic redshifts from four surveys) to obtain photometric redshift errors and lensing biases corresponding to our full SDSS DR8 lens and source catalogues. Our tests of the calibration sample also highlight the impact of observing conditions in the imaging survey when the spectroscopic calibration covers a small fraction of its footprint; atypical imaging conditions in calibration fields can lead to incorrect conclusions regarding the photo-z of the full survey. For the SDSS DR8 catalogue, we find $\sigma\Delta z/(1+z)= 0.096$ and 0.113 for the lens and source catalogues, with flux limits of r= 21 and 21.8, respectively. The photo-z bias and scatter is a function of photo-z and template types, which we exploit to apply photo-z quality cuts. By using photo-z rather than spectroscopy for lenses, dim blue galaxies and L* galaxies up to z˜ 0.4 can be used as lenses, thus expanding into unexplored areas of parameter space. We also explore the systematic uncertainty in the lensing signal calibration when using source photo-z, and both lens and source photo-z; given the size of existing training samples, we can constrain

the lensing signal calibration (and therefore the normalization of the surface mass density) to within 2 and 4 per cent, respectively.

Full text link: https://tinyurl.com/yct24suf

Article title: Calibrated Tully-fisher Relations For Improved Photometric Estimates Of Disk Rotation Velocities

Authors: Reinabelle Reyes, R. Mandelbaum, J.E. Gunn, J. Pizagno

Publication title: American Astronomical Society, AAS Meeting #217, id.430.06; Bulletin of the American Astronomical Society, Vol. 43, 2011

Abstract:

We present calibrated scaling relations (also referred to as Tully-Fisher relations or TFRs) between rotation velocity and photometric quantities-- absolute magnitude, stellar mass, and synthetic magnitude (a linear combination of absolute magnitude and color)-- of disk galaxies at z 0.1. First, we selected a parent disk sample of 170,000 galaxies from SDSS DR7, with redshifts between 0.02 and 0.10 and r band absolute magnitudes between -18.0 and -22.5. Then, we constructed a child disk sample of 189 galaxies that span the parameter space-- in absolute magnitude, color, and disk size-- covered by the parent sample, and for which we have obtained kinematic data. Long-slit spectroscopy were obtained from the Dual Imaging Spectrograph (DIS) at the Apache Point Observatory 3.5 m for 99 galaxies, and from Pizagno et al. (2007) for 95 galaxies (five have repeat observations). We find the best photometric estimator of disk rotation velocity to be a synthetic magnitude with a color correction that is consistent with the Bell et al. (2003) color-based stellar mass ratio. The improved rotation velocity estimates have a wide range of scientific applications, and in particular, in combination with weak lensing measurements, they enable us to constrain the ratio of optical-to-virial velocity in disk galaxies.

Article title: Confirmation of general relativity on large scales from weak lensing and galaxy velocities

Authors: Reinabelle Reyes, Rachel Mandelbaum, Uros Seljak, Tobias Baldauf, James E. Gunn, Lucas Lombriser, Robert E. Smith

Publication title: Nature 464 (7286) March 2010

Abstract:

Although general relativity underlies modern cosmology, its applicability on cosmological length scales has yet to be stringently tested. Such a test has recently been proposed, using a quantity, E(G), that combines measures of large-scale gravitational lensing, galaxy clustering and structure growth rate. The combination is insensitive to 'galaxy bias' (the difference between the clustering of visible galaxies and invisible dark matter) and is thus robust to the uncertainty in this parameter. Modified theories of gravity generally predict values of E(G) different from the general relativistic prediction because, in these theories, the 'gravitational slip' (the difference between the two potentials that describe perturbations in the gravitational metric) is non-zero, which leads to changes in the growth of structure and the strength of the gravitational lensing effect. Here we report that E(G) = 0.39 +/- 0.06 on length scales of tens of megaparsecs, in agreement with the general relativistic prediction of E(G) approximately 0.4. The measured value excludes a model within the tensor-vector-scalar gravity theory, which modifies both Newtonian and Einstein gravity. However, the relatively large uncertainty still permits models within f(R) theory, which is an extension of general relativity. A fivefold decrease in uncertainty is needed to rule out these models.

Full text available: https://tinyurl.com/y7f5e744

Article title: Space Density of Optically Selected Type 2 Quasars

Authors: Reinabelle Reyes, Nadia L. Zakamska, Michael A. Strauss, Joshua Green, Julian H. Krolik, Yue Shen, Gordon T. Richards, Scott F. Anderson, Donald P. Schneider

Publication title: The Astronomical Journal, 136 (6) : 2373, November 2008

Abstract:

Type 2 quasars are luminous active galactic nuclei whose central regions are obscured by large amounts of gas and dust. In this paper, we present a catalog of type 2 quasars from the Sloan Digital Sky Survey, selected based on their optical emission lines. The catalog contains 887 objects with redshifts z < 0.83; this is 6 times larger than the previous version and is by far the largest sample of type 2 quasars in the literature. We derive the [O III]5007 luminosity function (LF) for 108.3 L ⊙ < L [O III] < 1010 L ⊙ (corresponding to intrinsic luminosities up to M[2500 Å] –28 mag or bolometric luminosities up to 4 × 1047 erg s–1). This LF provides robust lower

limits to the actual space density of obscured quasars due to our selection criteria, the details of the spectroscopic target selection, and other effects. We derive the equivalent LF for the complete sample of type 1 (unobscured) quasars and determine the ratio of type 2 to type 1 quasar number densities. Our data constrain this ratio to be at least ~1.5:1 for 108.3 L ⊙ < L [O III] < 109.5 L ⊙ at z < 0.3, and at least ~1.2:1 for L [O III] ~ 1010 L ⊙ at 0.3 < z < 0.83. Type 2 quasars are at least as abundant as type 1 quasars in the relatively nearby universe (z 0.8) for the highest luminosities.

Full text link: https://tinyurl.com/y73k448a

Article title: Erratum: "Space Density of optically selected type 2 quasars" (2008, AJ, 136, 2373)
Authors: Reinabelle Reyes, Nadia L. Zakamska, Michael A. Strauss, Joshua Green, Julian H. Krolik, Yue Shen, Gordon T. Richards, Scott F. Anderson, Donald P. Schneider
Publication title: The Astronomical Journal 139 (3) : 1295, February 2010

Abstract:

Figure 12 of the paper "Space Density of Optically Selected Type 2 Quasars" compares the obscured quasar fractions derived in our work with those of other studies. Unfortunately, some of the points from these other studies were shown incorrectly. Specifically, the results from X-ray data—Hasinger (2004; open circles) and Ueda et al. (2003; open squares)—which we had taken from Figure 16 of Hopkins et al. (2006), were affected by a luminosity conversion error, in the sense that the displayed luminosities for these data were too high by ~1 dex. With this erratum, we correct this problem and update the figure. The new version (Figure 12) shows more recent results from Hasinger (2008), in lieu of the Hasinger (2004) data points. These are based on data in the redshift range z = 0.2-3.2 (open circles) in that work. The best linear fit to these data (black dashed line) is consistent with that derived for the redshift slice z = 0.4-0.8, which overlaps with the highest redshift bin in our study, and is higher than that derived for redshifts smaller than 0.4 (corresponding to a shift of ~0.7 dex in luminosity). Figure 12 also shows estimates of the obscured quasar fraction derived from the ratio of IR to bolometric luminosities of an AGN sample at redshift z ~ 1 (Treister et al. 2008; filled triangles). Because the obscured quasar fractions derived from our analysis (colored arrows) are strict lower limits, there was already a hint in the previous version of Figure 12 that at high quasar luminosities, we find higher obscured quasar fractions than X-ray surveys. The correction and updates of

Figure 12 strengthen this conclusion. At face value, our derived obscured quasar fractions are consistent with those from IR data (Treister et al. 2008; filled triangles). However, we find that they are significantly higher than those derived from X-ray surveys at , especially those from the recent analysis by Hasinger (2008). This comparison strongly suggests that optical selection successfully identifies a population of luminous obscured quasars that are missed by X-ray selection.

Article title: Test of Gravity on Large Scales with Weak Gravitational Lensing and Clustering Measurements of SDSS Luminous Red Galaxies
Authors: Reinabelle Reyes, R. Mandelbaum, U Seljak, J. Gunn, L. Lombriser
Publication title: American Astronomical Society, AAS Meeting #213, id.425.08; Bulletin of the American Astronomical Society, Vol. 41, p.253 January 2009

Abstract:
We perform a test of gravity on large scales (5-50 Mpc/h) using 70,000 luminous red galaxies (LRGs) from the Sloan Digital Sky Survey (SDSS) DR7 with redshifts 0.16<z<0.47. Following Zhang et al. (2007), we define a quantity E_G-- a combination of measurements of weak gravitational lensing, galaxy peculiar velocities, and galaxy clustering-- that can discriminate between different theories of gravity and is largely independent of galaxy bias and sigma_8. In particular, E_G is sensitive to the relation between the spatial and temporal scalar perturbations in the space-time metric. While these two potentials are equivalent in concordance cosmology (GR+LCDM) in the absence of anisotropic stress, they are not equivalent in alternative theories of gravity in general, so that different models make different predictions for E_G. We find E_G=0.37±0.05 averaged over scales 5<R<50 Mpc/h, consistent with the prediction of LCDM, E_G = 0.375-0.425, for Omega_m=0.258±0.027. We also compare our measurements with preliminary predictions from modified gravity theories, including f(R), DGP, and TeVeS. This work serves as a proof of concept for the application of this test in future galaxy surveys such as LSST, for which a very high signal-to-noise measurement will be possible.

Article title: Improved optical mass tracer for galaxy clusters calibrated using weak lensing measurements
Authors: Reinabelle Reyes, Rachel Mandelbaum, Christopher Hirata, N.A Bahcall, Uros Seljak

Publication title: Monthly Notices of the Royal Astronomical Society 390(3) 1157-1169, November 2008

Abstract:

We develop an improved mass tracer for clusters of galaxies from optically observed parameters, and calibrate the mass relation using weak gravitational lensing measurements. We employ a sample of ~13 000 optically selected clusters from the Sloan Digital Sky Survey (SDSS) maxBCG catalogue, with photometric redshifts in the range 0.1–0.3. The optical tracers we consider are cluster richness, cluster luminosity, luminosity of the brightest cluster galaxy (BCG) and combinations of these parameters. We measure the weak lensing signal around stacked clusters as a function of the various tracers, and use it to determine the tracer with the least amount of scatter. We further use the weak lensing data to calibrate the mass normalization. We find that the best mass estimator for massive clusters is a combination of cluster richness, N200, and the luminosity of the BCG, LBCG: , where is the observed mean BCG luminosity at a given richness. This improved mass tracer will enable the use of galaxy clusters as a more powerful tool for constraining cosmological parameters.

Full text link: https://tinyurl.com/yalzjs5j

Article title: Space Density Of Optically-Selected Type II Quasars From The SDSS

Authors: Reinabelle Reyes, Nadia L Zakamska, Michael A Strauss, Joshua Green, Julian H Krolik, Yue Shen, Gordon T Richards, Scott F Anderson, Donald P Schneider

Publication Title: Astronomical Journal 139(3) 1295-96, March 2010

Abstract:

Type II quasars are luminous Active Galactic Nuclei (AGN) whose central regions are obscured by large amounts of gas and dust. In this poster, we present a catalog of 887 type II quasars with redshifts z